EXTENDING THE PALEOSEISMIC RECORD OF THE PROVO SEGMENT OF THE WASATCH FAULT ZONE, UTAH

Final Technical Report

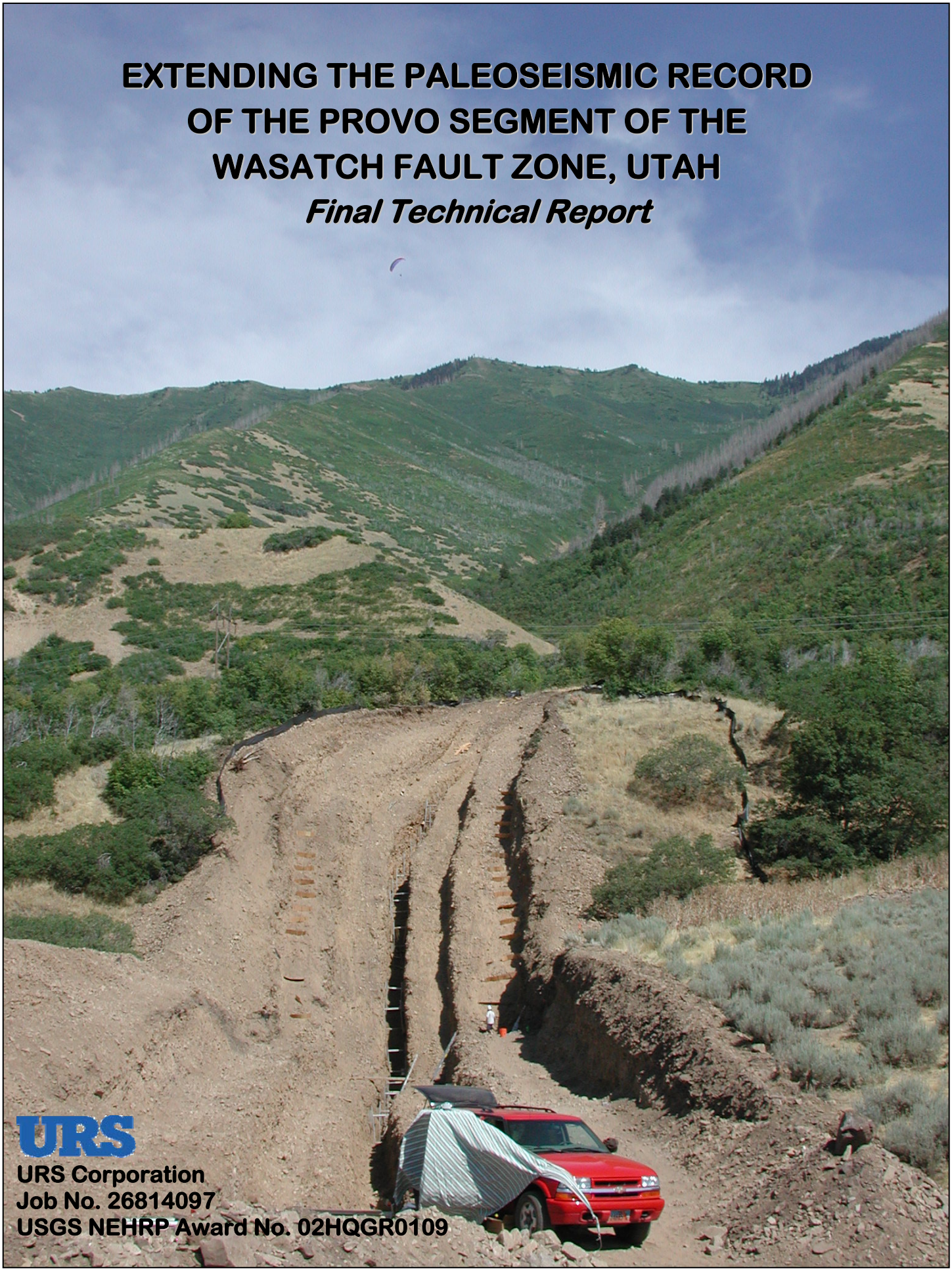

URS

URS Corporation
Job No. 26814097
USGS NEHRP Award No. 02HQGR0109

EXTENDING THE PALEOSEISMIC RECORD OF THE PROVO SEGMENT OF THE WASATCH FAULT ZONE, UTAH

Final Technical Report Submitted to:

U.S. Geological Survey
National Earthquake Hazards Reduction Program
Award No. 02HQGR0109

Submitted by:

Susan S. Olig (PI)
URS Corporation
1333 Broadway, Suite 800
Oakland, CA 94612
Ph: (510) 874-1729
FAX: (510) 874-3268
Email: susan_olig@urscorp.com

Assisted By: Greg McDonald[1], Bill D. Black[2], Christopher B. DuRoss[1,3], William R. Lund[1], Michael Hylland[1], David B. Simon[4], Richard E. Giraud[1] and Gary E. Christenson[5]

[1] Utah Geological Survey
[2] Western GeoLogic LLC
[3] Formerly University of Utah
[4] Simon Bymaster Inc.
[5] Formerly Utah Geological Survey

January 19, 2011

Research supported by the U.S. Geological Survey (USGS) Department of the Interior, under USGS award number 02HQGR0109. The views and conclusions contained in this document are those of the authors and should not be interpreted as necessarily representing the official policies, either expressed or implied, of the U.S. Government.

Job No. 26814097

We excavated an 11.65-m-deep, and ~105-m-long "megatrench" across a 19 to 23-m-high scarp on post-Bonneville fan alluvium along the Provo segment of the Wasatch fault zone, Utah, at the eastern margin of the Basin and Range Province. The purpose of our study was to extend the paleoseismic record back on the Provo segment to investigate if significantly longer latest Pleistocene to early Holocene recurrence rates observed on the Salt Lake and Brigham City segments also occurred on the Provo segment. The trench exposed 33 m of vertical relief across a complex, 50-m-wide deformation zone with evidence of multiple surface-faulting events that occurred throughout the Holocene on 4 footwall and 6 antithetic faults. Paleoseismic evidence included 18 colluvial-wedge and fissure-fill deposits, 7 buried scarp free-faces, stratigraphic truncations and differential offsets of fan sediments, and fault terminations. Debris flows and stream alluvium comprise the exposed fan deposits and ages range from historic to ~15,100 cal B.P. based on radiocarbon analyses of 46 charcoal samples from the trench and soil pits. Surprisingly, 6 to 7 m of mid to late Holocene fan alluvium draped a large, steep (>30°) paleo-scarp created by older (>7.3 ka) events on footwall faults over 16 m upslope from the main fault at the base of the slope. This highlights the importance of adequately exposing the entire deformation zone to obtain complete faulting histories, particularly where longer paleosesimic records are the goal.

Our preliminary evaluation indicates that at least 7, probably 10, possibly 11 or more, large surface-faulting earthquakes occurred since 13,040 cal B.P., and recurrence does not appear to have varied significantly during the Holocene. Most of the uncertainty is due to uncertainty in how older events on footwall faults may or may not correlate to each other, and additional analyses are needed to further evaluate possible correlations for older events. Fortunately, correlations between younger events on graben faults were more straightforward. At least 4, possibly 5 earthquakes occurred since ≈6.1 ka, including compelling evidence for a previously unrecognized event on the Provo segment that occurred about 1,600 (1,100 to 1,800 cal B.P.; all event ages rounded to the nearest half-century with 2 σ range). The four youngest events occurred between 500 (350 to 650) cal B.P. and 4,750 (4,400 to 5,000) cal B.P., which yields a preferred average mid to late Holocene recurrence interval of 1,400 years. Resulting preferred estimates for individual recurrence intervals range from 1,100 to 1,600 years. These values are much shorter than determined by previous studies, and the preferred consensus value of 2,400 years assigned by the Utah Quaternary Fault Parameters Working Group. However, our shorter recurrence interval is similar to average mid to late Holocene intervals of 1,300 to 1,400 years for the adjacent Salt Lake City, Weber, and Brigham City segments, and it is more consistent with the prominent Holocene geomorphic expression of the Provo segment. Overall, our results highlight the importance of striving to obtain not only longer, but more complete paleoseismic records to improve probabilistic seismic hazard evaluations.

Cover Photograph: View looking east at the Mapleton megatrench located near the mouth of Big Slide Canyon on the Provo Segment of the Wasatch fault zone. The trench was 105 m long, 11.5 m deep and exposed over 33 m of vertical relief on a fault that is 19 to 23 m high.

TABLE OF CONTENTS

Abstract i

Acknowledgements iv

Section 1 Introduction 1-1

1.1 Seismotectonic and Geologic Setting 1-1
1.2 Previous Work 1-3
1.3 Scope 1-8

Section 2 Results for the Mapleton Megatrench Site 2-10

2.1 Surficial Geology 2-10
2.2 Subsurface Investigations 2-11
2.2.1 Trench Exposure 2-13
2.2.2 Soil Pits 2-28

Section 3 Analysis of Paleoseismic Parameters and Discussion of Fault Behavior 3-1

3.1 Surface-Faulting Event Summary for the Provo Segment 3-1
3.1.1 Paleoearthquake Summary for the Mapleton Megatrench 3-1
3.1.2 Paleoearthqauke Correlations With Other Provo Segment Sites 3-2
3.2 Recurrence 3-4
3.3 Paleomagnitudes 3-5
3.4 Discussion 3-5

Section 4 References 4-1

Figure Captions

1 Map showing segments (in bold) of the Wasatch fault zone (after Machette *et al.*, 1992), the location of this study and the location of previous megatrench studies (BC – Brigham City site of McCalpin and Forman, 2002; LCC – Little Cottonwood Canyon site of McCalpin, 2002).

2 Location map of trench sites on the Provo and northern Nephi segments of the Wasatch fault zone (modified from Lund and Black, 1998).

3 Aerial view looking east at the Mapleton megatrench site (photograph from R.L. Bruhn).

4 Surficial geology of the Mapleton megatrench site. Topography (with 2 foot contour intervals) is superimposed on an orthophotograph base provided by Olympus Aerial Survey (with the permission of RB&G Engineering).

5 Schematic trench diagram showing general fault locations.

6 Logs of soil pits SP1 through SP3. See Figure 4 for locations.

7 Schematic diagram of graben stratigraphy and surface-faulting event horizons (Event Z_g – pink, Event Y_g – blue, Event X_g – green, Event W_g – orange, and Event V_g(?) – purple). Red circles show radiocarbon samples and ages (with 1σ errors) used in the final analysis (see Figure 8). Gray circles show outlier samples. Jagged lines indicate unconformities. Unit thicknesses and displacements are not to scale.

8 Age analyses of graben faulting event sequence. Ages (with 2 σ ranges) were calendar calibrated and modeled using OxCal 4.1.5 (Bronk Ramsey, 2009) and the IntCal09 calibration curve (Reimer et al., 2009).

9 Modeled distributions and preferred ages of graben faulting events (from analysis shown in Figure 8). See Section 2.2.1 for discussion of selection of preferred ages.

10 Preliminary schematic diagram of footwall stratigraphy and surface-faulting event horizons (Event $Z_{FZ2\&3}$ – orange, Events Y_{FZ2} and Y_{FZ3}(?) – brown [uncertain if event pre- or post-dates deposition of Unit 5c/5cc/5ccc(?)], Event X_{FZ2} – teal, Event W_{FZ2} – lavender, Event Z_{FZ1} – green, Event Y_{FZ1} – magenta). Dark blue shows a non-tectonic slumping event horizon that included secondary faulting on FZ2. Jagged lines indicate unconformities. Red circles show radiocarbon samples and ages (with 1σ errors). Unit thicknesses and displacements are not to scale.

11 Paleoearthquake space-time diagram for central segments of the Wasatch fault zone comparing ages of the 4 youngest events in this study (shown in color) with consenus ages of the UQFPWG (Lund, 2005) determined from previous studies (modified from DuRoss, 2008). As discussed in the text, Event Y (in red) was previously unrecognized on the Provo segment.

List of Tables

1 Event Chronologies From Previous Wasatch Fault Megatrench Studies

2 Comparison of Consensus Recurrence Intervals Assigned by the UQFPWG for the Central Segments of the Wasatch Fault Zone

3 UTM Coordinates for the Mapleton Megatrench, Soil Pits, and Boreholes

4 Radiocarbon Analyses for the Mapleton Megatrench and Soil Pits

5 Summary of Paleoseismic Evidence for Graben Faulting Events

6 Stratigraphic Throw, Differential Displacements and Vertical Slip per Event Measured Across Antithetic Faults in the Graben

7 Measured Throw and Estimated Differential Vertical Displacements Per Event for Footwall Faults

8 Preliminary Summary of Faulting Events Exposed in the Mapleton Megatrench - Preferred Scenario

9 Minimum and Maximum Surface-Faulting Event Scenarios for the Mapleton Megatrench

10 Comparison of Event Ages for the Preliminary 10-Event Megatrench Scenario with Previous Paleoseismic Studies on the Provo Segment

11 Paleomagnitude Estimates for the Provo Segment of the Wasatch Fault Zone

List of Appendixes

A Lithologic Unit Descriptions

B Paleo Research Institute Report by Kathy Puseman on "Examination of Bulk Soil for Radiocarbon Datable Material From the Mapleton Megatrench, Utah"

List of Plates

(Not included here due to file size limitations. See the Working Group on Utah Earthquake Probabilities website: http://geology.utah.gov/ghp/workgroups/wguep.htm)

1 Mapleton Megatrench, Bench 1, South Wall, Sheet 1 of 6

2 Mapleton Megatrench, Bench 1, South Wall, Sheet 2 of 6

3 Mapleton Megatrench, Bench 1, South Wall, Sheet 3 of 6

4 Mapleton Megatrench, Bench 1, South Wall, Sheet 4 of 6

5 Mapleton Megatrench, Bench 1, South Wall, Sheet 5 of 6

6 Mapleton Megatrench, Bench 1, South Wall, Sheet 6 of 6

7 Mapleton Megatrench, Bench 2, South Wall, Sheet 1 of 8

8 Mapleton Megatrench, Bench 2, South Wall, Sheet 2 of 8

9 Mapleton Megatrench, Bench 2, South Wall, Sheet 3 of 8

10 Mapleton Megatrench, Bench 2, South Wall, Sheet 4 of 8

11 Mapleton Megatrench, Bench 2, South Wall, Sheet 5 of 8

12 Mapleton Megatrench, Bench 2, South Wall, Sheet 6 of 8

13 Mapleton Megatrench, Bench 2, South Wall, Sheet 7 of 8

14 Mapleton Megatrench, Bench 2, South Wall, Sheet 8 of 8

15 Mapleton Megatrench, Slot Trench, South Wall, Sheet 1 of 5

16 Mapleton Megatrench, Slot Trench, South Wall, Sheet 2 of 5

17 Mapleton Megatrench, Slot Trench, South Wall, Sheet 3 of 5

18 Mapleton Megatrench, Slot Trench, South Wall, Sheet 4 of 5

19 Mapleton Megatrench, Slot Trench, South Wall, Sheet 5 of 5

This study was funded by the U.S. Geological Survey (USGS) through their National Earthquake Hazard Reduction Program (Award No. 02HQGR0109), by the Utah Geological Survey (UGS), and with support for report preparation from the URS Professional Development Fund. We thank the Suburban Land Reserve and Don White (Zion Securities) for granting access and permission to conduct this study. We also thank Mapleton City and the Division of Wildlife Resources for their cooperation in issuing permits. Melinda Lee and Fabia Terra (URS) assisted with report preparation.

This project benefited measurably from contributions by many individuals, which is testimony to the cooperative spirit, technical expertise, and professional dedication of the community working to reduce earthquake hazards along the Wasatch Front. We would like to particularly thank:

- Craig Nelson (Western GeoLogic, LLC) and Ivan Wong (URS) for help with logistics and project management.
- Ronald Bruhn, Ann Mattson, and Gerald Schuster (University of Utah) for their support and assistance of the drilling to augment this study.
- Gary Christenson and Rick Allis for coordinating outstanding support by UGS and its staff, without which this study could not have been completed.
- Mark Petersen (USGS) for his interest and support.

We would also like to thank Eliza Nemser (URS) and Michael Hozik for their field assistance, Justin Johnson (UGS) for constructing photo mosaics, and the members of the Utah Quaternary Fault Parameter Working Group and others for helpful field review comments (particularly Michael Machette, David Schwartz and Alan Nelson [USGS] and Gordon Seitz [UCSD]). Chris Busch and Scott Cragen helped with setting shores, Joergen Pilz (AMEC) kindly loaned shores, and Bob Gunnell (RB&G) released aerial survey data. We also thank Michaele Kashgarian (Lawrence Livermore National Laboratory) for her adept expertise at radiocarbon analyses and Kathy Puseman (Paleo Research Institute) for presorting samples and identifying organic material. Finally, the PI would like to personally thank the field crew (particularly my coauthors) for braving hail, searing heat, dust, long days, debris floods, and rattlesnakes (but no milksnakes!).

Large variations in rates of earthquake activity through time have been observed for many faults throughout the Basin and Range Province, which can significantly impact probabilistic seismic hazard evaluations (e.g., Wong and Olig, 1998; Wong *et al.*, 2002; Wong *et al.*, 2004). A good example of large rate variations can be found along portions of the Wasatch fault zone (Figure 1), one of the longest and most active faults in the Basin and Range Province. This 343-km-long fault extends along the urbanized Wasatch Front corridor, where 1.6 million people live. Previous "megatrench" studies (with unusually large or extensive excavations) conducted on two of the ten segments of the Wasatch fault zone provide an extended paleoseismic record for the Salt Lake and Brigham City segments (Figure 1). Results from these studies suggest that recurrence intervals between large surface-faulting earthquakes have occurred relatively regularly during the past 6 ka, but were as much as six times longer between 9 and 17 ka (McCalpin and Forman, 2002; McCalpin, 2002; Table 1).

Recent probabilistic ground motion evaluations in the region indicate that these large rate variations can significantly impact the hazard, increasing it by 60% or lowering it by 20%, depending on how the data are incorporated into probabilistic analyses (Olig *et al.*, 2001; 2005). A significant issue in how the paleoseismic data are used is whether the large rate variations were casually related to fluctuations of prehistoric Lake Bonneville, or were they just random variations inherent in the earthquake process? Thus, better understanding these rate variations, what causes them, and how to address them in hazard assessments is critical to adequately evaluating earthquake hazards along the Wasatch Front. More generally, a better understanding of large rate variations through time is important to addressing the fundamental question of how periodically do large earthquakes occur?

The purpose of this study was to excavate a megatrench across the Provo segment of the Wasatch fault zone (Figure 1) to extend the detailed paleoseismic record back from less than 6 ka to over 13 ka. Our intent was to investigate if large rate variations have occurred on the Provo segment, and if so, how event chronologies might compare to those of the Salt Lake City and Brigham City segments. This would help us better understand the rate variations, what causes them, and how to best characterize them in hazard evaluations.

Preliminary results from this study do not indicate lower rates of activity on the Provo segment for the early Holocene to latest Pleistocene, even though the paleoseismic record likely remains incomplete prior to 6 ka. However, we emphasize that these results are preliminary for older (> 5 ka) faulting event pending additional ongoing analyses. Perhaps even more important were surprising observations of multiple, significant, active faults buried high in the footwall; and, evidence for previously unrecognized surface-faulting events that occurred since 6 ka. The latter observation of additional events yields shorter recurrence intervals for the Provo segment and has obvious implications for higher seismic hazards in Utah Valley. The former observation highlights a more general caveat for normal fault investigations everywhere: Beware of buried footwall faults! Both observations emphasize the importance of striving for completeness in the paleoseismic record to adequately evaluate seismic hazards.

1.1 SEISMOTECTONIC AND GEOLOGIC SETTING

The Wasatch fault zone is a west-dipping, range-bounding, normal fault that strikes north-south through south-central Idaho and north-central Utah (Figure 1). It forms the eastern boundary of the Basin and Range Province, separating the Basin and Range Province to the west from the Wasatch Range of the Middle Rocky Mountains Province to the east. The Wasatch fault zone

also lies within the southern portion of the Intermountain Seismic Belt (ISB), a north-south trending zone of shallow, diffuse, intraplate seismicity that extends from Montana, through central Utah, into northern Arizona (Smith and Arabasz, 1991). Similar to the Basin and Range Province, the ISB is characterized by late Cenozoic extension on normal faults and episodic surface-faulting earthquakes (**M** 6½ and greater).

The Provo segment of the Wasatch fault zone lies within the central Wasatch Front region of the southern ISB, which is undergoing east-west extension (Zoback, 1983). Seismological (Arabasz *et al.*, 1992) and geological (Hecker, 1993) characteristics of the Wasatch Front include: (1) dominantly normal slip on generally north-south striking Quaternary faults; (2) moderate background seismicity exhibiting dominantly normal faulting (for comparison, the background seismicity in central Utah is lower by a factor of four to six than that along the San Andreas fault system in California); (3) diffuse seismicity that generally does not correlate to Quaternary faults and is typically located at focal depths of less than 15 to 20 km; (4) relatively long and often variable recurrence intervals for surface faulting on individual fault segments (typically more than 1,000 years); (5) vertical slip rates of late Quaternary faulting (typically less than 2 mm/yr); and (6) the historical absence of any surface-faulting earthquake larger than the 1934 **M** 6.6 Hansel Valley earthquake, despite the presence of abundant late-Pleistocene and Holocene fault scarps.

Although diffuse seismicity has occurred in the area of the Provo segment, no historical earthquakes have been directly attributed to the segment, a pattern typical of seismic activity in the Wasatch Front region (Arabasz *et al*., 1992). Regardless, compelling geologic evidence indicates that large earthquakes have repeatedly occurred prehistorically on the Wasatch fault, and indeed, that it is the longest, most active fault in the region (Hecker, 1993), with vertical slip rate estimates ranging from about 0.5 to over 2 mm/yr during the past 20 ka (Machette *et al.*, 1992). Rate data and particularly variations of rates through time on the Wasatch fault are discussed further in the next section.

The Provo segment of the Wasatch fault zone forms the boundary between Utah Valley to the west and the Wasatch Range to the east. The late Quaternary stratigraphic and geomorphic framework of this area is critical to deciphering the paleoseismic record of the Provo segment. Late Quaternary sedimentation along the western base of the Wasatch Range has been dominated by alluvial-fan sediments shed from the mountains and deposition of lacustrine sediments in Utah Valley (Machette *et al.*, 1992).

Utah Valley lies within the Bonneville basin, which was repeatedly inundated by paleolakes during the late Quaternary. The most significant of these to this study is the youngest deep-lake cycle, the Bonneville cycle, which lasted between 32 and 10 ka. Lake Bonneville reached its highstand, forming the Bonneville Shoreline about 15,000 ^{14}C yr B.P. (Oviatt *et al*., 1992) and intermittently overflowed its basin until about 14,500 ^{14}C yr B.P.. Altitudes of the Bonneville Shoreline range from 1,553 to 1,587 m in Utah Valley (Machette, 1992). The lake level then catastrophically dropped about 110 meters to the Provo Shoreline during the Bonneville Flood. This drop resulted in subsequent isostatic rebound and rapid erosion of Bonneville shoreline deposits throughout Utah Valley. These sediments were reworked and deposited at lower altitudes as alluvial fan-delta complexes and terraces graded to the Provo Shoreline. Recent studies suggest that the Provo phase was actually much longer than previously thought and the lake oscillated near the Provo Shoreline for more than 2,500 ^{14}C yr B.P. (Godsey et al., 2005). After ~12,000 ^{14}C yr B.P., the lake rapidly regressed at a rate of 25 cm/yr, which subsequently

isolated Utah Lake from Lake Bonneville. At its present altitude of ~1,368 m, Utah Lake is still separated from the modern Great Salt Lake today, however, the Jordan River flows from Utah Lake into Great Salt Lake, partially connecting these two modern remnants of Lake Bonneville.

1.2 PREVIOUS WORK

Wasatch Fault Zone

The Wasatch fault zone is the most studied Quaternary fault in Utah and only an abbreviated summary is provided here. Lund (2005) provides a more comprehensive summary and review of previous studies. Since the pioneering studies of Gilbert (1890; 1928), there have been a series of landmark studies in neotectonics and paleoseismology along the Wasatch fault. Some of these include early application of low-sun angle aerial photographs for identifying and mapping active faults for urban planning (Cluff *et al.*, 1973), using trench excavations to develop paradigms of colluvial wedge stratigraphy and earthquake event identification along normal faults (Swan *et al.*, 1980; Hanson *et al.*, 1982; Schwartz *et al.*, 1983), developing new ideas on controls and characteristics of fault segmentation and earthquake recurrence models (Schwartz and Coppersmith, 1984; Smith and Bruhn, 1984; Machette *et al.*, 1991, 1992; Wheeler and Krystinik, 1992), and successful application of new dating techniques such as luminescence and AMS radiocarbon dating of organics within soil horizons (e.g., Forman *et al.*, 1989; McCalpin *et al.*, 1994; Machette *et al.*, 1992). This list is by no means complete, but all of these studies have contributed significantly to our understanding of the earthquake behavior and potential of the Wasatch fault zone overall, or the Provo segment in particular.

Abundant compelling evidence indicates that the Wasatch fault is separated into segments (Figure 1) with relatively persistent segment boundaries between prehistoric surface ruptures (Schwartz and Coppersmith, 1984; Machette *et al.*, 1991; Wheeler and Krystinik, 1992). Initially, Schwartz and Coppersmith (1984) proposed that the fault was divided into 6 segments, but subsequent detailed mapping (Scott and Shroba, 1985; Personius, 1990; Machette, 1992; Personius and Scott, 1992; Nelson and Personius, 1993; and Harty *et al.*, 1997) and dozens of trench investigations (see Table 1 in Machette *et al.*, 1992, and McCalpin and Nishenko, 1996 for summaries), all compose a comprehensive paleoseismic record of fault behavior that indicates a 10-segment model best fits the data (Machette *et al.*, 1991; Machette *et al.*, 1992). This model is also generally consistent with statistical analyses of geophysical and geological properties of potential segment boundaries (Wheeler and Krystinik, 1992) that indicate that salients along the Wasatch Range front appear to have formed at persistent segment boundaries between the central most-active segments.

As persistent as these segment boundaries appear to have been, recent studies strongly suggest that they have not been absolute. Evidence for occasional partial rupture of segments, ruptures extending beyond boundaries, and possible multisegment ruptures (e.g., Hylland and Machette, 2008; DurRoss et al., 2008; Nelson *et al.*, 2006; DuRoss, 2004; Ostenaa, 1990) indicate that more complex rupture patterns have also occasionally occurred on the Wasatch fault zone. Even though these complexities do not appear typical, they can impact seismic hazard evaluations (e.g., Chang and Smith, 2002; Wong *et al.*, 2002). Of particular relevance to this study, is evidence that suggests that the boundary between the Provo and Nephi segments has not been an

absolute barrier to all recent ruptures (Ostenaa, 1990; DuRoss et al., 2008). This is discussed further in the next section on the Provo segment.

Dozens of detailed paleoseismic trench investigations have documented repeated Holocene surface-faulting events along the five central, most-active segments of the Wasatch fault (Brigham City, Weber, Salt Lake City, Provo, and Nephi). Holocene vertical slip rates are typically between 1 and 2 mm/year, whereas recurrence intervals since the mid Holocene are generally between 1,000 and 3,000 years (e.g., Machette *et al.*, 1991; 1992; McCalpin and Nishenko, 1996). Preferred consensus vertical slip rates assigned by the Utah Quaternary Fault Parameter Working Group (UQFPWG) to the five central segments range from 1.1 to 1.4 mm/yr (Lund, 2005). Preferred consensus recurrence intervals are more variable for the central segments, ranging from 1,300 to 2,500 years (Table 2). In contrast to the central segments, the northern (Malad City, Clarkston Mountain, and Collinston) and southern (Levan and Fayette) segments toward the ends of the Wasatch fault are much less active than the central segments, as indicated by more subdued and sinuous range fronts, a general lack of Holocene fault scarps, and more discontinuous and degraded fault scarps (Machette *et al.*, 1992; Hylland and Machette, 2008; Hylland, 2007).

Of particular interest to this study are extensive trench investigations on the Salt Lake City and Brigham City segments, which provide unusually long paleoseismic records (since about 15 to 17 ka) for these two central segments (Table 1). Deep trenches excavated across two main fault scarps near Little Cottonwood Canyon exposed evidence for seven surface-faulting events that occurred since the Bonneville Flood (McCalpin, 2002; McCalpin and Nelson, 2000). The timing of these events indicates that recurrence intervals have been fairly uniform between the past 4 events, averaging about 1,300 years (Table 1). In contrast, recurrence intervals average about 4,750 years, are more variable, and are as long as 8,000 years for the period between 7.5 and 17 ka (Table 1). McCalpin (2002) suggests that this period of quiescence may be related to desiccation of Lake Bonneville and a related suppression of fault movement due to a reduced load on the hanging wall of the Wasatch fault zone. He also notes that McCalpin and Forman (2002) found evidence for a similar period of quiescence on the Brigham City segment. On this segment, a series of trenches across seven fault scarps on a Provo-age delta at Brigham City exposed evidence for seven surface-faulting events (Table 1) with recurrence intervals being fairly uniform and averaging about 1,300 years between the past 6 events. Again this is in contrast to a longer recurrence interval prior to 8.5 ka, which is about 6,300 years or longer. However, they also note that they cannot preclude the possibility of an additional event (not shown in Table 1) occurring around 12 ka, although there is not direct evidence for this event.

Incorporating these rate variations into hazard evaluations for the Wasatch Front can significantly impact the hazard, particularly for time-dependent models. For example, on the Salt Lake City segment it can increase the hazard by 45% if one assumes low coefficients of variation (COV) and only the shorter paleoseismic record (Olig *et al.*, 2001; 2005). This characterization might be appropriate if you believe earthquakes occur very periodically, and that the lower activity rates during the early Holocene and latest Pleistocene were related to conditions caused by lake desiccation, which would no longer apply. In contrast, using high COVs and the longer paleoseismic record can decrease the hazard by nearly 20% (Olig *et al.*, 2001; 2005). This characterization is consistent with more random earthquake occurrence and the belief that the rate variations are not casually related to lake desiccation. Obviously, better

understanding these rate variations and how to incorporate them is important to improving probabilistic seismic hazard evaluations for the region.

It is worth noting that many investigators have speculated on possible causal relations between variations in lake level and rates of fault activity for various faults along the Wasatch Front (e.g., Machette *et al.*, 1992; McCalpin *et al.*, 1992; Keaton *et al.*, 1993; Olig *et al.*, 1994; McCalpin and Nelson, 2000). Perplexingly, patterns of variation are not consistent in that some faults show evidence for quiescence or slowed rates of activity variously during pluvial periods (e.g., West Valley fault zone), during major regressions following pluvial periods (e.g., Brigham City and Salt Lake City segments of the Wasatch fault zone), or throughout interpluvial periods (e.g., Hansel Valley fault). Similarly inconsistent, some faults show evidence of apparently higher rates of activity during pluvial transgressions (i.e., Provo segment of the Wasatch fault zone and Oquirrh fault), while others show higher rates sometime after regressions and several thousand years into the interpluvial cycle (e.g., Salt Lake City and Brigham City segments). Thus, if a causal relation exists, it must explain these complex patterns of variation.

Provo Segment

The Provo segment is the longest segment of the Wasatch fault, extending for 70 km (curvilinear trace length) along the eastern margin of Utah Valley, from the Payson salient north to the Traverse Mountains salient (Machette, 1992). It is characterized by nearly continuous Holocene fault scarps that show complex trace patterns, with near-right-angle bends, multiple overlapping branches, anastomosing splays, step-overs, and gaps. Machette *et al.* (1986) originally subdivided the Provo segment into three subsections (the American Fork, Central or Provo-restricted, and Spanish Fork) based primarily on preliminary mapping, scarp profiling, and geometrical arguments (Figures 1 and 2). However, all of these subsections show clear evidence for repeated Holocene movement, and in a summary analysis of all the paleoseismic data from detailed mapping and trench sites on each of the subsections (Figure 2), Machette *et al.* (1991; 1992) concluded that these subsections likely comprise one segment as originally proposed by Schwartz and Coppersmith (1984).

Holocene and latest Pleistocene vertical slip rate estimates are fairly consistent between all three subsections of the Provo segment and are comparable to estimates for the other central segments of the Wasatch fault. Vertical slip rates generally range from 0.5 to over 2.5 mm/yr (Swan *et al.*, 1980; Lund *et al.*, 1991; Machette *et al.*, 1992). However, there is also evidence for significant variations in slip rate through time, including very high rates between the Lake Bonneville transgression and regression (as high as 10 mm/yr), and two orders of magnitude lower rates over the past 130 to 250 ka (0.1 to 0.3 mm/yr) (Machette *et al.*, 1992). Lund (2005) provides a more detailed summary of all the available slip rate data for the various sites along the Provo segment. Based on their evaluation of all this data, the UQFPWG assigned a preferred vertical slip rate of 1.2 mm/yr, and 5th and 95th percentile estimates of 0.6 and 3.0 mm/yr to the Provo segment (Lund, 2005).

Although mid to late Holocene slip rates on the Provo segment are generally comparable to the other central segments of the Wasatch, previous trenching studies indicated that recurrence intervals were longer for the Provo segment than the Salt Lake City, Weber and Brigham City segments. Detailed trench investigations at seven trench sites along the main trace of Provo segment (Figure 2) reveal evidence for the occurrence of multiple Holocene surface-faulting events (Swan *et al.*, 1980; Schwartz *et al.*, 1983; Forman *et al.*, 1989; Ostenaa, 1990; Lund *et al.*,

1991: Machette *et al.*, 1992; Lund and Black, 1998). The site-specific data for events are discussed in more detail below. However, based on all the available data, the UQFPWG determined the following preferred ages for the three youngest events on the Provo segment:

Event Z: 600 ± 350 cal B.P.
Event Y: 2,850 ± 650 cal B.P.
Event X: 5,300 ± 300 cal B.P.

This resulted in a preferred average recurrence interval of 2,400 years for the Provo segment, and 5th and 95th percentile estimates of 3,200 and 1,200 years, respectively (Lund, 2005). In contrast, the preferred recurrence intervals for the Salt Lake City, Weber and Brigham City segments are much shorter at 1,300 to 1,400 years (Table 2).

Comparable slip rates but longer recurrence may appear incongruous. However, one possible explanation for apparently longer recurrence, but comparable slip rates on the Provo segment may be larger displacements per event. For previous studies along the Provo segment, estimates of net vertical displacement per event range from 0.8 to 3.3 m, but average 2.3 m for six well-constrained measurements and 2.2 m for all of the data (Swan *et al.*, 1980; Lund *et al*. 1991; Machette *et al.*, 1992; Lund and Black, 1998). Assuming a recurrence interval of 2,400 years with these displacements yields a slip rate of nearly 1 mm/yr, which is only slightly less than the preferred UQFPWG consensus rate for the Provo segment.

Due to the particular relevance to this study, we review in more detail here the paleoseismic record deciphered from previous trench investigations on the Provo segment. The first detailed trenching study along the Provo segment was at Hobble Creek (Figure 2). Swan *et al.* (1980) and Schwartz *et al.* (1983) found evidence for 6 or 7 surface-faulting events that produced 11.5 to 13.5 m of cumulative net vertical displacement since a Provo delta formed between 14,500 and 12,000 ^{14}C yr B.P. (revised Provo phase ages by Godsey and Chan, 2005, as discussed in the previous section). Calendar calibrations of the regression age (using CALIB 5.0.1) yields 2 σ age estimates of 13,660 to 14,080 cal B.P. These revised ages in turn yield revised vertical slip rates of 0.82 to 0.99 mm/yr for the Hobble Creek site. Unfortunately, additional absolute age constraints for individual events were lacking.

Forman *et al.* (1989) and Machette *et al.* (1992) found evidence for four surface-faulting events that occurred at the American Fork Canyon site (Figure 2). The oldest event (Event W_{AF}) occurred between 5.3 and 8.1 ka, the third event back (Event X_{AF}) occurred around 5,300 ± 300 cal B.P., the second or penultimate event (Event Y_{AF}) occurred around 2,650 ± 250 cal B.P., and the youngest event occurred around 500 ± 200 cal B.P. It is particularly relevant when comparing their results to this study that their three trenches did not expose the entire deformation zone (see Figure 3 of Machette, 1992). In particular, west-dipping fault traces that offset post-Bonneville fan deposits and lie east of Trenches AF1 and AF2 were not trenched and studied because of landowner restrictions. The implications of this are discussed later in our report.

Results from the Mapleton North (MN) and Mapleton South (MS) trench site of Lund *et al.* (1991) are particularly relevant to this study as our megatrench was located at their MN site, immediately north of their two trenches (Figure 3). At both MN and MS, Lund *et al.* (1991) found evidence for two surface-faulting events, a very large event that occurred at about 600 ± 80 cal B.P. and an earlier event that occurred shortly before 2,820 (+150, -130) cal B.P.

However, at both MN and MS sites, they only exposed the lower third of the main fault scarp. The implications of this are discussed later in our report. The age of the youngest event was constrained by several ages from the MN trenches, whereas ages for the penultimate event all came from the MS trench. Comparison of this record with the apparent correlative timing of the youngest events at the American Fork Canyon site, along with evidence for a well-constrained event at Rock Canyon that occurred at 650 (+50, -110) cal B.P. (Lund and Black, 1998), formed much of the basis for the conclusion that the entire length of the Provo segment likely ruptured together during the two youngest events, rather than rupture of independent subsections (Lund *et al.*, 1991; Machette *et al.*, 1991; Machette *et al.*, 1992).

Finally, unpublished results from the southernmost trench site on the Provo segment, Water Canyon, reveal a somewhat different record of faulting than sites to the north, perhaps because the site is only 4 km from the boundary with the Nephi segment to the south (Figure 2). Two trenches revealed evidence for at least 4, or possibly 5 surface-faulting events since 4,600 ± 75 ^{14}C yr B.P. (D. Ostenaa, USBR, personal communication, 1/11/06). Trench WC1 was across a small fault scarp offsetting an inset terrace and revealed compelling evidence for 2 surface-faulting events (Y_{WC1} and Z_{WC1}). The older event (Event Y_{WC1}) occurred shortly after 890 ± 60 ^{14}C yr B.P. based on radiocarbon analysis of a bulk soil sample from an A horizon directly underlying the penultimate event colluvial wedge. The younger event (Event Z_{WC1}) occurred shortly after 320 ± 120 ^{14}C yr B.P., based on radiocarbon analysis of a bulk sample from an A horizon developed on the older wedge that is faulted and underlies the youngest colluvial wedge. The older event in trench WC1 (Event Y_{WC1}) could correlate to the youngest event observed elsewhere (Event Z) on the Provo segment, whereas the youngest event in trench WC1 does not appear to have ruptured at any other Provo segment sites to the north. Based on this, Ostenaa (1990) postulated that this event may actually correlate to the youngest event on the northern Nephi segment. A recent trench investigation near Santaquin (Figure 2) indicates that the youngest event on the northern strand of the Nephi segment occurred at about 500 (+100, -150) cal B.P. and had a net vertical displacement of 3.0 (±0.2) m (DuRoss *et al.*, 2008). Thus, the ages for the youngest events at the Water Canyon and Santaquin sites do overlap within the 2 σ error range.

Trench WC2 at Water Canyon was across a much larger fault scarp on an older fan surface. This trench exposed evidence for 3 surface-faulting events: Events Z_{WC2}, Y_{WC2}, and X_{WC2}. The youngest event, Event Z_{WC2}, occurred shortly after 1,530 ± 60 ^{14}C yr B.P. (bulk soil sample from under the colluvial wedge exposed on the north wall) to 1,850 ± 70 ^{14}C yr B.P. (bulk soil sample from under the colluvial wedge exposed on south wall), and before distal colluvial wedge sediments were deposited 710 ± 90 ^{14}C yr B.P. Given the uncertainties, Event Z_{WC2} may or may not correlate to Event Y_{WC1} (and Event Z elsewhere on the Provo segment).

Event Y_{WC2} occurred at or just before deposition of colluvium 3,455 ± 100 to 3,655 ± 120 ^{14}C yr B.P., and Event X_{WC2} occurred after 4,600 ± 75 ^{14}C yr B.P. This older event may correlate to Event X_{AF} at American Fork Canyon. However, Event Y_{WC2} at the Water Canyon site does not appear to correlate with any other events previously identified on the Provo segment to the north. Perhaps this event too was actually associated with rupture of the northern Nephi segment. Obviously, calendar calibrations of the ages from Water Canyon are important to interpreting and comparing the paleoseismic record form this site. Therefore, we recalibrate and analyze the

radiocarbon ages generously provided by D. Ostenaa and discuss these further, particularly in regard to how they compare with our results, in Section 3.1.

1.3 SCOPE

Our study included: (1) interpretation of color and black and white stereo aerial photographs of the trench site at different scales; (2) detailed mapping of the surficial geology at the trench site; (3) topographic profiling of fault scarps; and (4) excavation, interpretation, logging, and analysis of trench and soil pit exposures; (5) description of lithologic units; and (6) accelerator mass spectrometer (AMS) radiocarbon analyses of 46 charcoal samples to determine numerical ages. Our methods for these tasks are described further in the respective parts of Section 2. This report does not discuss result from boreholes or seismic surveys conducted by the University of Utah at the Mapleton site (Buddensiek et al., 2007).

Table 1
Event Chronologies From Previous Wasatch Fault Megatrench Studies

Event	Age (± 2 σ) [1] (cal B.P. except as noted)	
	Brigham City Segment (McCalpin and Forman, 2002)	Salt Lake City Segment (McCalpin and Nelson, 2000; McCalpin, 2002)
Z (most recent)	2,100 (± 800)	1,300 (± 650)
Y	3,450 (± 300)	2,450 (± 550)
X	4,650 (± 500)	3,950 (± 550)
W	5,950 ± 250	5,300 (± 750)
V	7,500 (± 1,000)	~7.5 ka
U(?)	8,500 (± 1,500)	~9 ka
T	14,800 (± 1,200) to 17,000	~17 ka
Average Recurrence Interval (years) [2]	1,300 (500 – 2,800)	1,300 (500 – 2,400)

[1] Concensus values of the Utah Quaternary Fault Parameters Working Group (UQFPWG) (Lund, 2005) based on data in the megatrench studies cited above. See Lund (2005) for a complete list and discussion of all previous trench studies on these two segments.

[2] Consensus preferred values (with 2 σ range) of the UQFPWG based on the record since 6 ka, which was considered a more complete and reliable indicator for future activity than the record since 17 ka.

Table 2
Comparison of Consensus Recurrence Intervals (in years) Assigned by the UQFPWG to the Central Segments of the Wasatch Fault Zone (Lund, 2005)

Segment	Preferred	5th Percentile	95th Percentile
Brigham City	1,300	500	2,800
Weber	1,400	500	2,400
Salt Lake City	1,300	500	2,400
Provo	**2,400**	**1,200**	**3,200**
Nephi	2,500	1,200	4,800

2.1 SURFICIAL GEOLOGY

The Mapleton megatrench site is located 15½ km southeast of downtown Provo on the Spanish Fork subsection of the Provo segment (Figures 1 and 2). Figure 3 shows an aerial view of the trench site. It lies along the eastern margin of Utah Valley at the base of the Wasatch Range. Our trench was located just north of the mouth of Big Slide Canyon, whose headwaters initiate on the northwest flank of Spanish Peak, which lies about 4 km southeast of the site. At an elevation of 3,107 m, Spanish Fork Peak is one of the highest peaks along this portion of the Wasatch Range (Provo Peak and Mt. Timpanogos to the north are higher).

At Big Slide Canyon, the Wasatch fault zone lies at the base of the range, but several subparallel, primarily steeply west-dipping normal faults are also exposed within the range to the east (Baker, 1972; Davis, 1983; Machette, 1992). The closest is about 0.8 km east of the Wasatch fault. These faults all appear to be confined to bedrock, which consists of folded rocks of the Pennsylvanian-Permian Oquirrh Formation. These are the source rocks for sediments shed out of Big Slide Canyon, and they consist of gray to tan limy or quartzitic sandstone, tan quartzite, gray to blue to black limestone, and cherty limestone (Davis, 1983; Baker, 1972).

Figure 4 shows our surficial geology map of the site, which was originally prepared at a 1:3,600 scale on a topographic base with 2-foot contours registered to an orthophoto base. This map is based on a variety of data sources, including: (1) Machette (1992) and Figure 2 of Lund *et al*. (1991); (2) our interpretation of aerial photographs (1970, 1:12,000-scale, low-sun-angle black and white stereo pairs and 1989, 1:6,600-scale, natural color stereo pairs); (3) field checking stream cuts, gravel pits, etc.; (4) an aerial overflight (conducted as part of the University of Utah's study); and (5) 32 soil pits, excavated in the area west of the Wasatch fault and east of the Mapleton canal for a hazards and geotechnical investigation conducted by Western GeoLogic, LLC (C. Nelson, Western GeoLogic, personal communication, 2003). Using a total station, we also measured a long (>760 m) topographic Profile (P1 on Figure 4) to estimate vertical displacements across the fault zone. This profile compares favorably with a profile constructed from the aerial survey map data, and with a shorter profile measured in 1987 using a stadia rod and abney level by Lund et al. (1991).

At elevations ranging from 1,468 to 1,545 m, our trench site lies just below the Bonneville shoreline ("B" on Figure 4), and above the Provo shoreline, which is mapped at an elevation of 1,451 m (4,760 feet) west of Big Slide Canyon (Machette, 1992). The chronology for the Bonneville lake cycle (Oviatt *et al*., 1992) indicates that the fault scarp at the site was transgressed by this ancient lake about 16,000 to 17,000 ^{14}C yr B.P. Indeed, we found transgressive beach gravels, with a distinctive boulder lag at the scarp base ("T" on Figure 4), overlying older alluvial-fan gravels (af_3 on Figure 4) exposed in gravel pits on the main fault scarp both north and south of our trench site. Overlying these gravels is an apparently complete transgressive and regressive sequence of lake sediments of the Bonneville lake cycle (lb on Figure 4). The transgressive beach deposits are not clearly exposed in the hanging wall, but boulders weathering out in the colluvium at the base of a knob near a stock pond south of the trench site are suggestive of their presence.

Overlying the Lake Bonneville deposits are latest Pleistocene to Holocene fan sediments (af2 on Figure 4) that were deposited at the mouths of Big Slide and Middle Slide Canyons after the

Bonneville Flood. These fans appear larger (in both areal extent and volume) than younger Holocene fans (af1 on Figure 4) and are generally graded to shorelines of the Provo phase.

The Wasatch fault zone is expressed geomorphically at our trench site as a single, large, west-facing main fault scarp and two small east-facing antithetic fault scarps that form a distinctive graben, which is 18 to 40 m wide (Figure 4). The main fault scarp is 19 to 23 m high, has a maximum scarp angle of 58½° (located just above the scarp base) and six additional prominent scarp bevels located upslope on the scarp face. Three of these bevels have scarp angles exceeding 40° (46½°, 49°, and 41°) and were approximately coincident with significant footwall faults exposed in the trench (discussed further in the next section).

Based on the surficial mapping, both the af2 and af1 deposits are offset by scarps of the Wasatch fault, but af1 deposits appear to be primarily deposited in the hanging wall. Additionally, the scarp profile and surficial mapping suggest apparent net vertical tectonic displacements of 19.8 to 25.9 m down to the west on the af2 surface. However, this is misleading as the trench revealed that actually a considerable thickness (6 to 7 m) of younger (mid to late Holocene) fan deposits were present in the footwall and were draping a buried scarp on af2 deposits. These relations and their implications to displacements are discussed further in Section 3.2.

2.2 SUBSURFACE INVESTIGATIONS

We excavated one large trench across the fault zone and three soil pits (SP1, SP2, and SP3) located west of the trench (Figure 4). Our megatrench was located north of the two previous Mapleton North (MN) trenches of Lund *et al.* (1991) (Figure 3). The megatrench was generally oriented perpendicular to the scarp (cover photograph) with an azimuth of 290° on the scarp face. However, due to logistical constraints the east end of the trench bent 10° southward near the scarp crest. As part of a separate study conducted by the University of Utah and funded by the National Science Foundation, three boreholes were also drilled in the hanging wall of the fault (B1, B2, and B3 on Figure 4). Table 3 shows UTM coordinates for all the excavations. Results from the boreholes are not included in this report, but will be included in a separate report.

The trench was over 105 m long, 11 to 15 m wide, as much as 11.65 m deep and exposed over 33 m of vertical relief. It was constructed with upper (Bench 1) and lower (Bench 2) benches symmetrically flanking both sides of a deeper slot trench extending down the center (Figure 5 and cover photograph). The soil pits were nearly 3 m deep and T-shaped for better safety and visibility. The trench was excavated with a D-9 bulldozer and a Cat 325B track-mounted excavator. The bulldozer first roughly cut the benches and the excavator then “cleaned up” bench walls and excavated the slot trench. Walls were further scraped and cleaned with hand tools to remove bucket smear. Rapid dust accumulation obscured key features, and so we periodically blew dust off the walls with a leaf blower to maintain optimum visibility.

Due to field-time constraints, we only logged the south walls of the trench (Plates 1 through 19) and a representative stratigraphic column for each soil pit (Figure 6). Detailed descriptions of all the stratigraphic units exposed in the trenches are included in Appendix A. Benches 1 and 2 were logged on color photograph mosaics. The slot trench was logged at a scale of 1 inch = 0.5 meter (≈1:20 scale) on a planimetric grid (Plates 15 through 19) using more traditional methods. Specifically, we strung level lines and marked stations at one-meter intervals to provide reference lines. Locations of samples, faults, and stratigraphic and pedologic contacts were

marked with flagging and nails, and/or spray paint, and measured relative to a level line to the nearest centimeter.

Our photo mosaics for Benches 1 and 2 were constructed using Photoshop Version 6, but due to field-time constraints we did not string grids as is typically done to rectify or un-distort the photo mosaics (A. Nelson, USGS, written communication, 2003). Instead, prior to shooting photographs of the trench wall, we constructed a series of targets (T1-1 through T1-36 in Bench 1 and T2-0 through T2-36 in Bench 2). Using a total station, we surveyed these points, along with our slot trench level line to: un-distort the photo mosaic logs, register the different levels together into the same reference frame, and tie these together with our topographic profile, and the borehole and soil pit locations. In this reference frame the origin (st. 0,0 m) is the easternmost point on our topographic profile. Horizontal stations increase westward and vertical stations decrease downward so that all horizontal stations are positive and all vertical stations are negative. To un-distort the photo mosaic logs, we first projected survey points onto a flat reference plane (approximated by the south wall of the slot trench on the scarp face), and then restored target points in the photo mosaics to their respective projected survey point. For the most part this required relatively minor manipulations (small rotations or stretching, splicing, or shrinking less than a few centimeters between targets). Amazingly we found errors of ≤ 4 cm in the slot trench. However, errors are larger in the bench logs, particularly for Bench 2 on the scarp, which we estimate to be ≤ 10 cm, with maximum errors occurring near the scarp crest and scarp base.

We collected 53 organic samples from the trench and soil pits, and conducted 46 AMS radiocarbon analyses to provide numerical age constraints for faulting events (Table 4). The locations of all the samples collected are shown on Plates 1 through 19 and the respective plate for each sample is noted in Table 4. Radiocarbon ages in Table 4 are shown with 1 σ errors. We calendar calibrated all individual radiocarbon ages using CALIB 5.0.1 as noted in the footnotes of Table 4. Calibrated ages are reported with 2 σ errors. Discussions with Paula Reimer (coauthor of CALIB) about combining and sequencing our ages given some of the stratigraphic complexities, resulted in our using OxCal 4.1.5 (Bronk Ramsey, 2009) for analysis of multiple ages in a sequence to better estimate the timing of earthquakes by incorporating stratigraphic and pedologic information into the analysis using Bayesian statistics. These analyses vary depending on information available for each event and are specifically discussed in the next section. In the OxCal analyses, we used the updated calibration curve (IntCal09) by Reimer *et al.* (2009), and report all calibrated ages rounded to the nearest decade with 2σ errors.

Note that the OxCal model we present here is consistent with ongoing analyses of the Mapleton North site, and the entire Provo segment, which are being conducted by the OxCal Subcommittee of the Working Group of Utah Earthquake Probabilities to better constrain paleoearthquake ages along the five central segments of the Wasatch fault zone (DuRoss et al., 2011). The primary difference between this model and the WGUEP model for the Mapleton North site is that the latter combines data from the Megatrench with the Mapleton North trenches of Lund et al. (1991).

Except for MM-RC25a and MM-RC25b, all of the samples were collected as individual pieces of charcoal. Samples MM-RC25a and 25b were collected as a bulk sediment sample (from 1 to 5 cm below the top of the buried A horizon on Unit 6t). Note that this A horizon (on the top of Unit 6t) was not generally logged due to the organic-rich nature of this unit, and so it is only

subtly distinguishable as a horizon with more concentrated roots and root pores, and granular to platy texture at the top of Unit 6t. PaleoResearch Institute sorted and identified organic fragments from MM-RC25 for potential AMS analyses (Appendix B). They found charcoal fragments of conifer, unidentified hardwood, and Roseacea. We selected the largest fragments of the Roseacea (MM-RC25a) and hardwood (MM-RC25b) to date because these species are generally located at lower elevations in Big Slide Canyon closer to the trench site, and Roseacea generally has a shorter lifespan.

Some of the charcoal samples were from buried A horizons, one was from a baked (or burn) horizon, but most were detrital pieces within channels or debris flows, and some caveats about the use of these ages are in order. If the charcoal was incorporated into the deposit shortly after the source plant was burned, then the radiocarbon age provides a close maximum limiting age for deposition of the alluvium or debris flow (that is the deposit is only slightly younger than the radiocarbon age of the charcoal). However, if the charcoal resides a long time on the floor of Big Slide Canyon (say hundreds to even a couple thousand years) before getting incorporated into the debris flow, or it is reworked from an older deposits, then the radiocarbon age can be much older than the age of the deposit. Where we have multiple samples from a single debris-flow deposit, we see evidence for both scenarios. The latter scenario is illustrated by analyses of three samples from Unit 6z, a thin dark, organic-rich, vesicular debris flow (Plates 4 and 5). Sample MM-RC23 from Unit 6z provided an age of 120 ± 35 yr B.P. and was a piece of charcoal burned *in situ* within a red baked horizon at the base of unit 6z (Plate 5). It therefore would be expected to provide a close minimum-limiting age for deposition of this debris flow. In comparison, samples MM-RC6 and MM-RC7, which were detrital charcoal and provide maximum-limiting ages for deposition of Unit 6z, yielded older ages of 275 ± 40 and 215 ± 35 yr B.P., respectively. After calibration, the ranges overlap at 2σ, but they test as significantly different from sample MM-RC23 at the 95% confidence level.

Regardless of potential problems with detrital charcoal, radiocarbon ages from the graben were all stratigraphically consistent, with the exception of MM-RC38, which was obviously anomalously young (Table 4) and was likely invasive due to bioturbation. Samples from the footwall were overall stratigraphically consistent, but five samples do appear anomalously old (MM-RC15, MM-RC42, MM-RC19, MM-RC29, and MM-RC42), and we believe this is likely due to older charcoal being incorporated into these deposits. In contrast, sample MM-RC9 appears anomalously young (Table 4), possibly due to disruption by faulting. Radiocarbon ages and the specific constraints they provide on the timing of faulting events are discussed further in the following section.

2.2.1 Trench Exposure

The trench exposed a 50-m-wide deformation zone that included 4 significant footwall faults (from east to west, FZ1 through FZ4) and 6 significant antithetic faults (AFZ1 through AFZ6) that overall offset latest Pleistocene to Holocene fan deposits down to the west (Figure 5; Plates 1 through 19). For comparison, the previous MN trenches of Lund et al. (1991) only exposed faults between FZ4 and AFZ5, and were not as deep as Bench 1. All of these faults were normal faults and generally north-south striking. Faults FZ1 through FZ4 dipped steeply (>60°) westward, whereas all the antithetic faults dipped steeply eastward. Each of these faults have associated evidence for surface-faulting events and most show evidence for repeated surface faulting. We refer to the surface-faulting events with reversed alphabetical labels; Event Z being

the youngest. For bookkeeping purposes, we distinguish events on individual faults with respective subscripts so that Event Z_{FZ1} is the youngest event on FZ1, and Event Z_g is the youngest event on the graben faults (FZ4 and all the antithetic faults, AFZ1 through AFZ6).

The trench exposed latest Pleistocene to Holocene alluvial fan deposits in the footwall (Units 3a through 3g, Units 4a through 4b/4bb, and Units 5aaa through 5s.5ss?), and mid Holocene to historic fan deposits in the hanging wall (Units 6a through 6za; Appendix A). Alluvial fan units are alphabetically labeled from oldest to youngest. Fan deposits were dominantly debris flows but also included channel deposits. Although we could generally correlate stratigraphic units across the antithetic faults in the hanging wall, correlations across footwall faults were often more ambiguous due to variability and complexities in deposition on the steep scarp. Due to the difficulties in correlating fan deposits across footwall faults, we used single letters for designating deposits on the upthrown side of FZ2 (e.g., Unit 5c), whereas double letters show probable correlative units between FZ2 and FZ3 (e.g., Unit 5cc), and triple letters designate probable correlative units between FZ3 and FZ4 (e.g., Unit 5ccc?). The trench also exposed 18 colluvial wedge and fissure fill deposits. These deposits of colluvium along fault scarps are labeled according to the fault and surface-faulting event that they are associated with (e.g., Unit FC4Z is the fault scarp colluvium associated with Event Zg on FZ4). Detailed descriptions of all units are included in Appendix A and listed from youngest (e.g. Unit 6za) to oldest (Unit 3a).

Due to these uncertainties, the results presented here for the footwall faults are preliminary pending additional analyses. Our preliminary interpretations suggest that the trench revealed structural, stratigraphic, and pedologic evidence for the occurrence of at least 7, probably 10, possibly 11 or more, surface-faulting earthquakes on the Provo segment. The evidence for all events, along with their timing and the associated displacements, is described in detail in the following sections, first for the hanging wall, and then for the footwall.

2.2.1.1 Hanging Wall

In the hanging wall, the trench exposed a 35-m-wide graben defined by the main fault, FZ4, and the six significant antithetic faults (AFZ1 through AFZ6) that offset fan sediments that include debris flows, channel alluvium and colluvium. We identified 27 alluvial fan units in the hanging wall (Units 6a through 6za) and their ages range from 7,430-7,550 cal B.P. (oldest age for Unit 6c, Table 4) to historic, as indicated by several pieces of barbed wire observed in Unit 6za (Plate 4). Also exposed in the hanging wall were 10 distinct fissure-fill and/or colluvial wedge deposits. See Appendix A for detailed unit descriptions of all stratigraphic units in the hanging wall.

Overall, in the graben we found stratigraphic and structural evidence for at least 4, possibly 5, surface-faulting earthquakes (Events Z_g through V_g [?]) that occurred since ≈ 6.1 ka. The evidence for these faulting events is summarized in Table 5, and it includes stratigraphic and differential offsets, buried scarp free-faces and associated colluvial-wedge deposits, fissure fills, and fault terminations. The specific evidence for each event and their ages are discussed in more detail below. Table 6 shows measurements of stratigraphic throw, differential displacements, and estimates of vertical slip per event for each antithetic fault. These are all down-to-the-east vertical displacements and they range from 0.3 ± 0.05 m on AFZ4 for Event W_g, to 1.1 ± 0.4 m on AFZ5 for Event W_g. Figure 7 shows the relation of the five graben event horizons to faults, stratigraphic units and radiocarbon ages. From Figure 7 and Table 5 it is readily apparent that

activity has jumped around between antithetic faults and most of the faults have been repeatedly active. Most importantly, multiple lines of evidence on multiple faults provide compelling evidence for the 4 youngest surface-faulting events (Z_g through W_g) that occurred between 500 (350 to 650) and 4,850 (4450 to 5050) cal B.P. Evidence for an additional older earthquake, Event V_g (?), is more limited but still suggestive that it occurred at 5950 (4950 to 6100) cal B.P.

Figure 8 shows our age analysis of the graben faulting event sequence using OxCal v 4.1.5 (Bronk Ramsey, 2009) and the IntCal09 calibration curve (Reimer et al., 2009). In the analysis, calibrated radiocarbon ages (with 2 σ ranges) are rounded to the nearest decade. As previously mentioned, this OxCal model is consistent with ongoing analyses being conducted by the OxCal Subcommittee of the Working Group of Utah Earthquake Probabilities, with the main difference being that the latter combines data from the this study with the Mapleton North trenches of Lund et al. (1991).

Figure 9 shows the probability density functions of each of the faulting events that result from the Megatrench OxCal analysis, including our preferred ages, which are not always the mean or median values of the modeled distributions, but instead are selected based on the best constraining geologic data as discussed in detail below for each event. All our final faulting event ages are rounded to the nearest half-century, which we believe more realistically reflects all the uncertainties.

In constructing our stratigraphic-ordering model in OxCal we opted for generally minimizing the use of boundaries in the sequence to avoid over-constraining the model. We did group samples from the same stratigraphic units into phases (unordered groups). We also included the historical record constraint that no surface-faulting earthquakes are known to have occurred in Utah Valley since the Mormon pioneers arrived in 1847 (103 cal B.P. on Figure 8). We did not include the age for sample MM-RC38 from Unit 6k in our final model as it is obviously anomalously young (Table 4) and was probably invasive due to bioturbation (Appendix A). Indeed, when included it has an agreement index (A) of 0%, where A provides a measure of the agreement between the observed ages and the prior stratigraphic model. Bronk Ramsey (2009) recommends to consider discarding ages where A<60%. All the other 13 sample ages are stratigraphically consistent, showing a progressively younging-up sequence and having agreement indices of ≥93% (Figure 8). The model (A_{model}) and overall ($A_{overall}$) agreement indices for our final model were 99 and 99.2%, respectively, indicating that the stratigraphic model is internally consistent and in good agreement with the age data. Specific details of the age analysis for each event are discussed further below.

Event Z_g – Stratigraphic offsets, fault terminations, buried scarp free faces, and associated colluvial wedge deposits on faults FZ4, AFZ2 and AFZ5 provide compelling evidence for this youngest surface-faulting event in the graben (Figures 7 and 8; Table 6; Plates 3, 4 and 5). Additional evidence is provided by stratigraphic offsets and fault terminations at the top of Unit 6w on AFZ2 (Table 6, Plates 3 and 4). An impressive feature of this event is Unit $FC4Z_g$, an exceptionally large colluvial wedge, which was deposited against a fault scarp on FZ4 that was about 8 m high (Plates 3 and 4). Event Z_g occurred very soon after Units 6v, 6w and 6x were deposited, which are all faulted, directly underlie colluvial wedge deposits, and show no soil development. Unfortunately, ages are lacking from these units. The best age constraints are provided from samples MM-RC1 and MM-RC13a, which are from colluvium that respectively post-dates and predates Event Z_g (Figure 7, Plates 3 and 11). The 2 σ range for the modeled age distribution of Event Z_g is 370 to 630 cal B.P., whereas our preferred age of 520 cal B.P. is based

on the peak of the event age distribution, which minimizes the overlap in age distributions for samples MM-RC1 and MM-RC13a (Figures 8 and 9). This is also the median of the modeled age distribution for Event Z_g(Figure 9). Rounded to the nearest half century, our age analysis indicates that Event Z_g occurred about 500 (350 to 650) cal B.P.

Our age of 500 (350 to 650) cal B.P. for Event Z_g is slightly younger, but still compares favorably with, previously determined ages of 600 ±80 cal B.P. for the youngest earthquake in the MN trenches (Lund et al., 1991). Indeed, we believe that we could correlate some of the key units from their trenches to our trench. We correlate our Unit FCA5 Z_g (Plate 5) to their Units 8W, 8X and 8Y; and, we correlate our unit FC4Z_g to their Units 8A through 8U. Overall, the ages and stratigraphic evidence indicate that the youngest faulting event of Lund et al. (1991) correlates to our Event Z_g.

We can estimate the amount of net vertical slip that occurred during Event Z_g. Even though stratigraphic offsets cannot be measured across the main fault, FZ4, estimates of the minimum net vertical slip that occurred during Event Z_g can be made using heights of the buried scarp free face. We measure a minimum scarp height for FZ4 of 7.3 ± 0.1 m (height from the top of the buried free-face to the top of Unit 6w immediately adjacent to FZ4, which does not include the "heal" or fissure immediately adjacent to FZ4 at the base of Unit FC4Z_g; Plate 3). This is a minimum as the top of the free-face appears truncated and was likely partially eroded. Scarp height can be a reasonable estimate for vertical slip if we subtract all back-tilting and antithetic faulting (McCalpin, 1995). Summing the down-to-the-east throw measured on individual antithetic faults for Event Z_g yields 2.25 m (Table 6), but this does not include backtilting or all the complex deformation on AFZ1. Fortunately the top of Unit 6v (a channel deposit that closely predates Event Z_g) provides a good marker for estimating all of the vertical down-to-the-east deformation between FZ4 and AFZ2. We measure a cumulative down-to-the-east throw on the top of Unit 6v of 1.44 to 1.68 m. This includes a maximum of 2° of back-tilting and is measured by projecting the top of Unit 6v between st. 234.5 and 241.5 m back (eastward) to FZ4. We note that back-tilting appears negligible between AFZ2 and AFZ5. Adding the down-to-the-east throw on AFZ5 of 1.0 ± 0.3 m for Event Z_g (Table 6) yields a cumulative down-to-the-east vertical slip of 2.56 ± 0.3 m for Event Z_g. Subtracting this from the minimum scarp height of 7.3 ± 0.1 m on FZ4 yields 4.7 ± 0.5 m of net vertical slip for Event Z_g. We recognize that this is unusually large for a normal-slip earthquake, however we also emphasize that this estimate appears to be a minimum as we believe we have adequately accounted for back-tilting and all antithetic faulting, and our scarp height estimate for FZ4 is a minimum.

Event Y_g – Stratigraphic displacements, fault terminations, buried scarp free faces, and associated colluvial wedge/fissure-fill deposits on faults FZ4, AFZ5 and AFZ6 provide compelling evidence for this penultimate surface-faulting event in the graben (Figures 7 and 8; Plates 3, 4, 5 and 11; and Table 6). Event Y_g occurred shortly after deposition of Unit 6t, a very dark organic-rich debris flow. Reworking of this deposit into Units FC4Y_g, FCA5Y_g, and FCA6Y_g has resulted in distinctly dark colluvial wedges with blocks of organic-rich colluvium (Plates 3, 5 and 11). Although an unknown portion of the colluvial wedge on FZ4 was subsequently eroded away by graben-parallel channels that deposited Units 6u and 6v, a portion of the buried free-face were still preserved (Plate 3), and indicates that the scarp that formed during Event Y_g on FZ4 was at least a few meters high (see additional discussion below). Differential throw of 0.5 ± 0.2 m (Table 6) on the main splay of AFZ1 at st. 226 m, and preservation only locally of a small block of Unit 6t on the downthrown side of the fault (Plate

11) strongly suggests that AFZ1 was also active during Event Y_g, even though we did not observe any associated fault scarp colluvium along AFZ1, perhaps because it was eroded away by channels. The colluvial wedge on AFZ5 was partially eroded into by the channel 6v, and then was subsequently faulted during Event Z_g . We measure an average differential throw of 0.9 ± 0.3 m for Event Y_g on AFZ5 (Table 6). Along AFZ6 the geometry of Unit FCA6Yg is more like a fissure-fill than a wedge-shape. Two ambiguities are associated with the interpretation of Event Y_g on AFZ6. First, because units that post-date Event Y_g and predate Event Z_g (Units 6u, 6v and 6x) are not present along AFZ6, it is possible that this deformation was actually associated with Event Z_g and not Event Y_g. However, because the associated colluvial wedge and fissure fill lies directly on Unit 6t, we believe the deformation is most likely associated with Event Y_g. The second ambiguity is regarding the correlation of Unit 6s (or 6t?), a debris flow in the footwall of AFZ6 (Plates 5 and 6). This dark gray brown silty gravel with cobbles has some characteristics of both units: dark and less silty matrix like Unit 6t, but coarse with more cobbles and some carbonate in the matrix like Unit 6s (cf., detailed descriptions in Appendix A). However, it turns out that this uncertainty has a negligible effect on the estimated displacement on AFZ6 for Event Yg, which likely is about 0.5 to 0.6 m regardless of how it is estimated (Table 6).

The 2 σ range of the age distribution for Event Y_g is 1,100 to 1,800 cal B.P., and is best constrained by maximum limiting ages from samples MM-RC25a and MM-RC25b, and the minimum-limiting age from sample MM-RC13b (Figures 7, 8 and 9). Our preferred age estimate of 1,610 cal B.P. (Figure 8) allows for a minimal amount of soil development (≈100 years) after deposition of Unit 6t (minimum age of MM-RC25a is about 1,710 cal B.P.). We allow this time for some soil development because it seems most likely that the charcoal fragments of Roseacea in MM-RC25a (Appendix B) were part of the original debris flow deposit versus being incorporated into the soil horizon after deposition as wild rose bushes are present on the t2 terrace in Big Slide Canyon (Figure 4), but are not currently present at our site. Rounding to the nearest half-century, our analysis indicates an age of 1,600 (1,100 to 1,800) cal B.P. for surface faulting Event Y_g in our trench.

Our Event Y_g is quite a bit younger than the penultimate event identified by Lund et al. (1991) and although the ages do overlap at 2σ, we do believe that the two events most likely do not correlate. This may initially appear problematic, but Lund et al.'s (1991) age determination of 2820 (2690 to 2970) cal B.P. for their penultimate event is based on radiocarbon samples entirely from the MS trenches (over 1 km to the south), and it is important to note that these trenches only partially exposed the main fault scarp (lower third). We believe that Lund et al.'s penultimate event in the MS trenches most likely correlates to our next oldest earthquake, Event X_g (discussed below), and perhaps Event Y_g was not exposed in the MS trenches. As no ages were obtained from the MN trenches and we could not directly correlate older stratigraphy in our trench to that in the MN trenches, we cannot be certain that the penultimate event exposed in the MN trenches correlates to our Event Y_g or not, however it seems likely given the shallow depth of their trenches and that the evidence they found for the penultimate event is along structures we believe correlate along strike to our AFZ5, which had 0.9 ±0.3 m of throw in the Megtrench (Table 6). Thus, although we believe it is most likely that our Event Y_g is a newly recognized event on the Provo segment, it may possibly correlate to Lund et al.'s (1991) penultimate event.

Similar to Event Z_g, estimates of the net vertical slip that occurred during Event Y_g can be made using the height of the buried scarp free face along FZ4. Unfortunately there is additional

uncertainty due to only partial preservation of the free-face, and because it has been subsequently faulted during Event Z_g. After removing 7.3 m of slip associated with Event Z_g on FZ4 to reconstruct the free face and colluvial wedge of Event Y_g, we measure a minimum scarp height for Event Y_g on FZ4 of 2.5 to 4.2 m. However, backtilting and antithetic faulting must be subtracted from this to estimate the net vertical slip for Event Y_g. Cumulative down-to-the-east throw for both Events Z_g and Y_g can be measured on the top of Unit 6t. This cumulative down-to-the-east throw is 4.52 m (assuming 6s lies in the footwall of AFZ6) to 4.64 m (assuming Unit 6t lies in the footwall of AFZ6). Subtracting the net vertical down-to-the east slip of 2.56 ± 0.3 m for Event Z_g (discussed previously above) yields 2.02 ± 0.06 m of net vertical down-to-the east slip in the graben for Event Y_g. Subtracting this from the estimated minimum scarp height on FZ4 yields a minimum net vertical slip for Event Y_g of 0.5 to 2.2 m. Even though this is a minimum estimate, it seems reasonable that the net slip for Event Y_g appears to have been less than that for Event Z_g, because the measured total down to the east displacement on antithetic faults for Event Y_g is about 20% less than that measured for Event Z_g.

Event X_g – Compelling evidence for this antepenultimate faulting event in the graben comes from: (1) associated colluvial wedge/fissure-fill deposits along FZ4, AFZ2 and AFZ6 (Figure 7; Plates 11 and 5); (2) associated buried scarp free-faces preserved along AFZ2 and AFZ6; (3) stratigraphic offsets on FZ4 of un unknown amount, and differential offsets of 0.3 ± 0.2 m along AFZ2 and of ≈0.6 ± 0.2 m along AFZ6 (Table 6); and, (4) fault terminations of secondary fault splays at the event horizon along FZ4, AFZ1, AFZ2, and AFZ6 (Plates 5 and 11). Similar to Event Y_g, post-event channels (e.g., Unit 6u) appear to have significantly eroded into the colluvial-wedge deposits along the main fault (Unit $FC4X_g$) and AFZ2 (Unit $FCA2X_g$) (Plate 11). However, in contrast to Event Y_g, the associated scarp free-face along FZ4 was not preserved for Event X_g, and so we cannot directly estimate the net vertical slip for this event.

The maximum limiting age for Event X_g comes from sample MM-RC40 from Unit 6s, a tan silty debris flow, which directly underlies all colluvial wedge deposits associated with this event (Figure 7). Minimum limiting ages are from Unit 6t (samples MM-RC25a and MM-RC25b), which directly overlies Unit $FCA6X_g$, and likely was overlying the colluvial wedges along FZ4 and AFZ2 as well, but was nearly all eroded away by younger channels. However, a small block of Unit 6t(?) seems to have been preserved overlying Unit $FC4X_g$ between secondary fault splays adjacent to FZ4 (Plates 3 and 4). Unfortunately, maximum and minimum limiting ages do not tightly constrain the age for Event X_g and the modeled 2 σ age range is large at 1,870 to 4,470 cal B.P. (Figures 8 and 9). This is somewhat surprising as Unit 6t directly overlies Unit 6s, wherever there are no intervening colluvial wedge deposits, and there is no soil development evident anywhere on Unit 6s. We suspect that perhaps the age of the detrital charcoal sample MM-RC40 may be a bit older than the actual age of deposition of Unit 6s, possibly due to reworking of older charcoal into the deposit. However, with only one sample from this unit, this is highly speculative, and so for lack of a better constraint, we choose the mean of the distribution at 3,200 cal B.P. as our preferred age, which also equals the median, and acknowledge that our rounded age estimate of 3,200 (1,850 to 4,450) cal B.P. for Event X_g is poorly constrained.

Given the large age uncertainties, we believe that our Event X_g most likely correlates with the penultimate event previously identified and dated as 2820 (2690 to 2970) cal B.P. in the MS trenches by Lund et al. (1991). Alternatively, it is possible that Event Y_g correlates to the

penultimate event in the MS trenches and then Event X_g would be an older, previously unrecognized event on the Provo segment.

Event W_g – Strong evidence for this fourth youngest faulting event in the graben comes from: (1) a colluvial wedge along AFZ5 (Unit FCA5W_g on Figure 7 and Plate 12); (2) differential offsets of 0.3 ±0.05 m along AFZ3, and of 1.1 ± 0.4 m along AFZ5 (Table 6); (3) the termination of fault splays of AFZ3 at the top of a buried soil associated with this event horizon (Figure 7 and Plate 11); and, (4) terminations of secondary faults along AFZ5 at this event horizon (Plate 12).

We note that unlike the three youngest faulting events in the graben, FZ4 does not appear to have been active during Event W_g (Figure 7). Unit 6q directly overlies the event horizon and is suspiciously only present locally adjacent to FZ4 (Plate 11), and so we examined this unit thoroughly to investigate if it was a possible colluvial wedge. We concluded it was most likely channel alluvium because of its density, moderate sorting, tabular channel shape, and stratification of clast fabric that uniformly parallels the lower contact (Appendix A). Unit 6q also lacked any evidence of a fissure-fill or "heal" immediately adjacent to FZ4, or any blocks or even intraclasts that are abundant in all the other colluvial wedge deposits along FZ4. It is possible that colluvial wedge deposits along FZ4 were completely eroded away by channels, but as the underlying Unit 6p does not appear to have been eroded (it actually thickens considerably toward FZ4), this seems unlikely. Additionally, there are no associated fault terminations on secondary splays along FZ4 for Event W_g, like are evident for Events Z_g, Y_g, and X_g. Thus, we believe it is most likely that FZ4 was not active during Event W_g, and that other footwall fault(s) were active as the principal down-to-the-west structures during this event. Indeed, we believe that Event W_g likely correlates to the youngest faulting events on FZ2 and FZ3, which is discussed further in the *Footwall* section below.

Unfortunately, the sample that would provide the best maximum limiting age for Event W_g (MM-RC39 from Unit 6p, Plate 11), was too small to provide an age (Table 4). Additionally, the problems with sample MM-RC38 likely being invasive due to bioturbation and the reason for disregarding its age were already discussed. Thus, sample MM-RC21 from Unit 6k provides the best reliable maximum-limiting age for Event W_g, and sample MM-RC40 from Unit 6s provides the best minimum-limiting age (Figure 7). Surprisingly, these samples constrain the 2 σ range for Event Wg to be fairly narrowly between 4,410 and 4,980 cal B.P., with our preferred age at 4,760 cal B.P. based on the approximate midpoint of the peak of the modeled distribution, which minimizes overlap between maximum and minimum-limiting ages (Figures 8 and 9). This relatively narrow 2 σ range is somewhat surprising because we expected a longer time between the constraining ages. This is implied by the soil developed on Unit 6k, and the deposition of intervening Units 6p, FCA5Wg, and 6r (Figure 7). Regardless, the age of Event Wg is fairly well-constrained to be about 4,750 (4,400 to 5,000) cal B.P., rounded to the nearest half-century.

Event V_g(?) – Suggestive evidence for this oldest faulting event in the graben comes from differential offsets of 0.5 ± 0.1 m (Table 6) and fault terminations at the top of Unit 6d along AFZ4, differential offsets of 0.1 m on AFZ3.5, and differential tilting of Units 6a through 6d west of AFZ4 (Plate 18). Indeed, it appears that AFZ4 was only active during this oldest graben event. Although the main strand of AFZ4 continues as a fracture up into overlying Units 6i-j, 6k, and 6p, this fracture does not appear to displace these units (Plates 12 and 18). Thus, it appears

that just a fracture opened up on AFZ4 during Event W_g, but no measureable slip occurred on AFZ4 during this later event.

We observed no differential offsets along AFZ5 or AFZ6, indicating that these faults were not active during Event V_g(?). However, west of AFZ5, Units 6a through 6d do appear more tilted to the west than overlying units. For example, the base of unit 6b slopes an average of 8° to the west, whereas the top of unit 6i-j slopes 5° to 6° westward. After Event V_g(?), Units 6a through 6d were apparently eroded into by graben-parallel channels east of AFZ4, which deposited Units 6e through 6h (Plates 17 and 18). Thus, we do not know if faults FZ4, AFZ1, AFZ2, or AFZ3 were active during Event V_g(?).

It is noteworthy that we query our correlation of Units 6i-j(?) east of AFZ1 because this unit changes character east of st. 50 m, becoming coarser and more bioturbated, and the buried soil is missing from the top of the unit (Plate 17 and Appendix A). We originally thought that the soil on the top of Units 6i-j had been stripped away by the graben-parallel channels that deposited Units 6l through 6m (Plate 17). However, in retrospect, it is possible our Unit 6i-j(?) correlation is incorrect and that this brown gravelly silt with clay and cobbles is actually a colluvial wedge along FZ4 associated with Event V_g(?). Unfortunately, due to large boulders in the floor of the slot trench, the base of Unit 6i-j(?) immediately adjacent to FZ4 was never completely exposed. An erroneous correlation of Units 6i-j(?) on the downthrown side of AFZ1 would explain why the apparent throw measured on the top of Units 6i-j across AFZ1 is anomalously smaller by about a half of a meter than the throw measured on overlying units (Table 6). If Unit 6i-j(?) is actually a different unit, this might also explain why the large krotovina truncated by the fault at st. 49 m has no apparent counterpart on the other side of the fault (Plate 17). Thus, it is possible but remains uncertain as to whether FZ4 was active during Event V_g(?), and the evidence for this event remains only suggestive.

Event V_g(?) occurred shortly after Unit 6d was deposited and sample MM-RC12 provides the best maximum-limiting age for this event (Figure 7). Sample MM-RC21 from Unit 6k provides the best minimum-limiting age for Event V_g(?), but it is noteworthy that Units 6e through 6i-j were all deposited and a soil formed after the event and before deposition of Unit 6k, and so this minimum constraint is not close. To help address this, we added a zero boundary to the OxCal model between Event V_g(?) and the MM-RC21 date (Figure 8). The modeled 2 σ age range for Event V_g(?) is 5,090 to 6,080 cal B.P. (Figures 8 and 9). Our preferred age of 5,700 cal B.P. is based on the peak of the Event V_g(?) distribution (Figure 9). Rounding to the nearest half-century, our age analysis indicates that Event V_g(?) occurred about 5,700 (5,100 to 6,100) cal B.P.

2.2.1.2 Footwall

In the footwall the trench exposed three additional significant west-dipping fault zones, FZ1 through FZ3, all east and upslope of the main fault, FZ4 (Figure 6). Each of the footwall faults was generally coincident with a significant bevel on the main scarp. FZ1 had an associated slope angle of 41°, FZ2 had an associated slope angle of 49°, and FZ3 had an associated slope angle of 46.5°. This is in comparison to an average slope on the main scarp of 35°, and a maximum slope angle of 59.5° associated with FZ4. Due to the associated very large breaks in slope, we had suspected from the scarp profile that there might be additional faults near the locations of FZ2 and FZ3. However, the existence and location of FZ1 was a little more problematic to predict as

there were numerous bevels on the main scarp with slope angles between 36° and 40° that were nearly as prominent as the one associated with FZ1. However, these bevels did not turn out to be associated with faults. Indeed, given that FZ1 was actually buried by over 7 m of younger fan alluvium (Units 5c, and 5h through 5s on Plates 2, 8, and 16), it is actually surprising that there is any geomorphic signature to FZ1 preserved, but perhaps it is because this oldest footwall fault is also the most easternmost fault and very near the main fault scarp crest.

Stratigraphic units exposed in the footwall include older and younger fan alluvium and several colluvial wedge deposits along each of the footwall faults. Detailed descriptions of these units are included in Appendix A, whereas Figure 9 schematically shows the relation of these units to the footwall faults and associated faulting event horizons. As previously mentioned, the colluvial wedge deposits are labeled according to the fault they are associated with, and which surface-faulting event that they correlate to on that fault (e.g., Unit FC1Z on Figure 9 is colluvium associated with Event Z_{FZ1}, the youngest surface-faulting event on FZ1). The older fan alluvium includes Units 3a through 3g, 4a, and 4b/4bb (Figure 9, Plates 15 and 16), and generally correlates to af2 deposits on Figure 4. These deposits range in age from 15,110 to 10,730 cal B.P. (Table 4). As previously mentioned, due to more overall difficulty in correlating units across footwall faults, we used single letters for designating deposits on the upthrown side of FZ2, whereas double letters show probable correlative units between FZ2 and FZ3, and triple letters designate probable correlative units between FZ3 and FZ4. The younger fan alluvium includes Units 5aaa through 5s as shown on Figure 9. These deposits range in age from 7950 to <5590 cal B.P. (Table 4), and they generally correlate to af1 deposits on Figure 4.

We found evidence for repeated surface-faulting on each of the footwall faults. However, distinguishing and correlating surface-faulting events on footwall faults was much more difficult than in the graben, and the results presented here for footwall-faulting events are preliminary pending additional analyses. Our preliminary interpretations for the footwall faults suggest stratigraphic, structural and pedologic evidence for at least 3, possibly 6 or more separate surface-faulting earthquakes that are older and occurred before any of the graben faulting events. In addition, we also found evidence for a younger faulting event that occurred on FZ2 and FZ3, Event Z_{FZ2}-Z_{FZ3}, which we believe correlates to an older graben faulting event, most likely Event W_g. Table 7 shows measurements of stratigraphic throw and differential vertical displacements that could be estimated for each event on each footwall fault. Overall, faulting on footwall faults appears to have generally migrated basinward through time. In the following subsections we discuss the evidence and age for each event on each fault, and then we discuss the possible correlations of events and uncertainties.

Overall, the uncertainties in the number of separate surface-faulting events that occurred on footwall faults are due to several complicating factors. These include: possible slumping on FZ2 and FZ3, difficulties in sometimes correlating fan units across footwall faults, uncertainties as to whether some events on different faults correlate to each other due to overlapping ages, and problems with some radiocarbon ages apparently being out of stratigraphic order perhaps due to bioturbation and the reworking of older detrital charcoal into younger deposits. Additional analyses needed to help reduce the uncertainties include construction of a to-scale retrodeformation sequence of the entire megatrench log, and additional age analyses using the OxCal program to statistically test correlations and anomalous ages. Until these additional analyses are completed, the results presented here for the footwall faults should be considered preliminary.

Event Z_{FZ2} – Stratigraphic offsets, fault terminations, a buried scarp free face, and an associated colluvial wedge deposit provide compelling evidence for this youngest surface-faulting event on FZ2 (Figure 9; Plate 2; Table 7). FZ2 is a distributed zone of faults that is as wide as 6 m in Bench 2 (FZ2.1 to FZ2.6, st. 204 to 210 m on Plates 9 and 10). However, only the main splay, FZ2.1 (st. 203 m on Plate 2), has an associated colluvial wedge (Unit FC2Z). This wedge directly overlies Units 5oo and more distally overlies FC3Zb, and fault terminations along FZ2.2 also occur at the top of Unit 5oo (Plate 2). The top of Unit 5oo shows no soil development and has been significantly eroded into by the scarp eroding back from the free-face associated with Event Z_{FZ3} on FZ3. Unit FC2Z includes a Bk stage I+ to II– buried soil horizon. It is directly overlain by Unit 5ss(?) (Plate 2 and Appendix A), which likely correlates to Unit 5s, but Unit 5s has apparently been eroded from the main scarp crest (between sts. 197 and 202 m) and between st. 212 m and FZ4, probably as a result of uplift on FZ4 during Events Z_g and Y_g.

The average down to the west throw measured across the entire zone for Event Z_{FZ2} is 3.8 ± 0.3 m (Table 7). This is <u>not</u> net-slip as it does not account for any back-tilting, antithetic faulting, or slip on FZ3 if Event Z_{FZ2} correlates to Event Z_{FZ3}. Estimates of net slip are discussed later as they depend on possible correlations with graben events and Event Z_{FZ3}. Additionally, we note that displacements measured in Bench 2 are noticeably less than those measured in Bench 1 (Table 7), perhaps due to along-strike variations as the south wall of Bench 2 is about 4 m north of the south wall in Bench 1. Regardless, displacements on FZ2 for this event are large, as also indicated by the thick, associated colluvial wedge deposit, and the 2.1-m-high buried free-face along FZ2.1 (Plate 2).

The absolute age of Event Z_{FZ2} is poorly constrained and we can only be sure that it is younger than sample MM-RC2 from Unit 5k (Figure 9), i.e., younger than 5350 to 5590 cal B.P. (Table 4). Notably, this is young enough to correlate to one of the graben faulting events. Additionally, structural, stratigraphic, pedologic and geomorphic evidence all suggest that Event Z_{FZ2} correlates to Event Z_{FZ3}, and both of these events correlate to an older graben event, most likely Event W_g, but possibly Event V_g. These preliminary interpretations are discussed further below after the section on Event Z_{FZ3}.

Event Z_{FZ3} – Stratigraphic offsets, fault terminations, a buried scarp free-face, and an associated colluvial wedge deposit provide compelling evidence for this youngest surface-faulting event on FZ3 (Figure 9; Plates 2 and 3; Table 7). Similar to FZ2, FZ3 is a distributed zone of faults, but it is only as wide as 4 m (st. 208 to 212 m in Bench 1 on Plates 2 and 3). However, only the main splay at st. 209.5 m has an associated colluvial wedge (Unit FC3Z on Plates 2 and 3). Also similar to FZ2, the associated colluvial wedge for Event Z_{FZ3} includes a stage I+ to II- (carbonate) Bk horizon, directly overlies Units 5ooo (?), and is overlain by Unit 5ss(?). Additionally, fault terminations along other secondary splays of FZ3 also occur at the top of Unit 5ooo-ppp(?)(Plate 2). In contrast to FZ2, the buried scarp free-face is only 1 m high, however, the eroded scarp extends more than 3.6 m vertically upslope from FZ3 to the colluvial wedge on FZ2 (st. 208.5 m to 203.5 m on Plate 2).

The average down to the west throw for Event Z_{FZ3} measured across the entire zone is 4.1 ± 1.0 m (Table 7). Unfortunately, this estimate is not as robust as that for Event Z_{FZ2}, because correlations for some of the units across FZ3 are somewhat uncertain, most notably Unit 5lll cannot be distinguished as a distinct unit on the downthrown side of FZ3 in Bench 1 and neither can Unit 5ppp, and several of the units change significantly in thickness (Plates 2 and 3). Again,

this throw estimate is not the net slip, and estimates of net slip are discussed in the next section as they depend on possible correlations with graben events and Event Z_{FZ3}.

Similar to Event Z_{FZ2}, the absolute age of Event Z_{FZ3} is poorly constrained and we can only be sure that it is younger than sample MM-RC2 from Unit 5k (Figure 9), or younger than 5350 to 5590 cal B.P. (Table 4). However, if Events Z_{FZ3} and Z_{FZ2} correlate to an older faulting event in the graben, then ages can be more tightly constrained as discussed in the next section.

Correlation of Events Z_{FZ2} and Z_{FZ3} (Event $Z_{FZ2\text{-}FZ3}$) To Graben Events

As previously mentioned, our preliminary interpretation of the structural, stratigraphic, pedologic and geomorphic evidence suggests that Event Z_{FZ2} correlates to Event Z_{FZ3}, and both of these events correlate to an older graben event, most likely Event W_g, but possibly Event V_g(?).

Stratigraphic and pedologic relations suggest that Events Z_{FZ2} and Z_{FZ3} correlate because their respective event horizons stratigraphically correlate at the top of Units 5oo/5ooo-ppp(?) (Figure 9). However, this interpretation is somewhat complicated because Unit 5pp is missing on the downthrown side of FZ2. We suspect that Unit 5pp was overlying Unit 5oo on the downthrown side of FZ2, but this loose, spherical pea gravel exposed on a steep scarp uphill from FZ3 was quickly eroded and reworked into fault scarp colluvium (Plate 2). This interpretation is supported by the distinctive spherical pea gravel found in Units FC3Za and FC3Zb (Appendix A), but needs to be tested by a trench log reconstruction. Pedologic relations also support that Events Z_{FZ2} and Z_{FZ3} correlate because both colluvial wedges (Units FC2Z, FC3Za, and FC3Zb) include a buried Bk horizon that formed on the main fault scarp after Events Z_{FZ2} and Z_{FZ3}, and prior to deposition of Unit 5ss(?). This unit is a distinctly organic rich debris flow that directly overlies the colluvial wedges along both faults. However, it is notable that the distal portion of Unit FC2Z overlies the top of Unit FC3Zb (Plate 2), and so we cannot preclude the possibility that Event Z_{FZ3} is actually slightly older than Event Z_{FZ2}. However, these stratigraphic relations could also result from rapid raveling back of the FZ3 free-face along this very high and steep scarp. Based on all of the evidence, we prefer this interpretation and that Events Z_{FZ2} and Z_{FZ3} correlate, but this needs to be tested in a trench reconstruction. Assuming that these events correlate, the estimated down to the west throw for Event $Z_{FZ2\text{-}FZ3}$, is 7.23 ± 0.7 m as measured on the base of Units 5o/5ooo(?) across both FZ2 and FZ3.

The age overlap of Event $Z_{FZ2\text{-}FZ3}$, with graben faulting events and structural, stratigraphic, and pedologic considerations argue that this event may correlate to an older graben faulting event. It is notable that every event that occurred on FZ4 also had associated slip on multiple antithetic faults in the graben, and given the large amount of down-to-the-west displacement on FZ2 and FZ3 in Event $Z_{FZ2\text{-}FZ3}$, it seems highly likely that some backtilting and/or antitheic faulting also occurred during Event $Z_{FZ2\text{-}FZ3}$ as well.

Furthermore, structural considerations argue that Event $Z_{FZ2\text{-}FZ3}$ more likely correlates to one of the two older graben events, Events W_g or V_g, rather than any of the three youngest graben events where FZ4 was active. Estimated net vertical displacements for Events Z_g and Y_g are already very large, and based on what does remain for the colluvial wedge deposited along FZ4 during Event Xg, displacements for this event were likely very large as well. If Event $Z_{FZ2\text{-}FZ3}$ did correlate to Events Z_g, Y_g or Xg, this would imply respective net vertical displacements of 11.9, 11 and at least 7 m for a single event, and this seems highly implausible. As previously alluded to, our preferred interpretation is that Event $Z_{FZ2\text{-}FZ3}$ correlates to Event W_g, as FZ4 does not appear to have been active during this event.

Stratigraphic and pedologic evidence also supports an older age for Event $Z_{FZ2-FZ3}$. The Stage I+ to II- carbonate accumulation in both Units FC2Z and FC3Z (Appendix A) implies some relative age for these deposits (and the events). However, caution is warranted with making an age interpretation as carbonate can build-up more rapidly on slopes due to strong hydrologic gradients (Michael Machette, USGS, personal communication, September 2003). Regardless, both events predate formation of the Bk horizon and deposition of Unit 5ss(?) (Plate 2), which likely correlates to Unit 5s (Plate 1), and may correlate to Unit 6t in the graben based on many stratigraphic similarities (both are dark, organic-rich, vesicular, silty debris flows that are thicker and more cemented than Unit 6z; Appendix A). This correlation implies that Event Z_{FZ2} is older than 1710 to 1920 cal B.P. and occurred prior to Event Event Y_g**.**

Finally, geomorphic considerations also argue that Event $Z_{FZ2-FZ3}$ is older than Events Z_g or Y_g. Unit 5ss(?) is only preserved between FZ2 and FZ3, and appears eroded into at its western end by the large scarp created during Events Z_g and Y_g (Plates 2 and 3). Indeed, the overall crosscutting relations between, stratigraphic units, soil horizons and the scarp face, suggest the following sequence of events for Event $Z_{FZ2-FZ3}$:

1) deposition of Units 5o and5p sometime after 5350 to 5590 cal B.P.

2) the occurrence of faulting Event $Z_{FZ2-FZ3}$ on FZ2 and FZ3 (most likely with Event W_g)

3) rapid raveling back of the scarp and erosion of Unit 5p upslope of FZ3;

4) deposition of Units FC3Za, FC3Zb, and FC2Z

5) the fault-scarp slope stabilizes and a Bk horizon starts to form

6) Event Xg occurs downslope on FZ4

7) Unit 5s/6t is deposited

8) Event Yg occurs, etc.

This hypothesized sequence needs to be further tested by reconstruction of a composite log for the entire Mapleton trench. If Events Z_{FZ2} and Z_{FZ3} do both correlate with Event W_g, then the estimated net vertical displacement is 5.8 ± 0.7 m (7.23 - 0.3 - 1.1 m). This estimate still appears unusually large for a single event, and it may indeed be a maximum as it does not account for any backtilting that may have occurred between FZ3 and AFZ3.

Event Y_{FZ2} (??) – The only evidence for this suspect event on FZ2 is a possible 0.5 m or more of differential throw on the base of Unit 5c/5cc (Table 7, Plate 16). This displacement estimate is complicated by the complex geometry of FZ2, deposition of Unit 5c/5cc on a steep slope, dramatic changes in the geometry of Unit 5c/5cc across FZ2, and probable slumping that occurred soon after this event. Note that we believe that the somewhat unusual geometry of FZ2 (with multiple shallow listric splays), the backtilting of the contact between Units 5ii and 5hh, and the fault terminations at the top of Unit 5hh (Plate 16) are **not** related to this possible surface-faulting event but rather are evidence for minor slumping along FZ2 that occurred shortly **after** Event Y_{FZ2} (??), between 6460 and 6960 cal B.P. (between ages for samples MM-RC32 and MM-RC-41, Figure 9 and Table 4). Given that Unit 5ii overlies a backtilted buried soil with fault terminations along the downthrown side of FZ2, we thoroughly examined Unit 5ii to investigate if it was actually a colluvial wedge deposit. However, it does not look like fault scarp colluvium, but rather it looks just like Units 5i to the east and Unit 5iii to the west, a grayish to yellowish brown, relatively dense, matrix-supported, cobbley debris flow deposit with

a distinctive homogeneous clayey sandy silt matrix that is mottled with orange iron oxide staining, and includes disseminated charcoal fragments. Thus, we believe that the backtilting and fault terminations at the top of Unit 5hh are non-tectonic and related to slumping that occurred after Event Y_{FZ2} (??). This is supported by the observation that overall there appears to be no differential offset across FZ2 and FZ3 between units 5h/hh/5hhh, 5i/5ii/5iii, 5j/5jj/5jjj, and 5o/5oo/5ooo(?), at least within the large measurement uncertainties (Table 7).

In this regard, we cannot preclude that the differential slip estimated for Event Y_{FZ2} (??) may also be related to slumping, as no colluvial wedge was preserved for Event Y_{FZ2} (?) along FZ2 either. However, it is notable that a considerable amount of section is apparently missing both above and below Unit 5c/5cc on the upthrown side of FZ3 (Plates 15, 16 and 17, Figure 9). Additionally, Unit 5c/5cc/5ccc(?) was clearly deposited on a slope with a soil A horizon developed on it that was variably stripped in places, and Unit 5cc is missing between st. 208 and 210 m, immediately adjacent to FZ2 (Plate 16). Thus, a colluvial wedge may have been deposited after Event Y_{FZ2} (??), but was eroded away. Construction of a retrodeformation sequence from the composite trench log might provide insight into these apparently complex stratigraphic relations and better constrain the possible differential slip of Event Y_{FZ2} (??).

If this event did occur, it occurred after the buried soil formed that underlies Unit 5c and before deposition of Unit 5h, and it likely correlates to Event Y_{FZ3} (?), which is discussed below along with our preliminary interpretation of the event age.

Event Y_{FZ3} (?)– The evidence for this possible event on FZ3 is an apparent 3 m of differential throw on the base of Unit 5cc/5ccc(?), and substantial backtilting toward FZ3 (≥20°) of Unit 5ccc (?) and the underlying buried soil (Table 7, Plates 16 and 17). However, this displacement estimate is complicated by deposition of Unit 5c/5cc/5ccc(?) on a steep slope, changes in the geometry of Unit 5c/5cc/5ccc (particularly across FZ3), the slumping previously discussed that probably occurred on FZ2, and uncertainties in correlating Units 5cc and 5ccc(?). In regard to the latter uncertainty, although Units 5cc and 5ccc(?) are similar (both deposits overlie a buried soil A horizon and have a distinctive charcoal-rich, pinkish-brown silty matrix), and ages suggest that they may correlate, we acknowledge that the correlation of Unit 5cc to 5ccc(?) is ambiguous. There are distinct stratigraphic differences between the two units and it is possible that Unit 5ccc(?) is actually a graben-parallel channel that is reworked from Unit 5cc. Perhaps the most important uncertainty is the incomplete exposure of the event horizon, which was not exposed immediately adjacent to FZ3, so it is not known if there was a colluvial wedge associated with this event.

Regardless, there is a strong case for a significant amount of slip to have occurred on FZ3 sometime after the buried soil on Unit 5bbb and before Unit 5hhh was deposited to create the additional space on the downthrown side of FZ3 where Units 5ddd through 5ggg were deposited, as these units are not present on the upthrown side of FZ3. Additionally, Unit 5ccc(?) does appear significantly backtilted toward the east compared to Units 5c and 5cc (Plates 16 and 17). Again, due to the incomplete exposure at the base of FZ3, we cannot preclude the possibility that the slip and backtilting may have been related to slumping and not tectonic displacement.

Assuming Events Y_{FZ2}(?) and Y_{FZ3}(?) correlate, our preliminary interpretation is that Event $Y_{FZ2\text{-}FZ3}$ (?) occurred sometime after formation of the soil on Unit 5bbb, after 7,470 to 7,580 cal B.P. (age of sample MM-RC20), and before deposition of Unit 5h between 6,770 and 6,960 cal B.P. (age for sample MM-RC41). This age range of 6,770 to 7,580 cal B.P. overlaps with the ages for

all of the five samples from Unit 5c/5cc/5ccc(?), except sample MM-RC 15 (Figure 9 and Table 4), which appears to be anomalously old, possibly due to detrital reworking. Note that additional OxCal analyses and a trench reconstruction to determine if this event occurred prior to or after deposition of Unit 5c may help tighten the age constraints on this event. Regardless, this event is clearly older than any graben faulting events. Minor deformation (warping and small offsets less than 20 cm) may have also occurred on FZ1 during this event. This deformation must post-date deposition of Unit 5c, occurring sometime after 7,020 to 7,120 cal B.P. (age of MM-RC 16; Figure 9 and Table 4).

Event X_{FZ2} – Evidence for this event on FZ2 includes stratigraphic offsets, and an associated colluvial wedge deposit (Unit FC2X) that overlies a slightly backtilted buried soil (Plate 16). Additionally, fault terminations were observed at the top of the buried soil on Unit FC2Wb on the north wall of the trench, but time limitations prevented logging these relations. Although initially Unit FC2X appeared similar to Unit FC1Y (Plate 16), upon closer examination there were several minor stratigraphic differences (Appendix A) and Unit FC2X turned out to be much younger (Figure 9). The wedge-shape of Unit FC2X and its location only present immediately adjacent to FZ2, the presence of intraclasts and a block of debris colluvium, and the strong clast fabric that steepens toward FZ2.2 and is generally steeper than the lower contact of Unit FC2X, all indicate that Unit FC2X is fault-scarp colluvium deposited after Event X_{FZ2} occurred (Plate 16, Appendix A).

Unfortunately, vertical displacements cannot be measured for Event X_{FZ2}. However, the thickness of Unit FC2X indicates a minimum scarp height of about 2.4 m (Plate 16), suggesting relatively large displacements for this event.

Our preliminary interpretation of calendar calibrated ages indicate that Event X_{FZ2} occurred between 8460 and 10,410 cal B.P. (between the ages of samples MM-RC8a and MM-RC45, Figure 9 and Table 4), which slightly overlaps, but is most likely younger than the age of Event Z_{FZ1} (discussed below). Construction of a retrodeformation sequence would help test the spatial viability of Events Z_{FZ1} and X_{FZ2} correlating and additional OxCal analyses would test the likelihood that event ages correlate.

Event Z_{FZ1} – Similar to Event X_{FZ2}, evidence for this youngest event on FZ1 includes stratigraphic offsets and an associated colluvial wedge deposit (Units FC1Z) that overlies a slightly discordant buried soil on an older colluvial wedge deposit (Unit FC1Y) (Plate 16). Termination of a minor fault splay at st. 206 m, within Unit FC1Y, and the associated warping of the top of Unit FC1Y (Plate 16), which is marked by a stone line and buried soil, also provides supporting evidence for the occurrence of Event Z_{FZ1}.

Vertical displacements cannot be measured for Event Z_{FZ1}, but the thickness of unit FC1Z indicates a minimum scarp height of 1.6 m for Event Z_{FZ1}, suggesting relatively large displacements for this event. It is also noteworthy that we did observe about 20 cm of throw on the top of the buried soil formed on Unit FC1Z (along with the base of Unit 5c), but no discrete slip was observed on the top of Unit 5c, or any overlying units, although small fractures extended into the overlying unit 5h. This deformation does postdate Event Z_{FZ1}, but it appears relatively minor and may have been associated with the possible slumping previously discussed that occurred after Event Y_{FZ2} (??), or it may have even been associated with Event $Y_{FZ2\text{-}FZ3}$ (?).

Our preliminary interpretation of calendar calibrated ages for samples MM-RC37 and MM-RC48 (Figure 9 and Table 4) indicate that Event Z_{FZ1} occurred between 10,290 and 11,210 cal

B.P. This age range overlaps substantially with the age for Event W_{FZ2} , and our preferred preliminary interpretation is that these two events correlate with each other (Table 7). Alternatively, as previously mentioned, Events Z_{FZ1} and X_{FZ2} may correlate within the 2 σ range of age uncertainties. Again, construction of a retrodeformation sequence would help test the spatial viability of Event Z_{FZ1} correlating to either and Events X_{FZ2} or W_{FZ2}.

Event W_{FZ2} – Similar to Event X_{FZ2}, evidence for this oldest event on FZ2 includes stratigraphic offsets and associated colluvial wedge deposits (Units FC2Wb and possibly FC2Wa) that overlie a slightly discordant buried soil on older fan deposits (Unit 4b/4 bb) (Plate 16). Characteristics which indicate that Unit FC2Wb is fault-scarp colluvium include: (1) the shape and location of the deposit only adjacent to FZ2; and, (2) a slope-parallel clast fabric that steepens toward FZ2 and is generally steeper than the lower contact, which is somewhat discordant with the upper contact. The origin of Unit FC2Wa is not as clear because shearing (and slumping?) along FZ2.2 has distorted its characteristics and although it is loose and jumbled, it also has a few lenses of well-sorted sands that appear more fluvial-like than colluvial. Still, even if Unit FC2Wa was deposited by a graben-parallel channel, this does not change our interpretation of the occurrence of Event W_{FZ2}, as stratigraphic and pedologic relations, as well as radiocarbon ages, still indicate that Unit FCWa was deposited shortly after the faulting event that created the scarp that Unit FC2Wb was deposited against.

Based on our ages and stratigraphic descriptions Unit 4a may correlate to Unit 3g in the footwall of FZ1, but a rigorous reconstruction of the composite trench log is needed to test this preliminary interpretation. Regardless, vertical displacements cannot be measured for just Event W_{FZ2}, but the combined thickness of units FC2Wa and FC2Wb suggest a minimum scarp height of 1.4 m for Event W_{FZ2}.

Our preliminary interpretation is that the age of Event W_{FZ2} is best constrained as between 10,780 and 11,950 cal B.P. (between the ages of samples RC-MM-10 and MM-RC43). This is disregarding sample MM-RC 11b because it appears to be out of stratigraphic order and may by slightly anomalously young due to bioturbation, which is prevalent in the limited exposure of Unit 4b. As previously mentioned, based on the age constraints, Event W_{FZ2} most likely correlates to Event $Z_{FZ1.}$ However, once again we emphasize that constructing a retrodeformation sequence will provide insights into the likelihood of the various possible correlations.

Event Y_{FZ1} – Similar to Event Z_{FZ1}, evidence for the penultimate event on FZ1 includes stratigraphic offsets and an associated colluvial wedge deposit (Units FC1Y) that overlies a distinctly different gravel deposit (Unit FC1X) with a discordant contact (Plate 16). Several characteristics indicate that Unit FC1Y is fault-scarp colluvium including: (1) the shape and location of the deposit only adjacent to FZ1; (2) a strong slope-parallel fabric that steepens toward FZ1 and is generally steeper than the lower contact, which is somewhat discordant with the upper contact; and, (3) the heterogeneous lithology of the deposit with a lower portion that includes intraclasts, is more jumbled and likely includes debris-colluvium, versus the upper portion which is slope-wash colluvium. Vertical displacements cannot be measured for Event Y_{FZ1}, but the thickness of unit FC1Y suggests a minimum scarp height of 1.2 m for this event.

Event Y_{FZ1} occurred sometime shortly before 11,260 to 11,740 cal B.P., based on the age of sample MM-RC24 (Figure 9 and Table 4). Determining a maximum-limiting age for this event is more problematic. The age of sample MM-RC9 from Unit FC1X appears slightly out of

stratigraphic order and anomalously young (Figure 9), perhaps because it was actually out of place and translocated during faulting or slumping, as this charcoal sample was from a log truncated and sheared to the west along FZ2 (Plate 16). Unfortunately, no other samples directly provide a maximum-limiting age for Event Y_{FZ1}. However, Unit FC1X must be younger than the older fan deposits, Units 3a through 3e in the footwall, which were deposited before faulting on FZ1 initiated, as indicated by their daylighting into the paleoscarp created by uplift on FZ1 during Events Z_{FZ1}, Y_{FZ1}, and X_{FZ1} (Plates 15 and 16). Note that overlying Units 3f and 3g may also predate faulting on FZ1, but their relation to the paleoscarp is not as clear. Thus, we interpret that sample MM-RC33 from Unit 3e (Figure 9) provides the most reliable (but perhaps not the closest) maximum limiting age of 12,840 to 13,040 cal B.P. (Table 4) for the occurrence of Event Z_{FZ1}. In summary, our preliminary interpretation is that Event Y_{FZ1} occurred between 11,260 and 13,040 cal B.P., with a preferred age closer to the minimum. Constructing a retrodeformation sequence and further analyses of ages using OxCal, might better constrain the timing of this event.

Event X_{FZ1} – The evidence for the oldest event on FZ1 includes stratigraphic offsets and a probable associated colluvial wedge deposit (Units FC1X), however, the base of this unit (and the associated event horizon) is not exposed (Plate 16 and Figure 9), so the evidence for this event is not as strong as for younger events on FZ1. However, Unit FC1X is distinctly different from, and is in abrupt contact with the overlying Unit FC1Y. We also could not correlate Unit FC1X with any older fan units in the footwall (Units 3a through 3g). Unit FC1X does appear similar to Unit FC2Wa, but it is coarser and is in fault contact with Unit FC2Wa to the west. The similarities could be because Unit FC2Wa was reworked from Unit FC1X. Alternatively, if Unit FC1X does correlate to Unit FC2Wa, it would imply that Events X_{FZ1} and W_{FZ2} correlate, which we cannot preclude (Table 7). However, a possible alternative interpretation for Unit FC1X, which we cannot preclude due to its limited exposure, is that Unit FC1X is actually a graben-parallel channel deposit, but even so, a faulting event on FZ1 would necessarily still have predated Unit FC1X to create the space for this deposit as no correlative deposit can be identified on the upthrown side of FZ1.

We could not estimate displacements for Event X_{FZ1} and because the base of Unit FC1X was not exposed, we could not even estimate a minimum scarp height for Event X_{FZ1} based on colluvial wedge thickness. The age of this event is also poorly constrained as between 11,260 and 13,040 cal B.P. (the ages of samples MM-RC24 and MM-RC33, Figure 9 and Table 4), the same minimum- and maximum-limiting ages as for Event Y_{FZ1}. Event X_{FZ1} is obviously older than Event Y_{FZ1}, but the lack of soil development on the top of Unit FC1X suggests that these events may have occurred relatively closely together in time.

2.2.2 Soil Pits

Figure 4 shows the locations of the three soil pits (SP1, SP2 and SP3), and Figgure 6 shows schematic logs of the exposures. Except for Units SP3a and SP3b at the base of SP3, all of the units exposed in the soil pits are interbedded, debris flows and stream alluvium that appear to be relatively young (i.e., af1 deposits). These included a distinctive, dark, organic-rich, vesicular debris flow that was exposed at the top of all three pits (Units SP1c, SP2f and SP3e) and contained the modern soil. This deposit appeared very similar to, and may correlate to, Unit 6z exposed in the trench. In contrast, Units SP3a and SP3b exposed in the base of SP3 included a buried soil, with a Btk horizon, developed on loess and colluviated loess deposits (Table 5).

Radiocarbon analysis of charcoal from the loess indicates an age of 13,230 to 13,480 cal B.P. (sample MM-RC3 in table 4) for these deposits. Thus, the buried soil in SP3 appears to mark the contact between overlying af1 deposits and underlying, older af2 deposits. Additionally, the age of sample MM-RC3 correlates to the age of sample MMRC-35 from Unit 3d in the trench (Figure 9, Plate 16 and Table 4). This suggests that the buried soil in SP3 may correlate to the buried soil partially preserved on Unit 3g at the eastern end of the trench (Plate 15, Figure 9). Furthermore, radiocarbon ages for charcoal samples from older fan deposits recovered in Borings B1 and B2 range from 9710 to 12,900 cal B.P. (data not included in this report), and although additional analyses are still needed to better determine specific correlations and displacements, we are hopeful that these data will provide long-term slip rates at the Mapleton site.

Table 3

UTM Coordinates (NAD 27, Zone 12, CONUS) for the Mapleton Megatrench, Soil Pits, and Boreholes

Feature	Northing (m)	Easting (m)
Trench SW corner	4,439,838	451,912
Trench SE corner	4,439,798	452,022
Soil Pit SP1	4,439,837	451,710
Soil Pit SP2	4,439,858	451,607
Soil Pit SP3	4,439911	451,523
Borehole B1	4,439,819.6	451,926.4
Borehole B2	4,439,726.0	451,758.7
Borehole B3	4,439,997.0	451,690.2

Table 4
Radiocarbon Analyses for the Mapleton Megatrench

Field Sample No. (CAMS Lab No.)[1]	Unit	Material	Location	Comment	$\delta^{13}C$[2]	C^{14} Age[3] (yr B.P.)	Calendar Calibrated Age[4] (cal B.P.)
MM-RC1 (99536)	**Unit FC4Z** - fault-scarp colluvium of Event Z_g on FZ4	Charcoal (large)	Bench 1-HW of FZ4 (Plate 3)	From organic-rich horizon (A thin) in silty gravels, slopewash below dark vesicular mudflow	-25.0	380 ± 35	320 to 400 (0.38) 410 to 510 (0.62)
MM-RC2 (99539)	**Unit 5k** - Dark brown cobbley debris flow	Detrital charcoal (large)	Bench 2-FW (Plate 8)	Predates Events Z_{FZ2} and Z_{FZ3}, postdates Z_{FZ1}	-25	4,775 ± 35	5,350 to 5,360 (0.02) 5,460 to 5,590 (0.98)
MM-RC3 (99542)	**Unit SP3a** - Loess	Detrital charcoal (small)	Soil pit SP3 – HW (Figure 6)	Overlying reworked loess and colluvium (unit SP3b) has buried soil	-24.2	11,510 ± 60	13,230 to 13,480 (1.0)
MM-RC4 (99538)	**Unit 5m** - Dark brown debris flow	Detrital charcoal	Bench 2-FW (Plate 8)	From tan silty vfs bed within cobbley debris flow	-23.0	4,975 ± 35	5,610 to 5,760 (0.93) 5,830 to 5,870 (0.07)
MM-RC5a	**Unit 5m** - Chocolate dark brown debris flow	Detrital charcoal (small)	Bench 2-FW (Plate 8)	Back-up of MM-RC5b		Not analyzed	
MM-RC5b (114585)	**Unit 5m** - Chocolate brown debris flow	Detrital charcoal (medium)	Bench 2-FW (Plate 8)	Cf. to MM-RC4	-25	4,965 ± 40	5,600 to 5,760 (0.94) 5,830 to 5,870 (0.06)
MM-RC6 (99537)	**Unit 6z** - Dark vesicular mudflow	Charcoal	Bench 1-HW (Plate 4)	From thin and discontinuous organic-rich horizon that postdates Event Z_g	-25	275 ± 40	0 to 5 (0.01) 160 to 170 (0.01) 280 to 470 (0.98)
MM-RC7 (99535)	**Unit 6z** - Dark vesicular mudflow	Charcoal	Bench 1-HW (Plate 4)	Postdates Event Z_g (interbedded within Unit $FC4Z_g$)	-24.9	215 ± 35	0 to 30 (0.15) 130 to 220 (0.48) 260 to 320 (0.36)
MM-RC8a (106744)	**Unit FC2X** - Fault scarp colluvium of FZ2b	Detrital charcoal (very small)	Slot-FW (Plate 16)	Postdates Event X_{FZ2}. May correlate to MM-RC48.	-25	7,850 ± 90	8,460 to 8,980 (1.0)
MM-RC8b (99540)	**Unit 5cc** - Orange mottled debris flow	Detrital charcoal (small)	Slot-FW (Plate 16)	May correlate to MM-RC14, 15, and 16	-24.9	6,285 ± 40	7,080 to 7,100 (0.01) 7,150 to 7,310 (0.99)
MM-RC9 (99541)	**Unit FC1X** – Sub-rounded gravels in HW of FZ1, likely fault scarp colluvium	Charcoal (large)	Slot between FZ1 and FZ2a (Plate 16)	Test if Event X_{FZ1} correlates to Event W_{FC2} cf. to MM-RC43	23.3	9,670 ± 35	10,810 to 10,840 (0.03) 10,860 to 10,960 (0.23 11,070 to 11,210 (0.74)
MM-RC10 (114586)	**Unit 4a** - Organic-rich pod in indurated gravels	Charcoal	Slot-FW (Plate 16)	Oldest unit between FZ2a and FZ2b cf. to MM-RC34 in Unit 3g	-25	10,085 ± 35	11,400 to 11,830 (0.98) 11,920 to 11,950 (0.02)
MM-RC11a	**Unit 4b** - Buried soil	Charcoal	Slot-FW (Plate 16)	Back-up for MM-RC11b		Not analyzed	
MM-RC11b (107195)	**Unit 4b** - Buried soil	Charcoal	Slot-FW (Plate 16)	Provides better maximum-limiting age on Event W_{FC2} than MM-RC11a	-24.7	9,550 ± 30	10,730 to 10,890 (0.46) 10,930 to 11,080 (0.54)
MM-RC12 (106083)	**Unit 6d** - Mudflow in HW of AFZ6	Large charcoal	Slot-HW (Plate 19)	In mudlfow above black and below pea gravels, in HW of AFZ6	-24.5	5,305 ± 50	5,940 to 6,210 (1.0)
MM-RC13a (116403)	**Unit FC4Y** - fault-scarp colluvium	Small charcoal	Bench 2-HW (Plate 11)	Post-dates Event Y_g and closely predates Event Z_g	23.7	590 ± 35	540 to 650 (1.0)
MM-RC13b (114587)	**Unit FC4Y**- fault-scarp colluvium	Small charcoal	Bench 2-HW (Plate 11)	Post-dates Event Y_g (from block in colluvial wedge)	-25	1,130 ± 35	960 to 1,140 (1.0)

Field Sample No. (CAMS Lab No.)[1]	Unit	Material	Location	Comment	$\delta^{13}C$[2]	C^{14} Age[3] (yr B.P.)	Calendar Calibrated Age[4] (cal B.P.)
MM-RC14 (114588)	**Unit 5c** – Mudflow	Large detrital charcoal	Slot-FW (Plate 16)	Overlies FZ1. Should correlate to MM-RC16.	-25	6,335 ± 35	7,170 to 7,330 (0.99) 7,390 to 7,400 (0.01)
MM-RC15 (114589)	**Unit 5c** – Mudflow	Detrital charcoal	Slot-FW (Plate 16)	Overlies FZ1. Cf. to MM-RC14.	-25	8,815 ± 45	9,690 to 9,960 (0.77) 9,980 to 10,150 (0.23)
MM-RC16 (106742)	**Unit 5c** - Slopewash overlying FZ1	Large detrital charcoal	Slot-FW (Plate 16)	Postdates most faulting on FZ1. Should correlate to MM-RC14 and 15; may correlate to MM-RC8b.	-20.4	6,230 ± 30	7,020 to 7,120 (0.36) 7,140 to 7,250 (0.64)
MM-RC17 (114700)	**Unit 5aaa** - Silty very fine sand	Detrital charcoal	Slot-FW (Plate 17)	Oldest sample in FW adjacent to FZ4	-25	6,970 ± 35	7,700 to 7,870 (0.94) 7,890 to 7,920 (0.06)
MM-RC18	**Unit 5aaa** - Silty very fine sand	Detrital charcoal	Slot-FW (Plate 17)	Back-up of MM-RC17		Not analyzed	
MM-RC19 (114701)	**Unit 5bbb** - Buried soil under channel	Charcoal	Slot-FW (between FZ3 and FZ4) (Plate 17)	Back-up of MM-RC20	-25	7,030 ± 40	7,780 to 7,950 (1.0)
MM-RC20 (107194)	**Unit 5bbb** - Buried soil under channel	Charcoal	Slot-FW(between FZ3 and FZ4) (Plate 17)	To right of MM-RC19	-23.6	6,645 ± 30	7,470 to 7,580 (1.0)
MM-RC21 (106082)	**Unit 6k** - Gravelly silty debris flow	Detrital charcoal	Slot-HW (Plate 17)	From above weakly dev. Ak/Bk. Predates Event X_{graben}.	-25	4,380 ± 40	4,850 to 5,050 (1.0)
MM-RC22	Krotovina in FZ4 shear zone below FC4X	Invasive charcoal	Bench 2-HW (Plate 11)	Unsheared krotovina along FZ4 (younger than Event X_g?)		Not analyzed	
MM-RC23 (114702)	**Unit 6z** - Burn (baked) horizon at base of dark vesicular mudflow	*In situ* charcoal	Bench 1-HW (Plate 5)	Overlies MRE wedge on AFZ5. Cf. to MM-RC6 and MM-RC7	-25	120 ± 35	10 to 150 (0.63) 180 to 280 (0.37)
MM-RC24 (114703)	**Unit FC1Y** - Colluvium of FZ1	Detrital charcoal	Slot-FW (Plate 16)	Cf. to MM-RC37. Postdates Event Y_{FZ1}	-25	10,000 ± 60	11,260 to 11,740 (1.0)
MM-RC25a (116398)	**Unit 6t** - Buried A horizon on dark debris flow below Unit FCA5Y	Charcoal fragment of Rosceaceae[5]	Bench 1-HW (Plate 5)	Closely predates Event Y_g on AFZ5	-24.8	1,845 ± 30	1,710 to 1,860 (1.0)
MM-RC25b (123543)	**Unit 6t** - Buried A horizon on dark debris flow below Unit FCA5Y	Two charcoal fragments of vitrified unidentified hardwood[5]	Bench 1-HW (Plate 5)	Closely predates Event Y_g on AFZ5. From same bulk sediment sample as MM-RC25a.	-25	1,905 ± 35	1740 to 1920 (1.0)
MM-RC26 (106084)	**Unit 6c** - Sandy brown mudflow	Large detrital charcoal	Slot-HW (Plate 19)	In drag folded portion of HW of AFZ6 just east of small shear	-25	6,090 ± 80	6,750 to 7,170 (1.0)
MM-RC27 (116240)	**Unit 6c** - Base of sandy brown mudflow	Medium detrital charcoal	Slot-HW (Plate 18)	Cf. to MM-RC26, same unit, as MM-RC26 but on upthrown side of fault at st. 61 m with differential offset on black	-20.8	6,580 ± 30	7,430 to 7,520 (0.93) 7,530 to 7,550 (0.07)
MM-RC28 (111245)	**Unit 5jjj** - Tan silty debris flow	Large detrital charcoal	Bench 2-FW (between FZ3 and FZ4) (Plate 11)	cf. MM-RC2 and MM-RC31. Reanalyzed.	-25	5,400 ± 35	6,020 to 6,050 (0.03) 6,110 to 6,150 (0.06) 6,170 to 6,290 (0.91)

Field Sample No. (CAMS Lab No.)[1]	Unit	Material	Location	Comment	$\delta^{13}C$[2]	C^{14} Age[3] (yr B.P.)	Calendar Calibrated Age[4] (cal B.P.)
MM-RC29 (116241)	**Unit 5kkk** - Brown mudflow	Large detrital charcoal	Bench 2-FW (between FZ3 and FZ4) (Plate 10)	Provides check on stratigraphic correlations between FZ3 and FZ4	-24.1	5,525 ± 30	6,280 to 6,390 (1.0)
MM-RC30	**Unit 5kkk** - Brown mudflow	Large detrital charcoal	Bench 2-FW (between FZ3 and FZ4) (Plate 10)	Back-up of MM-RC29		Not analyzed	
MM-RC31	**Unit 5h** - Buried A horizon on buff debris flow	Large charcoal	Bench 2-FW of FZ2 (Plate 9)	Top of buff sandy debris flow with orange mottling in FW of FZ2	—	Too small	—
MM-RC32 (106740)	**Unit 5i** - Dark gray brown orange mottled debris flow	Large detrital charcoal	Bench 2-FW of FZ2 (Plate 9)	cf. to MM-RC42 and MM-RC44	-24.0	5,740 ± 30	6,460 to 6,630 (1.0)
MM-RC33 (107197)	**Unit 3e** - Silty interbed in cobbley fan gravels	Small detrital charcoal	Slot-FW of FZ1 (Plate 15)	Unit has lots disseminated charcoal	-25	10,970 ± 60	12,840 to 13,040 (1.0)
MM-RC34 (107196)	**Unit 3g** - Dark fine-grained subunit with intraclasts of reworked A horizon	Small charcoal	Slot-FW of FZ1 (Plate 15)	From intraclast of A horizon in mudflow	-27.3	9,965 ± 30	11,260 to 11,490 (0.87) 11,530 to 11,600 (0.13)
MM-RC35 (116242)	**Unit 3d** - Organic-rich subunit in mudflow	Medium charcoal	Slot-FW of FZ1 (Plate 16)	Compare to MM-RC36	-25	11,540 ± 60	13,250 to 13,540 (1.0)
MM-RC36 (107198)	**Unit 3d** - Organic-rich subunit in mudflow	Large charcoal	Slot-FW of FZ1 (Plate 16)	Collected from same subunit as MM-RC35. Oldest sample in FW of FZ1.	-23.5	12,210 ± 310	13,450 to 15,110 (1.0)
MM-RC37 (106745)	**Unit FC1Y** - A horizon on colluvial wedge of FZ1	Large charcoal	Slot-FW (Plate 16)	Predates Event Z_{FZ1} (youngest significant faulting event on FZ1)	-21.6	9,685 ± 30	10,880 to 10,930 (0.09) 11,080 to 11,210 (0.91)
MM-RC38 (116243)	**Unit 6k** - Debris flow	Medium charcoal	Bench 2-HW (Plate 12)	Likely invasive due to bioturbation	-25	190 ± 35	0 to 30 (0.17) 80 to 110 (0.03) 120 to 230 (0.57) 250 to 300 (0.23)
MM-RC39	**Unit 6p** - Alluvium with buff imbricated cobbles and dark tan silty matrix	Medium charcoal	Bench 2-HW (Plate 11)	Most closely predates Event W in graben	—	Too small	—
MM-RC40 (116244)	**Unit 6s** - Tan silty debris flow below Unit FC4X	Medium detrital charcoal	Bench 2-HW (Plate 11)	Predates Event X_{graben}	-25	4,100 ± 100	4,310 to 4,380 (0.01) 4,390 to 4,860 (0.99)
MM-RC41 (106741)	**Unit 5hh** - Buried A horizon on mudflow	Medium-large charcoal	Slot-FW (between FZ2 and FZ3) (Plate 16)	Cf. to MM-RC31 to test stratigraphic correlation. Closely predates faulting or slide Event Y_{FZ2}.	-22.9	6,020 ± 35	6,770 to 6,960 (1.0)
MM-RC42 (116245)	**Unit 5ii** - Mottled debris flow above buried soil	Medium-large detrital charcoal	Slot-FW (between FZ2 and FZ3) (Plate 16)	Cf. to MM-RC32 to test stratigraphic correlations. Postdates Event Y_{FZ2}.	-25	6,640 ± 50	7,440 to 7,590 (1.0)
MM-RC43 (116246)	**Unit FC2Wa** - Rounded gravels (fault colluvium ?) in HW of FZ2.2	Large detrital charcoal	Slot-FW (between FZ2.2 and FZ3) (Plate 16)	From below white fine sand lens. Cf. to MM-RC9 to check if Event W_{FZ2} correlates to Event X_{FZ1}.	-23.1	9,620 ± 40	10,780 to 11,040 (0.68) 11,050 to 11,170 (0.32)
MM-RC44 (106085)	**Unit 5i** - Dark brown mudflow at top of slot in FW of FZ1	Medium-large detrital charcoal	Slot-FW (Plate 16)	Cf. to MM-RC32 to check stratigraphic correlations	-23.5	5,895 ± 35	6,650 to 6,790 (1.0)

Field Sample No. (CAMS Lab No.)[1]	Unit	Material	Location	Comment	$\delta^{13}C$[2]	C^{14} Age[3] (yr B.P.)	Calendar Calibrated Age[4] (cal B.P.)
MM-RC45 (107192)	**Unit FC2Wb** - Buried A horizon on fault colluvium of FZ2.2	Medium charcoal	Slot-FW (between FZ2.2 and FZ3) (Plate 16)	Closely predates Event X_{FZ2} and postdates Event W_{FZ2}	-25	9,125 ± 45	10,210 to 10,410 (1.0)
MM-RC46 (116247)	**Unit FC2Wb** - Colluvium of FZ2.2	Medium detrital charcoal	Slot-FW (between FZ2.2 and FZ3) (Plate 16)	Cf. to MM-RC45 (not in A horizon like MM-RC45). More closely postdates Event W_{FZ2}.	-23.3	9,675 ± 40	10,800 to 10,960 (0.28) 11,067 to 11,210 (0.72)
MM-RC47 (107193)	**Unit 5ccc** - Openwork cobbley channel	Medium detrital charcoal	Slot-FW (between FZ3 and FZ4) (Plate 17)	Cf. to MM-RC14 and MM-RC16 to check if this correlates to openwork gravel below blue-white	-23.7	6,375 ± 35	7,250 to 7,410 (1.0)
MM-RC48 (106743)	**Unit FC1Z** - Colluvium of FZ1	Small charcoal	Slot-FW (between FZ1 and FZ2) (Plate 16)	Similar but distinctly different from FC2X	-25	9,640 ± 230	10,290 to 11,710 (1.0)

1 All samples analyzed by Michaele Kashgarian at the Center for Accelerator Mass Spectrometry, Lawrence Livermore National Laboratory.

2 $\delta^{13}C$ values are the assumed values according to Stuiver and Polach (1977) when given without decimal places. Values measured for the material itself are given with a single decimal place.

3 Age is in radiocarbon years before 1950 A.D., using the Libby half life of 5568 years, and following the conventions of Stuiver and Polach (1977). Errors are 1σ.

4 Calibrated using CALIB v. 5.0.1 (Stuiver and Reimer, 1993; downloaded 7/25/05 from http://radiocarbon.pa.qub.acuk/calib), a lab error of 1, and age span of 40 years, and the IntCal04 calibration curve (Reimer *et al.*, 2004). Reported with 2σ error and rounded to the nearest decade. Number in parentheses is the probability the age lies within the specified range.

5 Samples extracted from bulk soil sample, pretreated and identified by Kathryn Puseman at PaleoResearch Institute. See Appendix C for complete descriptions.

Table 5

Summary of the Paleoseismic Evidence for Graben Faulting Events[1]

Surface Faulting Event and Age	Main Fault	Antithetic Faults					
	FZ4	AFZ1	AFZ2	AFZ3	AFZ4	AFZ5	AFZ6
Z 500 (350 to 650) cal BP NVTD: 4.7 ± 0.5 m^2	– colluvial wedge – fault terminations – buried free-face – **stratigraphic offsets**	– fault terminations – **stratigraphic offsets**	– colluvial wedge – fault terminations – **stratigraphic offsets**			– colluvial wedge – buried free-face – **stratigraphic offsets**	
Y 1,600 (1,100 to 1,800) cal BP NVTD: 0.5 to 2.2 m^3	– wedge – fault terminations – buried free-face – **stratigraphic offsets**	– **differential offsets** – fault terminations				– colluvial wedge on buried soil – buried free-face – fault terminations – **differential offsets**	– colluvial wedge – buried free-face – **stratigraphic offsets**
X 3,200 (1,850 to 4,450) cal BP	– wedge/fissure-fill – **stratigraphic offsets** – fault terminations	– fault terminations with small offsets on one splay	– colluvial wedge – differential offsets – fault terminations – buried free-face				– fissure-fill/ colluvial wedge – **differential offsets** – fault terminations – buried free-face
W 4,750 (4,400 to 5,000) cal BP NVTD: 5.3 ± 1.4 m^4	Probably not active, possibly eroded	Probably not active, possibly eroded		– differential offsets – fault terminations at soil		– colluvial wedge on buried soil – fault terminations – **differential offsets**	
V (?) 5,700 (5,100 to 6,100) cal BP	Not Exposed	Not Exposed	Probably not active	– differential offset (on AFZ3.5)	– **differential offsets** and tilting 3° to west – fault terminations		

1. **Offsets** shown in **bold** signifies throw ≥ 0.5 m (see Table 6 for detailed measurements).
2. Based on an estimated scarp height of 7.3 ± 0.1 m for FZ4 and subtracting 2.56 ± 0.3 m for backtilting and down-to-the-east throw on all antithetic faults-see text for more details.
3. Based on an estimated minimum scarp height of 2.5 to 4.2 m for FZ4 and subtracting 2.02 ± 0.6 m for backtilting and down-to-the-east throw on all antithetic faults-see text for more details.
4. This estimate assumes that Event $Z_{FZ2\text{-}FZ3}$ correlates to Event W_g and that FZ4 was not active. Based on 6.75 ± 0.8 m of average down-to-the west throw measured across FZ2 and FZ3 (see Table 7) and subtracting 1.4 ± 0.45 m of down-to-the-east throw on AFZ3 and AFZ5 (see Table 6). Does not account for possible backtilting between AFZ2 and FZ3.

Not Active
Active

Table 6
Measured Throw, Calculated Differential Displacements, and Estimated Vertical Slip Per Event for Antithetic Faults

Fault (station location in slot trench)	Marker Horizon	Throw (m)	Vertical Differential Displacements and Slip per Event (m)
AFZ1 (main splay at st. 226 m)	Base of Unit 6w	0.5 ± 0.1	Average throw for Event Z_g = 0.55 ± 0.1
	Base of Unit 6u	0.6 ± 0.1	
	Top of Unit 6s	1.0 ± 0.1	Average throw = 1.05 and differential throw for Event Y_g = 1.05- 0.55 = 0.5 ± 0.2
	Top of Unit 6r	0.8 ± 0.1	
	Base of Unit 6r[a]	1.2 ± 0.3	
	Base of Unit 6q	0.8 ± 0.1	
	Base of Unit 6p	0.8 ± 0.1	
	Base of Unit 6o	0.9 ± 0.1	
	Top of Units 6i-j (?)	0.5 ± 0.1	Anomalously small throw could be due to problematic correlation of Unit 6i-j (?) on downthrown side
AFZ2 (st. 230 m)	Base of Unit 6x	0.6 ± 0.2	Average throw for Event Z_g = 0.7 ± 0.2
	Base of Unit 6v	0.8 ± 0.2	
	Base of Unit 6u	0.7 ± 0.2	
	Top of Unit 6s	1.2 ± 0.2	Average throw = 1.0, and differential throw for Event X_g = 1.0- 0.7 = 0.3 ± 0.2
	Top of Unit 6r	1.1 ± 0.1	
	Top of Unit 6p	1.0 ± 0.1	
	Base of Unit 6p	1.05 ± 0.1	
	Base of Unit 6k	0.8 ± 0.2	
	Base of Units 6i-j	1.0 ± 0.1	
	Base of Unit 6h	1.0 ± 0.1	
	Base of Unit 6g	1.0 ± 0.1	

Table 6 (continued)
Measured Throw, Calculated Differential Displacements, and Estimated Vertical Slip Per Event for Antithetic Faults

Fault (station location in slot trench)	Marker Horizon	Throw (m)	Vertical Differential Displacements and Slip per Event (m)
AFZ3 (st. 231.5 to 232 m)	Top of Unit 6p	<0.05	Fracture does not extend into overlying Unit 6r
	Base of Unit 6p	0.15 – 0.20	Average throw for Event $W_g = 0.3 \pm 0.05$
	Base of Unit 6k	0.25 – 0.35	
	Base of Unit 6i-j	0.30 ± 0.05	
	Base of Unit 6h	0.30 ± 0.05	
	Base of Unit 6g	0.30 ± 0.05	
	Base of Unit 6f	0.30 ± 0.05	
AFZ3.5 (st. 234 m)	Top of Unit 6s	~ 0.05	Assuming AFZ3.5 connects to the fault in Bench 1 at st. 236.5 m. The average throw for Event $X_g = 0.0.5$ m
	Top of Unit 6p	~ 0.05	
	Top of Unit 6k	0.18 ± 0.02	Average throw = 0.18, and differential throw for Event $V_g = 0.18 - 0.05 \approx 0.13$
	Top of Unit 6i-j	0.18 ± 0.02	
	Top of Unit 6h	0.18 ± 0.02	
	Top of Unit 6g	0.18 ± 0.02	
	Top of Unit 6f	0.18 ± 0.02	
	Top of Unit 6e	~ 0.20	
AFZ4 (st. 235.5 to 236.5 m)	Base of Unit 6i-j	<0.01	Shear crack extends to top of Unit 6p
	Base of Unit 6d	0.5 ± 0.1	Throw for Event $V_g = 0.5 \pm 0.1$
	Base of Unit 6c	>0.5	

Table 6 (continued)
Measured Throw, Calculated Differential Displacements, and Estimated Vertical Slip Per Event for Antithetic Faults

Fault (station location in slot trench)	Marker Horizon	Throw (m)	Vertical Differential Displacements and Slip per Event (m)
AFZ5 (st. 237.5 to 240 m)	FCA5Z_g thickness	0.5 ± 0.2	Estimated vertical slip for Event $Z_g \cong 1.0$ based on 2x colluvial wedge thickess (no markers postdate Event Y_g and predate Event Z_g)
	Top of Unit 6t	1.8 ± 0.2	Average throw = 1.9, and differential throw for Event Y_g = 1.9 – 1.0 = 0.9 ± 0.3
	Base of Unit 6t	1.8 ± 0.2	
	Base of Unit 6s	2.0 ± 0.2	
	Base of Unit 6r[b]	2.0 ± 0.4	
	Top of Unit 6p[b]	3.2 ± 0.5	Average throw = 3.0, and differential throw for Event W_g = 3.0 – 1.9 = 1.1 ± 0.4
	Base of Unit 6p[b]	3.0 ± 0.5	
	Base of Unit 6k[b]	3.0 ± 0.4	
	Base of Unit 6i-j[a]	2.9 ± 0.5	
	Base of Unit 6d[a]	2.9 ± 0.4	
	Base of Unit 6b	3.0 ± 0.4	
AFZ6 (st. 251.5 to 252 m)	Top of Unit 6s (?)	1.0 ± 0.1	Assuming deposit in footwall is Unit 6s, this is throw for both Events Y_g and X_g. Assuming deposit in footwall is Unit 6t then the indicated throw for only Event Y_g is 0.55 ± 0.1
	Top of Unit 6r	0.9 ± 0.2	Average throw is 1.2 and includes slip for two events (Y_g and X_g). Proportioning throw equally yields: Throw Event Y_g =0.6 ± 0.2 Throw Event X_g =0.6 ± 0.2 We did not proportion according to wedge thickness because Unit FCA6 Y_g is primarily a fissure fill
	Top of Unit 6p	1.3 ± 0.2	
	Top of Unit 6k	1.2 ± 0.1	
	Top of Unit 6i-j	1.3 ± 0.1	
	Top of Unit 6d	1.3 ± 0.3	
	Top of Unit 6c	1.5 ± 0.3	
	Top of Unit 6p	1.0 ± 0.3	

Table 7
Measured Throw and Estimated Differential Vertical Displacements Per Event for Footwall Faults

Fault (station location and bench)	Marker Horizon	Throw (m)	Comments/Vertical Differential Displacements and Slip per Event (m)
FZ2 (st. 202 to 207 m in Bench 1)	Base of Units 5o /5oo (within Bench 1)	3.82 ± 0.18	Average throw for Event Z_{FZ2} = 3.8 ± 0.3 m
	Base of Units 5m /5mm (within Bench 1)	3.88 ± 0.12	
	Base of Units 5l /5ll (within Bench 1)	4.0 ± 0.20	
	Base of Units 5k /5kk (within Bench 1)	3.82 ± 0.14	
	Base of Units 5j/5jj (within Bench 2)	3.36 ± 0.24	
	Base of Units 5i/5ii (within Bench 2)	3.0 ± 0.3	Slumping? (0 to 0.8 m differential throw and apparent backtilting with no associated colluvial wedge deposited)
	Base of Units 5i/5ii (Bench 2 to Slot)	4.6 ± 0.25	
	Base of Unit 5h/5hh (within slot)	3.06 ± 0.49	
	Base of Unit 5c/5cc (within slot)	5.1 ± 0.5	Event Y_{FZ2} (??) Possibly ≥0.5 m differential throw

Table 7 (continued)
Measured Throw and Estimated Differential Vertical Displacements Per Event for Footwall Faults

FZ3 (st. 208 to 211 m in Bench 1)	Base of Units 5oo/ 5ooo-ppp(?) (within Bench 1)	3.36 ± 0.16	Average throw for Event Z_{FZ3} = 4.1 ± 1.0
	Top of Units 5ll/ 5lll-kkk(?) (within Bench 1)	4.12 ± 0.28	
	Top of Units 5jj/jjj(?) (within Bench 1)	4.9 ± 0.3	
	Top of Units 5ii/iii (within Bench 2)	4.41 ± 0.39	
	Top of Units 5hh/hhh (within Bench 2)	4.1 ± 0.24	
	Top of Units 5hh/hhh (within slot)	3.62 ± 0.24	
	Base of Unit 5cc/5ccc(?) (within slot)	7.07 ± 0.32	Event Y_{FZ3} (?) Possibly ≈3 m of differential throw and backtilting
Both FZ2 and FZ3	Base of Units 5o/5oo/5ooo-ppp(?) (within Bench 1)	7.19 ± 0.28	Average throw for Event $Z_{FZ2\text{-}FZ3}$ = 6.75 ± 0.8
	Top of 5j/5jj/5jjj (within Bench 1)	6.75 ± 0.64	
	Top of 5i/5ii/5iii (within Bench 2)	7.07 ± 0.48	
	Top of 5h/5hh/5hhh (within Bench 2)	6.35 ± 0.40	

3.1 SURFACE-FAULTING EVENT SUMMARY FOR THE PROVO SEGMENT

3.1.1 Paleoearthquake Summary for the Mapleton Megatrench

The complexity of correlating and summarizing faulting events on 10 different faults in the Mapleton megatrench necessitates distinction of events in the overall summary chronology from events on individual faults. Therefore, for our summary paleoseismic chronology here we use the faulting-event nomenclature suggested by de Polo (2005), with P1 designating the overall youngest paleopearthquake in the Mapleton megatrench, P2 designating the overall penultimate event, and so on.

Preliminary interpretations suggest that the trench revealed structural, stratigraphic, and pedologic evidence for the occurrence of at least 7, probably 10, possibly 11 or more, surface-faulting earthquakes that occurred since 13,040 cal B.P. on the Provo segment. The uncertainty in the number and age of events are all associated with older events (P5 and older). Our summary of the older surface-faulting events (i.e., older than P4) exposed at the Mapleton megatrench site is still preliminary, pending the additional analyses of the footwall faults that are needed as discussed in Section 2.2.1.2. Table 8 shows the events and their ages for our preliminary preferred correlation of the events based on our analysis to date. It implies the occurrence of 10 separate paleoearthquakes since 13,040 cal B.P. We first discuss this scenario and then the alternative minimum (7-event) and maximum (11-event) scenarios.

As discussed in Section 2.2.1.1 and summarized in Table 5, multiple lines of evidence on multiple faults provide compelling evidence for the four youngest paleoearthquakes that occurred at the Mapleton megatrench site, Events **P1** ($\approx Z_g$) through **P4** ($\approx W_g$). The ages of these events (primarily as determined in the graben) are shown in **bold** on Table 8 as these results will not change with additional analyses. Our age analyses for these events indicate that they occurred: **P1**- 500 (350 to 650) cal B.P.; **P2**- 1,600 (1,100 to 1,800) cal B.P.; **P3**- 3,200 (1,850 to 4,450) cal B.P.; and, **P4**- 4,750 (4,400 to 5,000) cal B.P. Evidence for these events includes significant ($\geq$ 0.5 m) stratigraphic and differential displacements, fault terminations, buried scarp free-faces, and colluvial wedges on multiple faults (Table 5). Note that in this preferred scenario, Event P4 includes antithetic faulting on AFZ3 and AFZ5 (i.e., Event W_g), as well as down-to-the-west faulting on **both** FZ2 and FZ3 (i.e., Event $Z_{FZ2\text{-}FZ3}$) of 6.75 m. Although additional analyses will not revise the age of P4, they may result in a revised interpretation of the displacement for this event.

In contrast to the four youngest events, we emphasize that the interpretations for older events (P5 through P10) shown in Table 8 are still preliminary and may change with additional analyses. In our 10-event scenario, Event P5 (?) includes tilting and antithetic faulting of > 0.5 m on AFZ3 and AFZ4 (i.e., Event V_g) that occurred 5,700 (5,100 to 6,100) cal B.P. Furthermore, although it was not completely exposed, possible down-to-the west slip on FZ4 may have resulted in deposition of a colluvial wedge associated with Event P5(?), as previously discussed on p. 2-19. In the 10-event scenario, Event P6 (?) includes down-to- the-west slip on FZ3 (based on ≈3 m of differential offset and backtilting on Unit 5c/5cc/5ccc) and possibly minor faulting on FZ1 and FZ2 that occurred sometime between 6,770 to 7,580 cal B.P. Antithetic faulting is unconstrained for this and all older faulting events. A series of stacked colluvial wedges along FZ1 and FZ2

(Figure 9) provide the primary evidence for Events P7 through P10. In the 10-event scenario, Event X_{FZ2} on FZ2 is interpreted to be younger than Event Z_{FZ1} on FZ1, and Event Z_{FZ1} correlates with Event W_{FZ2} on FZ2 (Table 8). These correlations are primarily based on our age analyses to date and may change with additional analyses, particularly a trench log reconstruction. Preliminary age analyses suggest: Event P7 occurred between 8,460 to 10,410 cal B.P., Event P8 occurred between 10,780 to 11,210 cal B.P, Event P9 occurred between 11,260 to 13,040 cal B.P., and Event P10 occurred sometime before Event P9 and after 13,040 cal B.P. (Table 8).

Table 9 shows the minimum (7-event) and maximum (11 or more-event) scenarios that are permissible given the present uncertainties in the results. Note that other intermediate scenarios are also permissible. Some of the uncertainty in the number of footwall faulting events comes from the complications of apparent slumping along FZ2 and possibly FZ3, but the primary sources of uncertainty come from: incomplete exposure along FZ3 and FZ4 of events older than 6 ka, and how older events on FZ1 and FZ2 may or may not correlate to each other. Regardless, we emphasize that due to the limited exposure along FZ4 and FZ3 (Figures 7 and 9), the older record of paleoearthquakes (between 6 and 13 ka) is incomplete, hence the possibility of more than 11 events. The minimum 7-event scenario assumes that Events V_g(?), Y_{FZ2}(?) and Y_{FZ3}(?) were all non-tectonic and caused by mass-wasting. These events are all queried as their event horizons are only partially exposed, and/or the evidence for them only includes differential offsets and fault terminations, so the evidence is not as strong as for the other events with associated colluvial wedges. Also in the minimum 7-event scenario, Events Z_{FZ1} and X_{FZ2} correlate, and Events Y_{FZ1} and W_{FZ2} correlate, which is possible (but not as likely as the alternative correlation presented in the preferred 10-event scenario) within the 2 σ age range. The maximum 11-event scenario assumes that Events V_g(?), Y_{FZ2}(?) and Y_{FZ3}(?) were all tectonic and that none of the faulting events on FZ1 correlate with faulting events on FZ2 (Table 9).

3.1.2 Paleoearthqauke Correlations With Other Provo Segment Sites

Table 10 compares the results from this study for the 10-event scenario with the timing of surface-faulting earthquakes determined in previous studies on the Provo segment. Note that for the Water Canyon site we recalibrated unpublished radiocarbon ages generously provided by D. Ostenaa (as previously discussed in Section 1.2). Figure 11 compares the ages of the four youngest events at the Mapleton Megatrench (P1 through P4) with the consensus paleoearthquake ages for the central Wasatch fault segments determined by the UQFPWG (Lund, 2005) based on previous paleoseismic studies. Prior to the Mapleton Megatrench, the paleoseismic site on the Provo segment with the longest earthquake record was Hobble Creek, where Swan et al. (1980) found structural, stratigraphic and geomorphic evidence for 6 or 7 surface faulting events that occurred since 13,660 to 14,080 cal B.P.(Table 10). Unfortunately the lack of age constraints on individual events observed at Hobble Creek precludes specific correlations with any of these events to those identified at the Megatrench site. The next longest paleoseismic record on the Provo segment was at the American Fork Canyon site, where Machette et al. (1992) identified four events that occurred since 5.3 to 8.1 ka (Table 10). Correlations between paleoearthquakes identified at the Megatrench site with events identified at other sites on the Provo segment are discussed further below, but are preliminary as OxCal and

Matlab analyses of paleoearthauke age data for the entire Provo segment are being conducted by the Utah Working Group on Earthquake probabilities.

The youngest paleoearthquake, P1, has been identified and dated at most of the sites (Table 10) along the Provo segment (Figure 2). Our estimated age of 500 ± 150 cal B.P. for P1 at the Megatrench site is consistent with the consensus UQFPWG age of 600 ± 150 cal B.P. for this event (Figure 10). The implication that P1 ruptured the entire Provo segment is also supported by mapping and scarp profiling studies (Machette, 1992), and the large observed displacements for this event (DuRoss, 2008), which range from 1.4-3.0 m (Lund et al., 1991) to 4.7 ± 0.5 m (this study). The probability that a paleoearthquake with a 4.7 m displacement would rupture the entire 59-km-long segment is greater than 95% (Biasi and Weldon, 2006).

Of particular interest at the Mapleton Megatrench site is the penultimate paleoearthquake, Event P2, which occurred 1,600 (1,100 to 1,800) cal B.P. This event appears to have not been previously recognized elsewhere on the Provo segment, except perhaps in trench WC2 at Water Canyon (Table 10). Although P2 may correlate with the penultimate events at the Mapleton South and American Fork Canyon, it more likely does not correlate with any events at these sites. Event P2 at the Megatrench resulted in a minimum net vertical tectonic displacement of 0.5 to 2.2 m and had compelling evidence for surface-rupture along faults FZ4, AFZ1, AFZ5 and AFZ6 at the Megatrench site.

However, although the evidence for this event is compelling in the Megatrench, because of several uncertainties the question remains as to whether this event ruptured the entire segment and was missed in the paleoseismic record at other sites for various reasons, or the rupture was localized and did not rupture the entire segment. Assuming a 0.5-m-displacment, the probability that this event ruptured the entire segment is less than 30%, whereas for a 2.2-m-displacment the probability is > 60% (Biasi and Weldon, 2006). Perhaps, event P2 was not explicitly identified in the trenches of Lund et al. (1991) at either the Mapleton north (MN) or south (MS) sites because the penultimate event exposed in the MN trenches was not dated and /or the entire width of the deformation zone was not exposed in the relatively smaller trenches at either site. Perhaps event P2 was not identified at the American Fork Canyon site because trenches at this site also did not transect all of the fault traces. In particular, the easternmost, west-dipping trace that offsets post-Bonneville fan deposits (Machette, 1992) could not be trenched due to landowner restrictions (M. Machette, USGS, personal communication 2005). Or perhaps event P2 was not identified at the American Fork Canyon site because not all of the colluvial wedges exposed along primary faults were dated. The stream cut exposure at the Rock Creek site likely was not deep enough to expose event P2. However, the trench at Rock Creek exposed a1.6-ka debris flow as well as older sediments (Lund and Black, 1998), and yet evidence for a ~1.6-ka event was not observed. Trench WC1 at Water Canyon was likely not deep enough to expose event P2. In contrast, trenches at Hobble Creek and trench WC2 at Water Canyon may have exposed event P2, but age constraints were too poor to identify it explicitly. Thus, because there are plausible explanations of why event P2 has not been previously identified, and because the net vertical slip was 0.5 to 2.2 m at the Mapleton Megatrench site, we believe it is most likely that this event ruptured at least a good portion, if not all, of the Provo segment, but this hypothesis remains to be verified by additional studies at other sites.

Event P3 was identified at several sites along the Provo segment, from American Fork Canyon to Water Canyon, including the Mapleton Megatrench (Table 10). Although the age for P3 at the Megatrench site is poorly constrained at 3,200 (1,850 to 4,500), this is consistent with the better constrained ages at the American Fork Canyon and Mapleton South sites, and the consensus age determined by the UQFPWG of 2,850 (± 650) cal B.P (Figure 10). Displacement for this event was estimated to be 2.2 to 2.7 m at the American Fork Canyon site (Machette et al., 1992), which has a greater than 60% probability that it ruptured the entire segment (Biasi and Weldon, 2006).

Based on an age of 4,750 (4,400 to 5,000) cal B.P. for paleoearthquake P4 at the Megatrench site, this event most likely correlates to the antepenultimate event at the American Fork Canyon site, which was originally interpreted to have occurred at 5,300 (5,000 to 5,600) cal B.P. (Machette et al., 1992), but ongoing OxCal analysis by the WGUEP suggests a slightly younger age. P4 may also have occurred at the WC2 trench site; unfortunately the timing was poorly constrained for the two youngest events at that site. Alternatively, it is possible but less likely that paleoearthquake P5(?) in the Megatrench may correlate to the antepenultimate event at the American Fork Canyon site (Table 10). If so, this would imply that event P4 was not identified at the American Fork Canyon site, perhaps for the same reasons that event P2 was not identified at this site. Either way, the relatively large displacement of 2.2 to 2.7 m for the antepenultimate event at the American Fork Canyon site indicates a greater than 90% probability that this paleoearthquake also ruptured at the Megatrench site (Biasi and Weldon, 2006).

The oldest event identified at the American Fork Canyon site occurred between 5.3 and 8.1 ka and most likely correlates to paleoearthquake P5(?), but may correlate to event P6(?) at the Mapleton Megaterench site (Table 10). If so, this adds another event to our minimum scenario and implies that at least 8 events occurred on the Provo segment since 13 ka.

Finally, all older events identified in the Megatrench cannot be explicitly correlated to events at other sites because they were not exposed or age constraints are lacking at other sites.

3.2 RECURRENCE

Based on the ages of the four youngest events (**P1** through **P4)** that occurred between 500 (350 to 650) and 4,750 (4,400 to 5,000) cal B.P., we calculate a preferred average late Holocene recurrence interval of **1,400** years, and preferred estimates of individual recurrence intervals of 1,100, 1,600, and 1,550 years. These recurrence intervals are overall much shorter than determined by previous studies, and the preferred consensus value of 2,400 years assigned by the Utah Quaternary Fault Parameters Working Group (Table 2). However, our shorter average late Holocene recurrence interval estimate of 1,400 years is similar to average mid to late Holocene intervals of 1,300 to 1,400 years for the adjacent Salt Lake City, Weber, and Brigham City segments (Table 2), and it is more consistent with the prominent Holocene geomorphic expression of the Provo segment (Machette, 1992).

The shorter average late Holocene recurrence interval of 1,400 years is primarily due to identification of the newly recognized paleoearthquake P2 that occurred 1,600 (1,100 to 1,800) cal B.P. at the Megatrench site. Although we believe this event likely ruptured much if not all of the Provo segment, uncertainties remain, and this needs to be verified by additional studies.

For the longer term, based on our preliminary preferred scenario of 10 events we calculate an average recurrence interval of about 1,400 years for the past 13 ka ([13, 040-500]yrs /9 seismic cycles = 1,393 yrs). Similarly, for our minimum 7-event scenario we calculate an average recurrence interval of about 2,100 years ([13, 040-500]yrs /6 seismic cycles = 2,090 yrs), compared to 1,250 years calculated for our maximum 11-event scenario for the past 13 ka. Again, we emphasize that these longer term average recurrence estimates are preliminary and may change with additional analyses. Obviously, the resulting uncertainties in recurrence intervals associated with the range of scenarios would impact probabilistic hazard analyses and hopefully additional analyses can reduce these uncertainties.

3.3 PALEOMAGNITUDES

Table 11 shows our estimates of paleoearthquake magnitudes for the Provo segment based on various input parameters and empirical relations. Expected paleomagnitudes range from M_w 7.0 to 7.4. Estimates based on displacement are higher than those based on length or rupture area, but generally overlap within 1 σ. We bold the estimate of **M_w 7.3** (with 95% confidence limits of **Mw 7.1** to **7.6**), which is based on displacement data and using the empirical relation developed by Hemphill-Haley and Weldon (1999), because we judge this estimate to be the most robust based on the quality of the displacement data, and because the highly arcuate geometry of the Provo segment may bias the estimate based on surface rupture length to underestimate paleomagnitude. The curvilinear trace length of the Provo segment is 69.5 km (Machette et al., 1992), which does yield a slightly higher expected M_w of 7.2, compared to the expected M_w of 7.1 for the straight-line distance of 59 km (Table 11). Additionally, there is the uncertainty as to whether ruptures have extended beyond the segment boundaries, particularly to the south onto the Santaquin section of the Nephi segment. This could also result in an underestimated paleomagnitude. Except the estimates based on rupture area, all of the expected M_w estimates fall within the 95% confidence limits estimated using the Hemphill-Haley and Weldon (1999) relations (Table 11).

3.4 DISCUSSION

The timing of paleoearthquakes for our preliminary preferred 10-event and maximum 11-event scenarios suggests that events have occurred throughout the Holocene and relatively regularly on the Provo segment since 13 ka (cf. Tables 8 and 9). For these scenarios there is no evidence for a period of seismic quiescence or longer earthquake recurrence between 9 and 17 ka, as was interpreted for the long paleoseismic records from megatrench studies on the Brigham City and Salt Lake City segments.

In contrast, for our preliminary minimum 7-event scenario, one might be tempted to interpret that a period of seismic quiescence occurred on the Provo segment between 5 and 10 ka, but this interpretation is unsubstantiated and likely erroneous given the incomplete paleoseismic record along FZ3, FZ4, and all of the antithetic faults for this time period. Additionally, the evidence for the occurrence of an event at the American Fork Canyon site between 5.3 and 8.1 ka would also contradict an interpretation of seismic quiescence on the Provo segment between 5 and 10 ka. Indeed, given the buried footwall faults and previously unrecognized late Holocene event observed in the Mapleton Megatrench, the most significant lesson learned from this study is the

importance of completeness of the paleoseismic record in evaluating fault behavior and earthquake recurrence. We caution that the further back in time that one investigates, the more difficult it is to be confident of a complete paleoseismic record. We speculate that some (many?) of the apparent variations in rates through time that have been reported could be artifacts of an incomplete record. More emphasis on exposing the entire deformation zone and evaluating what periods are missing in the record is needed in future studies.

Table 8. Preliminary summary of preferred scenario of faulting events exposed in the Mapleton megatrench. Darker shading indicates faults were not active during events. Ages are in cal BP with 2 σ ranges. Ages for footwall faulting events are still preliminary and require further analysis. Preferred correlations between faulting events are shown (which suggests 10 events occurred since 13,040 cal BP), but alternative correlations are indicated by dashed lines (e.g., preliminary analysis suggests Event Z_{FZ1} most likely correlates to Event W_{FZ2}, but it could correlate to X_{FZ2} or to neither event on F_{Z2}). See Table 9 for minimum (7) and maximum (11) faulting-event scenarios permissible from alternative interpretations.

Summary Faulting Event: Age [2 σ]	Footwall Faults			Graben Faults							
	FZ1	FZ2	FZ3	FZ4	AFZ1	AFZ2	AFZ3	AFZ4	AFZ5	AFZ6	Graben Event Age
P1: 500 [350 to 650]				Z_g	Z_g	Z_g			Z_g		**500 [350 to 650]**
P2: 1,600 (1,100 to 1,800)				Y_g	Y_g		Y_g		Y_g	Y_g	**1,600 [1,100 to 1,800]**
P3: 3200 [1,850 to 4,450]				X_g		X_g				X_g	**3,200 [1,850 to 4,450]**
P4: 4,750 [4,400 to 5,000]		Z_{FZ2} < 5590	Z_{FZ3} < 5590				W_g		W_g		**4,750 [4,400 to 5,000]**
P5 (?): 5,700 [5,100 to 6,100]				Not Exposed			V_g (?)	V_g (?)			5,700 [5,100 to 6,100]
P6 (?): 6,770 to 7,580	Minor warping and possible slip (<20 cm) 6,770 to 7,020	Y_{FZ2} (??) (just slumping?) 6,770 to 7,580	Y_{FZ3} (?) 6,770 to 7,580								
P7: 8460 to 10,410		X_{FZ2} 8460 to 10,410	Not Exposed								
P8: 10,780 to 11,210	Z_{FZ1} 10,290 to 11,210	W_{FZ2} 10,780 to 11,950									
P9: 11,260 to 13,040	Y_{FZ1} 11,260 to 13,040										
P10: Before P9 and ≤ 13,040	X_{FZ1} 11,260 to 13,040										

Table 9. Preliminary minimum and maximum surface-faulting event scenarios for the Mapleton Megatrench. In the minimum 7-event scenario, differential displacements and tilting associated with Events V_g (?), Y_{FZ2} (?), and Y_{FZ3} (?) are assumed to be non-tectonic and caused by mass wasting. In the maximum 11-event scenario, Events V_g (?), Y_{FZ2} (?), and Y_{FZ3} (?) are assumed to be tectonic, and the events on FZ1 do not correlate with any of the events on FZ2.

Minimum Scenario – 7 Events			Maximum Scenario – 11 Events		
Surface Faulting Event and Age (cal B.P.)	**Correlation of Events**	**Participating Faults**	**Surface Faulting Event and Age (cal B.P.)**	**Correlation of Events**	**Participating Faults**
P1: 500 [350 to 650]	**Z_g**	**FZ4, AFZ1, AFZ2, AFZ5**	**P1: 500 [350 to 650]**	**Z_g**	**FZ4, AFZ1, AFZ2, AFZ5**
P2: 1,600 [1,100 to 1,800]	**Y_g**	**FZ4, AFZ1, AFZ5, AFZ6**	**P2: 1600 [1,100 to 1,800]**	**Y_g**	**FZ4, AFZ1, AFZ5, AFZ6**
P3: 3,200 [1,850 to 4,450]	**X_g**	**FZ4, AFZ2, AFZ6**	**P3: 3150 [1,850 to 4,450]**	**X_g**	**FZ4, AFZ2, AFZ6**
P4: 4,750 [4,400 to 5,000]	**$W_g = Z_{FZ2} = Z_{FZ3}$**	**FZ2, FZ3, AFZ3, AFZ5**	**P4: 4750 [4,40 to 5,000]**	**$W_g = Z_{FZ2}$**	**FZ2, AFZ3, AFZ5**
P5: 10,290 to 10,410	$Z_{FZ1} = X_{FZ2}$	FZ1, FZ2	P5: 5700 [5,100 to 6,100]	$V_g(?) = Z_{FZ3}$	FZ3, AFZ3
P6: 11,260 to 11,950	$Y_{FZ1} = W_{FZ2}$	FZ1, FZ2	P6: 6,770 to 7,580	$Y_{FZ2}(??) = Y_{FZ3}(?)$	FZ2, FZ3
P7: 11,260 to 13,040	X_{FZ1}	FZ1	P7: 8,460 to 10,410	X_{FZ2}	FZ2
			P8: 10,290 to 11,210	Z_{FZ1}	FZ1
			P9: 10,780 to 11,950	W_{FZ2}	FZ2
			P10: 11,260 to 13,040	Y_{FZ1}	FZ2
			P11: After P10 and ≤13,040	X_{FZ1}	FZ1

Table 10

Comparison of Event Ages for the Preliminary 10-Event Megatrench Scenario With Previous Paleoseismic Studies on the Provo Segment[1]

Surface-Faulting Event	**Mapleton Megatrench This Study**	**Entire Segment UQFPWG (Lund, 2005)**	**Mapleton Lund et al. (1991)**		**American Fork Canyon Machette et al. (1992)**	**Rock Canyon (Lund and Black, 1998)**	**Hobble Creek Swan et al. (1980); Schwartz et al. (1983)**	**Water Canyon Ostenaa (1990)[2]**	
			MN	**MS**				WC1	WC2
								After 540 (on Nephi?)[3]	
P1	**500 (350 to 650)**	600 (250 to 950)	600 (520 to 680)*	<1290 (<830 to 1550)*	500 (300 to 700)	650 (550 to 700)	6 or 7 events since Provo delta formed (Provo Phase ended by 13,600 to 14,080)	500 to 900	500 to 2,000
P2	**1,600 (1,100 to 1,800)**	Not recognized	Not dated	Not exposed?	Not exposed or no rupture?	Not exposed		Not exposed	
P3	**3200 (1,850 to 4,450)**	2,850 (2,200 to 3,500)	Not exposed	2,820 (2,690 to 2,970)*	2,650 (2,400 to 2,900)				1,600 to 4,400
P4	**4,750 (4,400 to 5,000)**	5,300 (5,000 to 5,600)			5,300 (5,000 to 5,600)				3,700 to 5,600
P5 (?)	5,700 (5,100 to 6,100)				5.3 to 8.1 ka				
P6 (?)	*6,770 to 7,580*	Considered Incomplete							Not exposed
P7	*8,460 to 10,410*				Not exposed				
P8	*10,780 to 11,210*								
P9	*11,260 to 13,040*								
P10	*Before P9, ≤ 13,040*								

1 All ages are cal B.P. with 2 σ errors unless noted with an *, which are 1 σ errors. Ages in italics are still preliminary pending additional analyses of footwall faults.

2 Based on radiocarbon ages and relations provided by D. Ostenaa, USBR, pers. comm. (1/11/2006) as discussed in Section 1.2. Recalibrated using OxCal 3.10 (Bronk Ramsey, 2001) and IntCal04 calibration curve (Reimer et al., 2004).

3 Evidence for this event is not observed at any Provo sites to the north. This event may be associated with the youngest rupture on the northern Nephi segment, which occurred after 500 (+100, -150) cal B.P. (DuRoss *et al.*, 2008). Therefore, this event was not assigned a separate letter in the overall Provo segment chronology.

Table 11. Paleomagnitude Estimates for the Provo Segment of the Wasatch Fault Zone

Empirical Relation	Input Parameters	Expected M_w [a]
$M_w = 5.08 + 1.16 \times \log(SRL)$; $\sigma = 0.28$ [b] Wells and Coppersmith (1994)-all fault types	SRL = 59 km[c] SRL = 63 km[d]	7.1 7.2
$M_w = 4.40 + 1.52 \times \log(SRL)$ Leonard (2010)-dip-slip plate earthquakes	SRL = 59 km[c] SRL = 63 km[d]	7.1 7.1
$M_w = 4.07 + 0.98 \times \log(A)$; $\sigma = 0.24$ Wells and Coppersmith (1994)-all fault types	A = 59 km x 18.3 km [e] = 1080 km^2	7.0
$M_w = 4.0 + \log(A)$ Leonard (2010)-dip-slip earthquakes	A = 59 km x 18.3 km [e] = 1080 km^2	7.0
$M_w = 6.69 + 0.74 \times \log(D_{max})$; $\sigma = 0.4$ Wells and Coppersmith (1994) -all fault types	D_{max} = 5.73 m [f]	7.3
$M_w = 6.93 + 0.82 \times \log(MD*MVCDS)$[g] **$M_{95max} = 6.93 + 0.82 \times \log[MD/UVCDS)*MVCDS]$[h]** **$M_{95min} = 6.93 + 0.82 \times \log[MD/LVCDS)*MVCDS]$[i]** **Hemphill-Haley and Weldon (1999)**	**MD = 3.56 m [j]** **MVCDS = 0.78 [k]** **UVCDS = 0.44 [k]** **LVCDS = 1.89 [k]**	**7.3** **(M_{95min} = 7.1;** **M_{95max} = 7.6)**
$M_w = ((2/3) \times \log M_o) - 10.7$ [l] Hanks and Kanamori (1979)	d = 3.56 m [m] A = 1080 km^2 $\mu = 3.3 \times 10^{11}$ dynes/cm^2	7.4

a M_w is moment magnitude.

b SRL is surface rupture length measured end to end in km. σ is standard deviation.

c Total length of Provo segment from Machette et al. (1992).

d For Provo segment + Santaquin section of Nephi segment as measured on http://earthquakes.usgs.gov/regional/qfaults/.

e A = rupture area (= length x downdip width). Assumes a 55º fault dip and a maximum seimogenic depth of 15 km.

f D_{max} is maximum surface displacement in meters and is based on 4.7 m of net vertical displacement for event P1 at the Megatrench site, and assuming a 55° fault dip and 100% dip slip.

g MD is the mean surface displacement of a paleoearthquake measured in meters at n sample sites. MVCDS is the mode value combined displacement statistic from Table 1 of Hemphill-Haley and Weldon (1999), and is dependent on n and the percent of the fault length that the n samples cover.

h M_{95max} is the maximum 95% confidence limit for the paleomagnitude estimate. Similar to MVCDS, UVCDS is the upper value combined displacement statistic from Table 1 of Hemphill-Haley and Weldon (1999) and is dependent on n and the percent of the fault length that the n samples cover.

i M_{95min} is the miminum 95% confidence limit for the paleomagnitude estimate. Similar to MVCDS, LVCDS is the lower value combined displacement statistic from Table 1 of Hemphill-Haley and Weldon (1999) and is dependent on n and the percent of the fault length that the n samples cover.

j We estimate a vertical mean displacement of 2.92 m for paleoearthquake P1 calculated from 5 sites along the Provo segment (American Fork Canyon, Hobble Creek, Rock Creek, Mapleton North, and Mapleton Megatrench; for individual estimates see Table 1 of DuRoss, 2008). Assuming a 55° fault dip and 100% dip slip, we then estimate MD = 3.56 m.

k Based on n = 5 sample sites that cover 66% of the fault.

l $M_o = \mu dA$. M_o is seismic moment, μ is shear modulus, A is rupture area, and d is average displacement over A.

m We assume d = MD (see footnote j above). A = 59 km * 18.3 km (assuming a maximum seismogenic depth of 15 km and a 55° fault dip).

Arabasz, W.J., Pechmann, J.C., and Brown, E.D., 1992, Observational seismology and the evaluation of earthquake hazards and risk in the Wasatch Front area, Utah, *in* P.L. Gori and W.W. Hays (eds.), Assessment of Regional Earthquake Hazards and Risk Along the Wasatch Front, Utah: U.S. Geological Survey Professional Paper 1500-A-J, p. D1-D36.

Baker, A.A., 1972, Geologic map of the northeast part of the Spanish Fork quadrangle, Utah: U.S. Geological Survey Open-File Report 72-9, scale 1:24,000.

Biasi, G. P., and Weldon II, R.J., Estimating surface rupture length and magnitude of paleoearthquakes from point measurements of rupture displacement: Bulletin of the Seismological Society of America, v. 96, no. 5, p. 1612-1623.

Buddensiek, M.–L., Sheng, J., Crosby, R., Schuster, G.T., Bruhn, R.L., and He, R., 2007, Colluvial wedge imaging using traveltime and waveform tomography along the Wasatch fault near Mapleton, Utah: Geophysical Journal International, v. 172, p. 686-697.

Bronk Ramsey, C., 2009, Bayesian analysis of radiocarbon dates: Radiocarbon, v.51, no. 1, p.337-360.

Chang, W.-L. and Smith, R.B., 2002, Integrated seismic-hazard analysis of the Wasatch Front, Utah: Bulletin of the Seismological Society of America, v. 92, p. 1904-1922.

Cluff, L.S., Brogan, G.E., and Glass, C.E., 1973, Wasatch fault, southern portion: Earthquake fault investigation and evaluation, unpublished consulting report prepared for the Utah Geological and Mineralogical Survey by Woodward-Lungren & Associates, Project G-12069A, Oakland, California.

Davis, F.D., compiler, 1983, Geologic map of the central Wasatch Front, Utah: Utah Geological and Mineral Survey Map 54-A, scale 1:100,000.

DuRoss, C.B., 2004, Spatial and temporal trends of surface rupturing on the Nephi segment of the Wasatch fault, Utah: Implications for fault segmentation and the recurrence of paleoearthquakes: MS thesis, University of Utah, Department of Geology and Geophysics.

DuRoss, C.B., 2008, Holocene vertical displacement on the central segments of the Wasatch fault zone, Utah: Bulletin of the Seismological Society of America, v. 98, p. 2918-2933.

DuRoss, C.B., Personius, S.F., Crone, A., Olig, S.S., and Lund, W., 2011, Integration of paleoseismic data from multiple sites to develop an objective earthquake chronology: Application to the Weber segment of the Wasatch fault zone, Utah [abs]: Seismological Research Letters (in press).

DuRoss, C., McDonald, G., and Lund, W., 2008, Paleoseismic investigation of the northern strand of the Nephi segment of the Wasatch fault zone at Santaquin, Utah: Utah Geological Survey Special Study 124 (CD).

Forman, S.L., Machette, M.N., Jackson, M.E., and Maat, Paula, 1989, An evaluation of thermoluminescence dating of paleoearthquakes on the American Fork segment, Wasatch fault zone, Utah: Journal of Geophysical Research, v. 94, no. B2, p. 1622-1630.

Gilbert, G.K., 1890, Lake Bonneville: U.S. Geological Survey Monograph 1, 438 p.

Gilbert, G.K., 1928, Studies of Basin-Range structure: U.S. Geological Survey Professional Paper 153, 89 p.

Godsey, H.S., Currey, D. R., and Chan, M.A., 2005, New evidence for an extended occupation of the Provo shoreline and implications for regional climate change, Pleistocene Lake Bonneville, Utah, USA: Quaternary Research, v. 63, p. 212-223.

Hanson, K.L., Swan, F.H., and Schwartz, D.P., 1982, Guidebook to late Pleistocene and Holocene faulting along the Wasatch Front and vicinity – Little Cottonwood Canyon to Scipio, Utah: American Geophysical Union, Chapman Conference on Fault Behavior and the Earthquake Generation Process, Snowbird, Utah, 40 p.

Harty, K.M, Mulvey, W.E., and Machette, M.N., 1997, Surficial geologic map of the Nephi segment of the Wasatch fault zone, eastern Juab County, Utah: Utah Geological Survey Map 170.

Hanks, T.C., and Kanamori, Haroo, 1979, A moment magnitude scale: Journal of Geophysical Research, v. 84, no B5, p. 2348-2350.

Hecker, S., 1993, Quaternary tectonics of Utah with emphasis on earthquake-hazard characterization: Utah Geological Survey Bulletin 127, 157 p., map scale 1:500,000.

Hemphill-Haley, M.A., and Weldon II, R.J., 1999, Estimating prehistoric earthquake magnitude from point measurements of surface rupture: Bulletin of the Seismological Society of America, v. 89, no. 5, p. 1264-1279.

Hylland, M.D., 2007, Paleoseismology of Utah, Volume 15: Surficial-geologic reconnaissance and scarp profiling on the Colliston and Clarkston Mountain segments of the Wasatch fault zone, Box Elder County, Utah - Paleoseismic inferences, implications for adjacent segments, and issues for diffusion-equation scarp-age modeling: Utah Geological Survey Special Study SS-121, 18 p.

Hylland, M.D. and Machette, M.N., 2008, Surficial geologic map of the Levan and Fayette segments of the Wasatch fault zone, Juab and Sanpete Counties, Utah: Utah Geological Survey Map M-229, 38 p., 1 plate.

Keaton, J.R., Currey, D.R., and Olig, S.J., 1993, Paleoseismicity and earthquake hazards evaluation of the West Valley fault zone, Salt Lake City urban area: Utah Geological Survey Contract Report 93-8, 55 p.

Lund, W.R., 2005, Consensus preferred recurrence-interval and vertical slip rate estimates: Review of Utah paleoseismic-trenching data by the Utah Quaternary Fault Parameters Working Group: Utah Geological Survey Bulletin, 134, 109 p.

Lund, W.R. and Black, B.D., 1998, Paleoseismology of Utah, volume 8-paleoseismic investigation at Rock Canyon, Provo segment, Wasatch fault zone, Utah County, Utah: Utah Geological and Mineral Survey Special Studies 75, 41 p.

Lund W.R., Schwartz, D.P., Mulvey, W.E., Budding, K.E., and Black, B.D., 1991, Paleoseismology of Utah, volume 1-fault behavior and earthquake recurrence on the Provo segment of the Wasatch fault zone at Mapleton, Utah County, Utah: Utah Geological and Mineral Survey Special Studies 75, 41 p.

Machette, M.N., 1992, Surficial geologic map of the Wasatch fault zone, eastern Utah Valley, Utah County and parts of Salt Lake and Juab Counties, Utah: U.S. Geological Survey Miscellaneous Investigations Series Map I-2095, scale 1:50,000.

Machette, M.N., Personius, S.F., and Nelson, A.R., 1986, Late Quaternary segmentation and slip-rate history of the Wasatch fault zone, Utah: EOS (Transactions, American Geophysical Union) v. 67, no. 44, p. 1107.

Machette, M.N., Personius, S.F., and Nelson, A.R., 1992, Paleoseismology of the Wasatch fault zone – A summary of recent investigations, conclusions, and interpretations, *in* P.L. Gori and W.W. Hays (eds.), Assessment of Regional Earthquake Hazard and Risk along the Wasatch Front, Utah: U. S. Geological Professional Paper 1500, p. A1-A71.

Machette, M.N., Personius, S.F., Nelson, A.R., Schwartz, D.P., and Lund, W.R., 1991, The Wasatch fault zone, Utah-segmentation and history of Holocene earthquakes: Journal of Structural Geology, v.13, p.137-149.

McCalpin, J.P., 2002, Post-Bonneville paleoearthquake chronology of the Salt Lake City segment, Wasatch fault zone, from the 1999 "Megatrench" site: Utah Geological Survey Miscellaneous Publication 02-7, 37 p.

McCalpin, J.P. and Forman, S.L., 2002, Post-Provo paleoearthquake chronology of the Brigham City segment, Wasatch fault zone, Utah: Utah Geological Survey Miscellaneous Publication 02-9, 46 p.

McCalpin, J.P., Forman, S.L., and Lowe, M., 1994, Reevaluation of Holocene faulting at the Kaysville site, Weber segment of the Wasatch fault zone, Utah: Tectonics, v. 13, p. 1-16.

McCalpin, J.P. and Nelson, C.V., 2000, Long recurrence records from the Wasatch fault zone, Utah: U.S. Geological Survey, National Earthquake Hazards Reduction Program Final Technical Report, Contract No. 99HQGR0058, 61 p.

McCalpin, J.P. and Nishenko, S.P., 1996, Holocene paleoseismicity temporal clustering, and probabilities of future large (M>7) earthquakes on the Wasatch fault zone, Utah: Journal of Geophysical Research, v. 101, p. 6,233-6,253.

McCalpin, J.P., Robison, R.M., and Garr, J.D., 1992, Neotectonics of the Hansel Valley-Pocatello Valley corridor, northern Utah and southern Idaho, in Gori, P.L. and Hays, W.W. (eds.), Assessment of Regional Earthquake Hazards and Risk Along the Wasatch Front, Utah: U.S. Geological Survey Professional Paper 1500, p. G1-G18.

Nelson, A.R., 1992, Lithofacies analysis of colluvial sediments – An aid in interpreting the recent history of Quaternary normal faults in the Basin and Range Province, western United States: Journal of Sedimentary Petrology, v. 63, p. 607-621.

Nelson, A.R. and Personius, S.F., 1993, Surficial geologic map of the Weber segment, Wasatch fault-zone, Weber and Davis Counties, Utah: U.S. Geological Survey Miscellaneous Investigations Series Map I-2199, 1:50,000 scale, 22 p.

Nelson, A.R., Lowe, M., Personius, S., Bradley, L., Forman, S.L., Klauk, R., and Garr, J., 2006, Holocene earthquake history of the northern Weber segment of the Wasatch fault zone, Utah: Utah Geological Survey Miscellaneous Publication 05-8 (CD).

Olig, S.S., Lund, W.R., Black, B.D., and Mayes, B., 1994, Earthquake potential evaluation of the Oquirrh fault zone, Central Wasatch Front, Utah: Utah Geological Survey Open-File Report 308, 46 p.

Olig, S.S., Thomas, P.A., and Wong, I.G., 2001, The use of time-dependent models in probabilistic seismic hazard analysis along the Wasatch Front, Utah [abs]: Seismological Research Letters, v. 72, p. 289.

Olig, S.S., Thomas, P.A., and Wong, I.G., 2005, Time-dependent probabilistic seismic hazard analyses along the Wasatch Front, Utah and the need for longer paleoseismic records (expanded abstract), *in* Proceedings Volume of the Basin and Range Province Seismic Hazards Summit II, Lund, W.R., (ed.), Utah Geological Survey Miscellaneous Publication 05-2, p. 39-40 (variously paginated).

Ostenaa, D., 1990, Late Holocene displacement history, Water Canyon site, Wasatch fault zone (abs.): Geological Society of America Abstracts with Programs, v. 22, p. 42.

Oviatt, C.G., Currey, D.R., and Sack, D., 1992, Radiocarbon chronology of Lake Bonneville, eastern Great Basin, U.S.A. Paleogeography, Paleoclimatology, Paleoecology, v. 99, p. 225-241.

Personius, S.F., 1990, Surficial geologic map of the Brigham City segment and adjacent parts of the Weber and Collinston segments, Wasatch fault zone, Box Elder and Weber Counties, Utah: U.S. Geological Survey Miscellaneous Investigations map I-1979, scale 1:50,000.

Personius, S.F. and Scott, W.E., 1992, Surficial geologic map of the Salt Lake City segment and parts of adjacent segments of the Wasatch fault zone, Davis, Salt Lake, and Utah Counties, Utah: U.S. Geological Survey Miscellaneous Investigations Map I-2106, scale 1:50,000.

Reimer, P.J., Baillie, M.G.L., Bard, E., Bayliss, A., Beck, J.W., Bertrand, C.J.H., Blackwell, P.G., Buck, C.E., Burr, G.S., Cutler, K.B., Damon, P.E., Edwards, R.L., Fairbanks, R.G., Friedrich, M., Guilderson, T.P., Hogg, A.G., Hughen, K.A., Kromer, B., McCormac, F.G., Manning, S.W., Ramsey, C.B., Reimer, R.W., Remmele, S., Southon, J.R., Stuiver, M., Talamo, S., Taylor, F.W., van der Plicht, J., and Weyhenmeyer, C.E., 2004, IntCal04 Terrestrial radiocarbon age calibration, 26-0 ka BP: Radiocarbon, v. 46, p. 1029-1058.

Reimer, P. J., Baillie, M. G. L., Bard, E., Bayliss, A., Beck, J. W., Blackwell, P. G., Bronk Ramsey, C., Buck, C. E., Burr, G. S., Edwards, R. L., Friedrich, M., Grootes, P. M., Guilderson, T. P., Hajdas, I., Heaton, T. J., Hogg, A. G., Hughen, K. A., Kaiser, K. F., Kromer, B., McCormac, F. G., Manning, S. W., Reimer, R. W., Richards, D. A., Southon, J. R., Talamo, S., Turney, C. S. M., van der Plicht, J., & Weyhenmeyer, C. E. (2009). IntCal09 and Marine09 radiocarbon age calibration curves, 0-50,000 years cal BP. *Radiocarbon, 51*(4), 1111-1150.

Schwartz, D.P. and Coppersmith, K.J., 1984, Fault behavior and characteristic earthquakes—examples from the Wasatch and San Andreas fault zones: Journal of Geophysical Research, v. 89, p. 5681-5698.

Schwartz, D.P., Hanson, K.L., and Swan, F.H., III, 1983, Paleoseismic investigations along the Wasatch fault zone – An update, *in* Gurgel, D.K. (ed.), Geologic Excursions in Neotectonics and Engineering Geology in Utah, Geological Society of America Rocky

Mountain and Cordilleran Sections Meeting, Salt Lake City, Utah, Field Trip Guidebook – Part IV: Utah Geological and Mineral Survey Special Studies 62, p. 45-48.

Scott, W.E. and Shroba, R.R., 1985, Surficial geologic map of an area along the Wasatch fault zone in the Salt Lake Valley, Utah: U.S. Geological Survey Open-File Report 85-448, pamphlet, 2 pls., scale 1:24,000.

Smith, R.B. and Arabasz, W.J., 1991, Seismicity of the Intermountain seismic belt *in* D.B. Slemmons, E.R. Engdahl, M.D. Zoback, M.L. Zoback, and D. Blackwell (eds.), Neotectonics of North America: Geological Society of North America, SMV V-1, p. 185-228.

Smith, R.B. and Bruhn, R.L., 1984, Intraplate extensional tectonics of the eastern Basin-Range: inferences on structural style from seismic reflection data, regional tectonics, and thermal-mechanical models of brittle-ductile deformation: Journal of Geophysical Research, v. 89, p. 5733-5762.

Stuiver, M. and Polach, H.A., 1977, Discussion: Reporting of 14C data: Radiocarbon, v. 19, p. 355-363.

Stuiver, M. and Reimer, P.J., 1993, Extended 14C database revised CALIB radiocarbon calibration program: Radiocarbon, v. 35, p. 215-230.

Swan, F.H., III, Schwartz, D.P., and Cluff, L.S., 1980, Recurrence of moderate to large magnitude earthquakes produced by surface faulting on the Wasatch fault zone, Utah: Bulletin of the Seismological Society of America, v. 70, p. 1431-1462.

Wells, D., and Coppersmith, K.J., 1994, New earthquake magnitude and fault rupture parameters, Correlations among earthquake magnitude, rupture length, and fault displacement: Bulletin of the Seismological Society of America, v. 84, p. 974-1002.

Wheeler, R.L. and Krystinik, K.B., 1992, Persistent and nonpersistent segmentation of the Wasatch fault zone, Utah: Statistical analysis for evaluation of seismic hazard: U. S. Geological Survey Professional Paper 1500-B, p. B1-B47.

Wong, I.G. and Olig, S.S., 1998, Seismic hazards in the Basin and Range Province: Perspectives from probabilistic analyses, in Western States Seismic Policy Council, Proceedings Volume, Basin and Range Province Seismic-Hazards Summit, W.R. Lund (ed.), Utah Geological Survey Miscellaneous Publication 98-2, p. 110-127.

Wong, I., Silva, W., Olig, S., Thomas, P., Wright, D., Ashland, F., Gregor, N., Pechmann, J., Dober, M., Christenson, G., and Gerth, R., 2002, Earthquake scenario and probabilistic ground shaking maps for the Salt Lake City, Utah, metropolitan area: Utah Geological Survey Miscellaneous Publication MP-02-05, 50 p. with CD ROM.

Wong, I., Olig, S., Dober, M., Silva, W., Wright, D., Thomas, P., Gregor, N., Sanford, A., Lin, K., and Love, D., 2004, Earthquake scenario and probabilistic ground-shaking hazard maps for the Albuquerque-Belen-Santa Fe, New Mexico corridor: New Mexico Geology, v. 26, p. 3-33.

Zoback, M.L., 1983, Structure and Cenozoic tectonism along the Wasatch fault zone, Utah, *in* D.M. Miller, V.R. Todd, and K.A. Howard (eds.), Tectonics and Stratigraphy of the Eastern Great Basin: Geological Society of America Memoir 157, pp. 3-27.

Appendix A

Lithologic Unit Descriptions

Trench Hanging Wall Stratigraphy (West of Main Fault, FZ4)

Unit 6za – Dark grayish brown (moist: 10 YR 3/2 with 3% mottling of 10 YR 5/4; wet: 2.5 Y 4/2) historic debris flow(s?); poorly-sorted, matrix-supported, gravelly silt with fine sand and some clay (5% cobbles, 25% gravel, 20% sand, 35% silt, 15% clay); clasts primarily quartzite, angular to subangular, randomly oriented, maximum size 20 cm, average size of 2-4 cm; massive; non- to slightly-plastic; low dry strength (no cementation); top of unit marks the ground surface and includes the modern A-horizon, bottom contact is clear to gradual, and wavy; matrix lacks carbonate; moderate roots and root pores; barbed wire observed at multiple locations throughout; deposit present throughout hanging wall but thickest between FZ4 and AFZ2.

Unit 6z – Dark brown (dry: 10 YR 5/3 to 4/3; wet: 10 YR 2/2), organic-rich, vesicular mudflow; poorly-sorted, generally matrix-supported gravelly silt with clay and fine sand (gravel 20%, sand 10%, silt 50%, clay 20%); clasts primarily quartzite with some gravel size red sandstone, angular to subangular, maximum size 8 cm, and average size 2 to 5 cm; generally massive except occasional pockets of clast-supported grave; non- to slightly-plastic; low dry strength (weak cementation); lower contact gradual and wavy; matrix lacks carbonate; localized burn (baked-red) horizon and pockets of abundant charcoal at base; deposit interfingers with slopewash facies of Unit FC4Z; only locally preserved in the trench hanging wall between FZ4 and AFZ2, but Unit 6Z likely correlates to Units SP1c, SP2d, and SP3e exposed in the soil pits, and may be included in the uppermost portion of Unit 5s in the footwall.

Unit 6y – Dark grayish brown channel alluvium; poorly-sorted, generally clast-supported silty sandy cobbley gravel; clasts primarily subangular to subrounded quartzite and sandstone; maximum size is 21 cm; organic-rich deposit similar to Unit 6x, but less matrix and more cobbles; nonplastic; noncemented; lower contact nondistinct to clear; deposit only locally present between AFZ2 and AFZ5.

Unit FC4Z_g – This unusually large wedge-shaped deposit of fault-scarp colluvium associated with the youngest graben event (Z_g) on the main fault (FZ4) consists of two parts: a very coarse-grained grayish brown (dry: 10 YR 5/2) talus-like distal western portion, and a finer grained yellowish brown (dry: 10 YR 5/4 to 10 YR 4/6, darkens upward) proximal slope wash portion to the east. The two facies are distinctly different and are described separately here, but they interfinger in a 1 to 2 m wide zone near the center of the wedge. Unit 6z, a thin, dark, vesicular, debris flow, is also interfingered within the western coarse talus-like facies of Unit FC4Z_g, but it is described separately because it is distinctive and laterally extensive across the site (also exposed in all three soil pits).

Eastern slope wash portion – Interbedded silty sand, gravelly sand, and sandy gravelly cobble layers, with the former two dominating (10% cobbles, 20% gravel, 40 to 60% sand, 20 to 40% silt, trace of clay); clasts are subangular to subrounded quartzite and limestone, showing slope-parallel imbrication that generally steepens toward the east where the deposit buries a 7½-m high scarp free-face of FZ4, forming an abrupt, subvertical contact; lower contact with Unit 6w is sharp to clear; maximum clast size is 33 cm and average size is medium sand; bedding is coarse to indistinct, laterally discontinuous, and slope-parallel; deposit is variably clast to matrix supported and sorting varies between horizons from poor to good; low plasticity and dry strength with no to very weak cementation; many clasts have relict carbonate coatings but deposit overall lacks carbonate accumulation except some weakly cemented sandy layers that efforvesce

violently (ev+); sandy horizons are vesicular; some localized and discontinuous organic-rich horizons with roots; deposit only locally present immediately adjacent to the downthrown side of FZ4; although the evidence for the genesis of Unit FC4Zg overall is irrefutable, it is noteworthy that the eastern proximal slopewash facies and the distal western coarser-grained facies are reversed from their usual slope positions observed along normal faults with the coarser debris facies usually located more proximal to the fault and the slopewash facies either overlying the debris facies or more distally located downslope (Nelson, 1992).

Western talus-like portion – cobbley gravel with sand (2% boulders, 45% cobbles, 30% gravel, 15% sand, 5% silt, trace of clay); clasts are subangular to subrounded quartzite, fewer limestone, and minor sandstone; extreme clast-supported texture with an open-boxwork structure and voids between clasts resulting in a loose deposit that unravels easily from the wall; maximum clast size is 40 cm and average is 5 to 10 cm; clasts weakly stratified (slope parallel) to more heterogenous and lacking bedding downslope; sorting varies from moderate upslope to poor downslope; no cementation, dry strength or plasticity; lower contact generally clear; clasts show occasional relict carbonate coatings but no carbonate evident in matrix; deposit only locally present adjacent to FZ4.

Unit FCA2Z_g – Very dark grayish brown (dry: 10 YR 3/2), organic-rich fault scarp colluvium associated with Event Z_g on the antithetic fault AFZ2; silty gravelly sand with cobbles to sandy gravel with cobbles and silt (10 to 15% cobbles, 30 to 35% gravel, 30 to 40% sand, 10 to 15% silt, trace of clay); clasts are primarily subangular quartzite with a distinct sparsity of limestone; maximum clasts size is 20 cm and average size is medium sand to fine gravel; generally no bedding except some slope-parallel alignment of elongate clasts in the distal portion; low plasticity and no cementation; very poorly sorted and matrix supported; lower contact is clear even though units below (and above) have a similar dark organic matrix; light reaction to HC1 (ev- to e+); pervasive roots, rootlets and vesicles resulting in a distinctive “dingle-berry” texture; deposit includes a small fissure-fill and buries a scarp free face at the top of AFZ2; deposit only present immediately adjacent to AFZ2.

Unit FCA5Z_g – Very dark grayish brown (dry: 10 YR 3/2), organic-rich fault scarp colluvium associated with Event Z_g on the antithetic fault AFZ5; dominantly silty sand with gravel but varies to cobbley gravelly sand with silt (trace of boulders, 10 to 15% cobbles, 20 to 25% gravel, 40 to 50% sand, 10 to 20% silt, trace of clay); clasts are primarily subangular to subrounded quartzite with some limestone and sandstone, maximum clast size is 40 cm and average size is sand to fine gravel; very poorly sorted, generally matrix supported, heterogenous and jumbled in lower portion (debris facies) but parallel alignment of elongate clasts in upper portion, particularly distally (slope-wash facies); low plasticity and no cementation; lower contact clear and includes buried scarp free-face; wedge-shaped deposit that is similar to Unit FCA2Z_g (loose matrix, lacks carbonate and organic-rich, concentration of roots, rootlets, and pores) but lacks “dingle-berry” texture); only present immediately adjacent to AFZ5.

Unit 6x – Dark brown (10 YR 3/2) organic-rich channel alluvium; moderately to poorly-sorted, generally matrix-supported gravelly sandy silt; clasts primarily subangular to subrounded quartzite, sandstone, and some limestone; weakly stratified with pockets of clast-supported gravels; maximum size is 13 cm; non to slightly plastic; noncemented; lower contact is clear and wavy; interfingers with Unit 6w to the west; although clasts do not appear imbricated, morphology suggests that sediment form a graben-parallel channel deposited at the base of the AFZ2 fault scarp just prior to Event Z_g.

Unit 6w – Yellow brown debris flow; poorly-sorted, matrix supported gravelly silt with sand and cobbles; clasts are randomly oriented angular to subangular quartzite and sandstone; maximum size clast is 21 cm, average size is medium gravel; non- to slightly plastic; loose (low dry strength); lower contact clear and wavy; matrix lacks carbonate; deposit only present locally adjacent to FZ4 under Unit FC4Z_g.

Unit 6v – Brown to dark grayish brown graben-parallel channel alluvium; poorly to moderately sorted; clast to matrix supported silty sandy gravel with cobbles; clasts are angular to subangular quartzite and sandstone; weekly stratified and imbricated to the northwest, grades upward (cobbley at base); nonplastic; loose; lower contact is clear to abrupt and wavy; matrix lacks carbonate; only locally present between AFZ5 and FZ4 (deposited after Event Y_g and before Event Z_g).

Unit 6u – Dark grayish brown graben-parallel channel alluvium; moderately sorted, matrix-supported gravelly sand silt; clasts are angular to subangular quartzite and sandstone; weakly stratified; distinctly finer-grained than overlying alluvium (Unit 6v) and underlying debris flow (Unit 6t); non- to slightly plastic; loose; lower contact is clear to abrupt and smooth to wavy; matrix lacks carbonate; deposit is only locally present between FZ4 and AFZ5.

Unit FC4Y_g – Heterogeneous fault-scarp colluvium associated with Event Y_g on the main fault (FZ4), varies in color from pale grayish brown to yellowish brown to very dark grayish brown (dry: 10 YR 4/6 to 3/4); cobbley sandy gravel (<1% boulders, 15 to 20% cobbles, 20 to 30% gravel, 30 to 40% sand, 5 to 10% silt, trace of clay) that also includes large blocks (as big as 66 cm) of underlying Units 6t and possibly 6s; clasts are subangular to subrounded limestone and quartzite, extremely jumbled, with maximum clast size of 70 cm (single limestone boulder) and average size of very coarse sand to gravel; deposit is faulted and only partially preserved, as it is truncated at the top and to the west of st. 221 m, apparently eroded into by overlying channels (Units 6u and 6v); what does remain of Unit FC4Y_g includes a large fissure or "heel" immediately adjacent to the downthrown side of FZ4 (better preserved in Bench 2 than Bench 1); it also buries a partially preserved scarp free-face on FZ4, which is characterized by a sub-vertical abrupt contact that truncates footwall units; very poorly sorted and variably matrix to clast-supported; non- to slightly plastic; matrix is very loose with no to slight cementation (blocks are weakly cemented); some relict carbonate coatings on clasts and matrix in fissure effervesces ev to ev+ to acid; deposit only locally present immediately adjacent to FZ4.

Unit FCA5Y_g – Dark brown (dry: 10 YR 3/3) fault scarp colluvium associated with Event Y_g on the antithetic fault AFZ5; silty gravelly sand (10 to 15% cobbles, 30 to 35% gravel, 30 to 40% sand, 15 to 20% silt); subangular to subrounded quartzite and limestone, maximum clast size is 26 cm and average size is sand to fine gravel; poorly sorted, matrix-supported, and some parallel alignment of elongate clasts, especially in distal portion of wedge; low plasticity and no cementation; abundant organics, roots, rootlets, and root pores; matrix generally lacks carbonate (none to e+ HC1 reaction) but some minor filaments on clast bottoms; lower contact clear and includes buried scarp free-face; deposit is faulted and likely eroded by overlying channel alluvium (Unit 6x) but is generally wedge-shaped and locally only present adjacent to AFZ5.

Unit FCA6Y_g – Very dark grayish brown (dry: 10 YR 3/2), organic-rich, fault scarp colluvium of Event Y_g on antithetic fault AFZ6; silty gravelly sand with cobbles (10 to 15% cobbles, 25 to 30% gravel, 30 to 35% sand, 10 to 20% silt, trace of clay); clasts are dominantly quartzite with some sandstone and limestone, maximum size is 25 cm and average size is sand to fine gravel;

poorly sorted and matrix supported, generally massive but some slope-parallel alignment of elongate clasts; deposit includes a large fissure-fill and smaller wedge-shaped deposit that buries a scarp free face on AFZ5; low plasticity and no cementation (loose); lower contact is clear to indistinct (similar to underlying organic-rich Unit 6t); no HC1 reaction; deposit only locally present adjacent to AFZ6.

Unit 6t – Very dark grayish brown (dry: 2.5 Y 4/3; wet: 2.5 Y 3/1 to 3/2) debris flow; poorly-sorted, generally matrix-supported, gravelly silt with clay and some sand (10% cobbles, 25% gravel, 5% sand, 35% silt, 25% clay); clasts are primarily angular to sub-angular quartzite, next in abundance is fine-grained, gray and yellow-brown calcareous sandstone, dark red (2.5 YR 4/6) sandstone, and cobble-sized bioclastic limestone (with crinoid stems); maximum clast size is 18 cm and average size is 1 to 6 cm; generally massive except occasional pockets of clast-supported gravel; non- to slightly plastic; slightly indurated; lower contact clear and wavy; matrix lacks carbonate; minor rootlets and occasional root pores; deposit is distinctly darker than underlying and overlying units, and has more clay and is more cemented than overlying units; deposit is present between FZ4 and AFZ6 except where locally eroded by channels (Units 6u and 6v) that cut into faults blocks, which were apparently uplifted during Event Y_g; may correlate to Unit 5s in the footwall.

Unit FC4X_g – Brown (dry: 10 YR 5/3) fault scarp colluvium associated with Event X_g on the main fault (FZ4); cobbley sandy gravel (20 to 25% cobbles, 30 to 35% gravel, 25 to 30% sand, 5 to 10% silt, trace of clay); clasts primarily subangular to subrounded limestone and quartzite, randomly oriented, maximum size is 22 cm and average size is coarse sand to fine gravel; heterogenous, poorly sorted and matrix- to clast-supported; none to very low plasticity; slight to no cementation, but distinctly more dense than overlying younger colluvial wedges (Units FC4Y_g and FC4Z_g); lower contact is clear to gradual (wedge rests on a similar-looking unit creating some uncertainty in exact contact location); truncated to the east by FZ4 and eroded at the top by channels (Unit 6v), deposit includes a large, coarse fissure-fill immediately adjacent to FZ4 and a narrow elongate distal wedge, both of which are faulted; matrix shows strong reaction to HC1 (ev+) and some carbonate accumulation on bottom of clasts; deposit only locally present adjacent to FZ4 (more extensive than overlying Unit FC4Y_g, but much less extensive than Unit FC4Z_g).

Unit FCA2X_g – Pale brown (dry: 10 YR 6/3 to 5/3) fault scarp colluvium associated with Event X_g on AFZ2; this colluvial wedge on AFZ2 is very similar in appearance to Unit FC4Z_g, but this matrix is slightly lighter in color; very poorly-sorted, clast to matrix supported, sandy cobbley gravel (trace of boulders, 20 to 25% cobbles, 30 to 35% gravel, 25 to 30% sand, 5 to 10% silt, trace of clay); clasts are subangular to subrounded limestone and quartzite, with a maximum size of 44 cm (single subangular limestone boulder) and an average size of coarse sand to gravel; generally no bedding or stratification except slope-parallel alignment of clasts in distal (easternmost) portion; deposit is heterogeneous, includes blocks of underlying Unit 6s; this wedge-shaped deposit buries a partially preserved free-face of AFZ2, which has been faulted (apparently in Event Z_g); very low plasticity and slightly cemented; highly reactive to HC1 (ev+), some carbonate filaments in matrix and thin discontinuous carbonate coatings on clast bottoms; present adjacent to AFZ2.

Unit FCA6X_g – Brown (dry: 10 YR 5/3) fault scarp colluvium of Event X_g on antithetic fault AFZ6; cobbley gravelly sand with silt (10 to 20% cobbles, 20 to 30% gravel, 30 to 40% sand, 10 to 15% silt); clasts are subangular to subrounded limestone and quartzite; poorly sorted, matrix

supported, and generally massive except some slope-parallel alignment of elongate clasts; low plasticity and slight cementation; deposit is faulted and primarily includes a fissure-fill with a thin colluvial wedge that buries a scarp free-face of AFZ5; lower contact is clear to indistinct (wedge portion overlies a similar looking deposit, Unit 6x); HC1 reaction is low to none (much less carbonate that other correlative colluvial wedge deposits of Event X_g); deposit only locally present immediately adjacent to AFZ6.

Unit 6s – Yellowish olive brown (dry: 2.5 Y 6/6; wet: 2.5 Y 4/3) debris flow; poorly-sorted matrix-supported, gravelly silt with sand and some clay (20% cobbles, 10% gravel, 10% sand, 55% silt, 5% clay); clasts are angular to subangular "sugary" quartzite, dark gray fine-grained sandstone, and some dark red sandstone; maximum clast size is 24 cm and average size is 5 to 10 cm; some stratification in upper half of unit where clasts are concentrated; nonplastic; weakly cemented (medium dry strength); lower contact clear and wavy; moderate HC1 reaction for matrix, some thin carbonate coatings on tops and bottoms of clasts; deposit is present through hanging wall (west of FZ4) but is generally darker and coarser (more clasts) west of AFZ6.

Unit 6r – Gray brown (dry: 10 YR 6/3 to 10 YR 5/3; wet: 10 YR 4/3 to 3/3) debris flow; poorly-sorted, generally matrix-supported gravelly silt with sand and some clay (5% cobbles, 35% gravel, 10% sand, 37% silt, 3% clay); clasts are angular to subangular and carbonaceous, composition is primarily dark gray quartzite, some cobble-sized red sandstone and fine-grained yellow-brown sandstone; maximum clast size is 26 cm and average size is 3 to 6 cm; slight fabric to clasts and localized pockets that are clast-supported; nonplastic; weak cementation (medium dry strength); lower contact is gradual and wavy; moderate HCI reaction for matrix, some thin carbonate coatings on tops and bottoms of clasts; deposit is present throughout hanging wall (west of FZ4).

Unit 6q – Brown (dry: 10 YR 4/3) localized debris flow or channel alluvium; generally poorly sorted with pockets of moderately sorted pea-gravel; variably clast- to matrix-supported, sandy cobbley gravel with silt; clasts are subrounded to subangular dark gray quartzite and sandstone; deposit is generally channel-shaped and uniform in thickness except where it pinches out near st. 228.5; lower contact is clear and wavy; weak and variable stratification with clast fabric paralleling lower contact; nonplastic; weakly cemented; only present within inner graben between FZ4 and AFZ2.

Unit FCA5W_g – Yellowish brown to brownish yellow (dry: 10 YR 5/6 to 6/6) fault scarp colluvium associated with Event W_g on antithetic fault AFZ5; cobbley sandy gravel (20 to 25% cobbles, 30 to 35% gravel, 25 to 30% sand, 5 to 10% silt); subangular to subrounded limestone and quartzite clasts, maximum size is 25 cm and average size is coarse sand to gravel; poorly sorted, matrix supported and no bedding except some slope parallel alignment of elongate clasts; very low plasticity and weakly cemented; wedge-shaped deposit that is coarser and denser than any other colluvial wedge on AFZ5; lower contact clear to indistinct; some carbonate in matrix (ev+ HC1 reaction) and coating on clast bottoms; some root pores and vesicles; deposit only locally adjacent to AFZ5.

Unit 6p – Pale brown (dry: 10 YR 5/3 to 6/3; wet: 10 YR 4/3) dense debris flow; poorly-sorted cobbley silty gravel (20% cobbles, 30% gravel, 10% sand, 37% silt, 3% clay); angular to subangular randomly oriented clasts, primarily dark gray quartzite, some yellowish brown and light reddish brown (2.4 YR 6/3) gravel-size sandstone; maximum clast size is 30 cm and average size is 4 to 7 cm; nonplastic; massive, dense and variably matrix- to clast-supported;

strong HCI reaction to matrix and more continuous carbonate coats on clasts than Unit 6r; slightly moist; deposit is present throughout hanging wall (west of FZ4) and thickens noticeably between AFZ1 and FZ4.

Units 6l through 6o – Pale gray brown to brown, graben-parallel, channel deposits only present between FZ4 and AFZ2; sandy gravels to silty gravels with sands; poorly to moderately-sorted; clast to matrix supported; clasts angular to subrounded; stratification variable (e.g., Unit 6l unstratified versus Unit 6m moderately stratified with distinctive lenses of pea gravel); contacts generally clear and smooth to wavy.

Unit 6k – Brown (dry: 10 YR 4/3; moist: 10 YR 3/3) massive debris flow; poorly-sorted, matrix-supported gravelly silt with clay (5% cobbles, 20% gravel, 5% sand, 55% silt, 15% clay); clasts are randomly oriented, angular to subangular, primarily "sugary" dark gray quartzite with some light redish brown (2.5 YR 6/3) sandstone and yellow (2.5 YR 7/6) sandstone; maximum clasts size is 30 cm and average size is 5 to 7 cm; slightly plastic; very stiff; lower contact is gradual and wavy; matrix shows strong HC1 reaction (carbonate mottling) and carbonate coats on tops and bottoms of many clasts (Stage I – Bk horizon in upper 15 to 20 cm); a weak concentration of darker organics, roots and rootlets form a thin buried A horizon at the top of this unit that is only preserved locally on the downthrown side of AFZ5 (Plate 12) and does not appear evident elsewhere (either on the upthrown side of AFZ5 to the west or east of st. 233 m); some areas are extensively bioturbated, including filled cicada burrows where carbonate has preferentially precipitated; deposit present throughout the hanging wall except between FZ4 and AFZ1 where it was likely eroded away by channels (Units 6l through 6o).

Units 6i and 6j – Brown to dark yellowish brown (dry: 10 YR 5/3 to 5/4; moist [*in situ*]: 10 YR 4/4) debris flow; Unit 6j is the upper portion that generally has less matrix, more gravel, and is darker than Unit 6i; but is only broken out separately at the west end of the slot trench (west of st. 266.5 m); poorly-sorted, generally matrix supported gravelly silt with clay and cobbles (20% cobbles, 15% gravel, 5% sand, 40% silt, 20% clay); clasts are angular to subangular, randomly oriented quartzite, light reddish brown (2.5 YR 6/3) and yellow (2.5 Y 7/6) sandstone, maximum size is 30 cm and average is 3 to 8 cm; massive; non-plastic, dense and stiff; lower contact clear to gradual and smooth; thin discontinuous carbonate coats on clasts and moderately strong HC1 reaction for matrix (but not as strong as Unit 6k); the top includes a weak Bk horizon (Stage I) that appears variably preserved (e.g., apparently stripped by channels east of st. 226 m in the slot trench, and stripped on the upthrown side of AFZ2 west of st. 231 m in Bench 2); deposit present throughout the hanging wall (west of FZ4) but correlation is somewhat ambiguous east of st. 226 m because the top is stripped, and the deposit becomes coarser, less dense, and more bioturbated east of st. 226 m.

Units 6e through 6h – Pale gray-brown to brown, graben-parallel channel alluvium only present between AFZ1 and AFZ4 in the hanging wall within the slot trench: these deposits cut into and unconformably overlie Units 6c and 6d; these units vary from clast- to matrix-supported, from moderately- to poorly-sorted, and from a silty, gravel with sand to a sandy cobbly gravel; bedding also varies with gravel-rich lenses, and units 6h, 6f, and 6e include a coarser, clast-supported basal lag that varies from a pea-gravel to cobbly gravel.

Unit 6d – Tan debris flow only present west of AFZ3 in graben, but similar radiocarbon ages suggest it may correlate to Unit 5j in the footwall; cobbly sandy silty gravel; more homogeneous

than Unit 6c; matrix-supported and poorly sorted, clasts randomly oriented with no bedding; carbonate stringers in matrix.

Unit 6c – Tan channelized debris flow deposits with localized lenses of brown channel gravels and brown mudflows; silty sandy gravel with cobbles and boulders to sandy gravelly silt; generally matrix- supported except gravel lenses; heterogeneous and varying from very poorly to moderately sorted; only present west of AFZ3 in graben; extensively bioturbated toward the east.

Unit 6b – Thin brown mudflow only present west of AFZ4 with a small section eroded from the upthrown side of AFZ5; sandy gravelly silt; matrix-supported, poorly sorted, clasts randomly oriented, carbonate filaments and vesicles present in matrix; lower contact is smooth wavy and conformable; overlying contact with Unit 6c appears disconformable.

Unit 6a – Tan (dry: 2.5 Y 7/3 , in situ moist: 10YR 6/3, wet: 2.5 Y 4/3) "chalky" debris flow; silty, sandy gravel with cobbles (trace of boulders, 15% cobbles, 30% gravel, 25% sand, 20% silt, 10% clay); primarily angular to subangular pale quartzite, maximum clast size is 40 cm and average size is bimodal: fine sand to gravel; massive, poorly-sorted, matrix-supported with randomly oriented clasts; relatively homogeneous but variably bioturbated, increasing to the east; slightly plastic and weakly to non-cemented, matrix effervesces violently (ev); only present west of AFZ3 in the hanging wall.

Trench Footwall Stratigraphy (East of Main Fault, FZ4)

Unit 5s, 5ss(?) – Dark to very dark grayish brown (in situ moist: 2.5 Y 4/2 to 3/2) debris flow; poorly-sorted, matrix-supported, gravelly silt with clay and sand (5% cobbles, 30% gravel, 15% sand, 35% silt, 15% clay); clasts are primarily randomly oriented, angular to sub-angular quartzite, with some red and tan sandstone sandstone; maximum clast size is 13 cm and average size is a few cm; generally massive and non-stratified except occasional pockets of gravel; non- to slightly plastic; slightly indurated; lower contact clear and wavy, forms angular unconformity with underlying units; lacks carbonate; abundant vesicles, roots, rootlets and occasional root pores; deposit is distinctly darker than underlying units; variable thickness (~3/4 m at east end of trench, 0 m at scarp crest , and Unit 5ss(?) is over 1 m on scarp between FZ2 and FZ3, eroded away west of st. 212 m); includes modern A horizon (upper portion includes discontinuous highly vesicular and very dark subhorizon); unit 5ss(?) likely correlates to Unit 5s and both units may correlate to Unit 6t in the hanging wall, uppermost portion may correlate to Unit 6z in the hanging wall, but overall Unit 5s is too thick and indurated to correlate to just Unit 6z alone.

Unit 5r – Grayish brown debris flow; silty sandy cobbley gravel; clasts are angular to subrounded, randomly-oriented quartzite, limestone and sandstone; deposit pinches out or was eroded away west of st. 174.5 m; it includes B_w and weak B_k (Stage I- to I+) soil horizons that apparently developed on the scarp prior deposition of overlying Unit 5s, but were apparently eroded away west of st. 198 m after Event Z_{FZ2-3}.

Unit 5q – Light grayish brown to dark grayish brown heterogeneous channelized debris-flow deposits; gravelly sandy silt to cobbley, silty, sandy gravel; siltier channels inter-fingered with more gravelly channels; daylighting into the main scarp, this unit is only present east of st. 198 m; it includes a buried soil consisting of a B_w and weak B_k (Stage I- to I+) horizons that apparently developed on the scarp prior deposition of overlying Unit 5s, but were apparently eroded away west of st. 198 m after Event Z_{FZ2-3}.

Unit FC2Z – Dark brown to pale brown, heterogeneous, fault-scarp colluvium associated with Event Z_{FZ2} on the footwall fault FZ2; silty cobbley gravel with occasional boulders to cobbley silty gravel with sand (0 to 10% boulders, 20 to 25% cobbles, 35% gravel, 10 to 15% sand, 15 to 20% silt; 5 % clay); clasts are primarily subangular to subrounded quartzite and limestone, maximum clast size is 30 cm and average size is gravel; lower debris-facies portion is very poorly-sorted, heterogeneous, jumbled, loose clast-supported, with some voids; grades to upper (20 to 50 cm) slopewash facies that is poorly sorted, matrix to clast-supported, with some slope-parallel alignment of elongate clasts, especially in distal portion of wedge; moderate to no cementation; no plasticity; thin carbonate coats on clast bottoms and ev+ HCl reaction of matrix indicates stage I+ to II- carbonate accumulation; this deposit buries a 2.1-m-high scarp free-face on FZ2; lower contact is abrupt and smooth to wavy; deposit only present between st. 202 and 204.5 m immediately adjacent to FZ2 on the downthrown side.

Unit FC3Zb – Brown to pale brown, slopewash facies of fault-scarp colluvium associated with Event Z_{FZ3} on the footwall fault FZ3; silty cobbley gravel with sand (25% cobbles, 40% gravel, 10% sand, 20% silt; 5 % clay); clasts are primarily subangular to subrounded quartzite and limestone, maximum clast size is ≈17 cm and average size is gravel; strong slope-parallel fabric

of clasts; generally poorly sorted but pockets of clast-supported, moderately sorted pea gravel, which increases in abundance upslope and appears to be reworked from Unit 5p; moderate to no cementation; no plasticity; thin carbonate coats on clast bottoms and ev+ HCl reaction of matrix indicates stage I+ to II- carbonate accumulation; this deposit buries an elongated eroded free-face that forma a ?? slope , which extends from FZ3 to FZ2 upslope; lower contact is gradational; deposit only present between st. 203 and 212 m generally between FZ2 and FZ3.

Unit FC3Za – Brown to pale brown, fault-scarp colluvium associated with Event Z_{FZ3} on the footwall fault FZ3; sandy cobbley silty gravel (15% cobbles, 40% gravel, 15% sand, 25% silt; 5 % clay); clasts are primarily subangular to subrounded quartzite and limestone, maximum clast size is ≈15 cm and average size is gravel; jumbled, and loose debris faces near base, grades to slopewash with slope-parallel fabric of clasts; poorly sorted, and clast- to matrix-supported; moderate to no cementation; no plasticity; thin carbonate coats on clast bottoms and ev+ HCl reaction of matrix indicates stage I+ to II- carbonate accumulation; this deposit buries a 1.4- to 1.8-m-high scarp free-face on FZ3; it grades conformably into the overlying Unit FC3Zb, which buries the eroded free-face of Event Z_{FZ3}; lower contact is abrupt and smooth to wavy; deposit only present between st. 208 and 211 m immediately adjacent to FZ3 on the downthrown side.

Unit 5p – Grayish brown (10YR 5/2) thin, channel of pea-gravel; silty sandy gravel (65% gravel, 20 to 25% sand, 10 to 15% silt); clasts are distinctively spherical and rounded fine gravel, mostly quartzite, sandstone and some limestone; maximum size is 10 cm; clast-supported, moderately-sorted, somewhat stratified alluvium; pinches out to the east at st. 187.5 m and is truncated to the west by erosion, daylighting into the main scarp at st. 198 m; the upper portion to the west includes a thin A horizon formed on the main scarp; based on the distinctive pea gravel, this unit may correlate to, or be reworked into, Unit 6m in the hanging wall.

Units 5o, 5oo, 5ooo-ppp(?) – very pale brown to pale brown debris flow or package of flows; gravelly sandy silt to sandy silty gravel (5 to 10% cobbles, 20 to 30% gravel, 25% sand, 30 to 35% silt, 5% clay); angular to subrounded clasts of dominantly quartzite with some limestone; maximum clast size is 28 cm and average size is 3-7 cm; poorly sorted heterogeneous deposit that is generally matrix supported with random clast orientations, but lenses of weakly stratified gravels are also evident (in particular lenses of spherical pea gravels in the upper portion of Unit 5ooo-ppp(?); nonplastic and stiff; matrix has moderate to strong HCl reaction (e to e+) and clasts have thin, variable carbonate rinds (reworked?); Unit 5ooo-ppp(?) has more carbonate in the matrix and on clasts; lower contact is clear and wavy; units are present from east end of trench to FZ4 but are disrupted by faulting.

Unit 5n – Pale brown debris flow; sandy silty gravel with cobbles; poorly sorted and generally matrix supported with random clast orientations, but weakly stratified channels with more gravel are also evident; unit is only present from east end of trench to st. 200.5 m where it pinches out against Unit 5o.

Units 5m, 5mm, and 5mmm(?) – Brown to dark brown cobbley debris flow; cobbley sand silty gravel; angular to subrounded clasts of dominantly quartzite (reddish brown and dark gray) with some sandstone and limestone; maximum clast size is 32 cm and average size is 4-9 cm; overall poorly sorted, generally clast supported and stratified, with lenses of sandy silt that contain disseminated charcoal; lower contact is clear and wavy; units are present from east end of trench to FZ4, however Unit 5mmm(?) between FZ3 and FZ4 is anomalously thick and includes more matrix.

Units 5l, 5ll, and 5lll – Thin, very pale brown to pale yellow debris flow (dry: 10 YR 7/4 to 2.5 Y 7/3; wet 10 YR 4/3); gravelly sandy silt (5 % cobbles, 10 to 15% gravel, 20% sand, 55 to 60%silt, 5% clay); subangular to subrounded clasts of dominantly quartzite (some reddish brown) with some yellow sandstone; maximum clast size is 26 cm and average size is 3-6 cm; poorly sorted and matrix supported with random clast orientations; plastic and stiff; matrix has strong HCl reaction (e+) and clasts have thin, variable carbonate rinds (reworked?); lower contact is generally clear and wavy but becomes indistinct west of FZ3; although it is thin, this debris flow deposit provides a distinct marker horizon from st. 178.5 m to FZ3, however between FZ3 and FZ4 the contact between Units 5kkk and 5lll becomes indistinguishable so we mapped the two units together (Unit 5kkk-lll?).

Units 5k, 5kk, and 5kkk – Thick, very pale brown to pale brown debris flow or package of flows (dry: 10 YR 7/4; wet 10 YR 3/3); gravelly sandy silt to sandy silty gravel (5 to 10% cobbles, 25% gravel, 30% sand, 30 to 35% silt, 5% clay); angular to subrounded clasts of dominantly quartzite (reddish brown and dark gray) with some limestone; maximum clast size is 23 cm and average size is 4-9 cm; poorly sorted heterogeneous deposit that is generally matrix supported with random clast orientations, but lenses and pockets of weakly stratified coarser gravels are also evident; nonplastic and stiff; some disseminated pieces of charcoal; matrix has strong HCl reaction (e+) and clasts have thin, variable carbonate rinds; lower contact is gradual and wavy; units are present from east end of trench to FZ4, however between FZ3 and FZ4 the contact between Units 5kkk and 5lll becomes indistinguishable so we mapped the two units together (Unit 5kkk-lll?).

Units 5j, 5jj, and 5jjj –Tan (dry: 2.5 Y 7/3 to 10 YR 6/3; wet: 10YR 4/2 to 4/3) silty debris flow with "chalky" texture; gravelly silt with sand to silty cobbley gravels with sand (trace of boulders, 7-25% cobbles, 13-30% gravels, 15-20% sand, 20-55% silt, 5-10% clay,); dominantly subangular to subrounded quartzite clasts with minor limestone and light reddish-brown (2.5 YR 6/3) fine-grained sandstone, maximum clast size is 35 cm and average size is 4 to 8 cm; massive and clasts are randomly oriented; low to medium plasticity and weakly cemented; some carbonate filaments in matrix and on clasts (iron staining on clasts as well), effervesces violently (ev); although the percentage of gravels and cobbles varies in this unit its matrix and other characteristics are relatively homogeneous and distinctive compared to other debris flows in the footwall and it serves as a marker bed; upper and lower contacts are sharp to gradual and wavy; present throughout the footwall (east of FZ4);this unit appears similar in many respects to Unit 6a in the hanging wall, but the radiocarbon age of 5400 ±35 for MMRC-28 from Unit 5jjj suggests it is actually younger, and may correlate to Unit 6c in the hanging wall.

Units 5i, 5ii, and 5iii – Pale brown to light yellowish brown to dark grayish brown (dry: 10 YR 6/3 to 10 YR 4/6; wet: 10 YR 5/4 to 10 YR 4/2) mudflow that is strongly mottled with iron-oxide straining; cobbly gravelly sandy silt to gravelly silty clay (10 to 20% cobbles, 15 to 25% gravel, 5 to 30% sand, 20 to 40% silt, 15 to 45% clay); clasts are angular to subrounded and include gray limestone, tan calcareous sandstone (with sulfur odor and broken crinoid stems), reddish brown sandstone and tan quartzite; maximum clast size is 32 cm and average size is 6 cm; poorly sorted, matrix supported and generally massive, but locally some weak slope-parallel imbrication of clasts (30° to 35° to east) is evident; slightly plastic and medium stiff to stiff with poor to moderate cementation; many clasts have weathering rinds and discontinuous carbonate coats (reworked?); some carbonate stringers in matrix and effervesces moderately (e); occasional small

pieces of charcoal; lower contact is generally abrupt and wavy; units are only present between st. 199 m and FZ4 in the footwall.

Units 5h, 5hh, and 5hhh – Pale yellow to light olive brown dense debris flow with yellowish brown iron-oxide mottling (dry: 2.5 Y 7/4 to 2.5 Y 5/3 to 10 YR 5/6; wet: 2.5 Y 4/3 to 10 YR 4/3 to 10 YR 4/4); cobbley, gravelly silt with sand to cobbley sandy silt (15 to 20% cobbles, 10 to 30% gravel, 10 to 30% sand, 30 to 50% silt, 5% clay); clasts are angular to subrounded and include gray limestone, tan calcareous sandstone, reddish brown sandstone and quartzite; maximum clast size is 28 cm and average size is 4-7 cm; poorly sorted, matrix supported and generally massive, but some weak stratification of cobbles; nonplastic and dense; discontinuous carbonate coats on clasts (reworked?); some carbonate stringers in matrix and effervesces moderately to strongly (e to e+); variable "pin" holes in matrix; lower contact is clear to gradual and wavy; Units 5hh and 5hhh include a weak, thin (3 to 4 cm) A horizon that is characterized by a concentration of roots and root pores, disseminated organics and a granular structure; units are only present between st. 200 m and FZ4; Unit 5hh appears anomalously thick between FZ2 and FZ3-lower portion could possibly include indistinguished equivalents of Units 5ggg, 5fff, 5eee or 5ddd .

Unit 5ggg – Mottled light brownish gray to light gray ("buff") debris flow; gravelly sandy silt with cobbles similar to underlying Unit 5fff but less matrix, more carbonate and base marked by stone line of cobbles; generally massive, well cemented and matrix-supported; maximum clast size is 25 cm; top includes weak buried A horizon; lower contact is diffuse except for stone line, which becomes less distinct to the west where Units 5fff and 5ggg are undifferentiated; only mapped between FZ3 and FZ4.

Unit 5fff – Thick, light brownish gray to light gray debris flow package with orange mottling; gravelly sandy silt with cobbles; maximum clast size is 34 cm; matrix supported; overall homogeneous, well-cemented and massive, but some weak stratification, more burrows and less indurated in the upper meter; zones of more iron-oxide mottling; lots of vesicles; the lower contact is diffuse and roughly horizontal; only mapped between FZ3 and FZ4.

Unit 5eee – Mottled light brownish gray debris flow; gravelly sandy silt with cobbles; maximum clast size is 32 cm; similar to units 5fff and 5ddd, but slightly darker with more iron oxide staining and no stratification; lower contact is diffuse; only mapped between FZ3 and FZ4.

Unit 5ddd – Mottled light brownish gray to light gray debris flow; cobbly gravelly sandy silt; similar to Unit 5ggg in that it has less matrix and iron oxide staining than Unit 5eee; lower contact is clear and slightly backtilted to the east; only mapped between FZ3 and FZ4.

Units 5c, 5cc, and 5ccc(?) – Organic-rich pale brown to very dark grayish brown (*in situ* moist:10YR 6/3 to 10YR 5/3; wet: 10YR 3/2) mudlow and slopewash colluvium; poorly-sorted, generally matrix-supported (with clast-supported pockets) clayey silt with gravel and fine sand (10% cobbles, 15% gravel, 15% fine sand, 40% silt, 20% clay); clasts are dominantly subangular quartzite; maximum clast-size is 17 cm, average size is 4 to 8 cm; generally massive but stratification varies from none (randomly oriented clasts in mud matrix) to weak slope-parallel fabric in clast-supported pockets; plastic to nonplastic; medium stiffness; weakly cemented; slow dilatency; lower contact abrupt and wavy (generally an angular unconformity); abundant disseminated charcoal; some discontinuous carbonate coats on clasts, e- to e+ HCl reaction for matrix; this thin, discontinuous deposit was only exposed in the slot trench between st.198 m and FZ2, between st. 210.5 m and FZ3, and between st. 217.5 m and FZ4; it apparently draped

a scarp created by older faulting events on FZ1; although Units 5c and 5cc are very similar, Unit 5ccc (?) is generally more stratified and coarser with less clay, and more sand and gravel (10% cobbles, 25% gravel, 20% sand, 35% silt, 10 to 15% clay), but matrix has similar distinctive pinkish brown color with lots of organics.

Unit 5bbb – Pink to brown silty clayey channel gravels; maximum clast size is 12 cm and average is 3 to 6 cm; clasts are primarily subangular to subrounded tan quartzite with some gray limestone and reddish brown sandstone; slightly graded with basal lag; lots of disseminated charcoal; top includes 3 to 5 cm thick buried A horizon; lower contact is abrupt and undulating and appears slightly tilted to east; unit only exposed between st. 218 m and FZ4.

Unit 5aaa – Light brown silty fine sand with gravel; debris flow or channel deposit; maximum clast size is 14 cm and average is fine sand; clasts are primarily subangular to subrounded quartzite with some limestone; moist in situ; lots of disseminated charcoal; lower contact not exposed; no apparent bedding and gravels are "floating" in massive matrix; extensively bioturbated near FZ4; only exposed between st. 218 m and FZ4.

Unit FC2X – Brown to yellowish brown to very dark brown (dry: 10YR5/3 to 4/3; wet: 10YR 3/4 to 2/2), heterogeneous fault-scarp colluvium associated with Event X on FZ2 (specifically splay FZ2.2); this wedge-shaped deposit is locally only present adjacent to FZ2.2 and varies from moderate- to poorly-sorted; it is a dominantly clast-supported silty sand gravel with cobbles (occasional boulders, 10% cobbles, 40 to 60% gravel, 20 to 30% sand, 10 to 20% silt); clasts are dominantly subrounded to subangular (occaisional angular) tan and red quartzitie, calcareous sandstone, gray limestone, red sandstone and some orange sandstone; maximum clast size is 39 cm and average size is medium gravel (3 to 4 cm); somewhat stratified with lenses of moderately sorted gravels; stratification and clast fabric generally parallels upper slope contact and steepens upslope toward FZ2.2 (with dips as much as 47° W); generally fines upward, but a distinct contact between debris- and wash-facies could not be identified; slightly plastic, slightly cemented; lots of disseminated organics with dark gray brown coatings on some clasts (charring from fire?); matrix generally shows no HCl reaction, except rare carbonate stringers and discontinuous (reworked?) coatings on clasts; deposit truncated to the east by FZ2.2 and to the west by FZ3.

Unit FC1Z – Yellowish brown (dry: 10YR 5/4; wet: 10YR 4/4 to 3/4) heterogeneous fault-scarp colluvium associated with the youngest surface-faulting event on FZ1; gravelly silty sand with cobbles (10 to 20% cobbles, 10 to 15% gravel, 40 to 50% sand, 25 to 30% silt); poorly-sorted, matrix-supported, deposit only present locally adjacent to FZ1 with weak slope parallel clast fabric that steepens toward FZ1; clasts are dominantly angular to subrounded gray limestone, quartzite and some red sandstone; maximum size is 16 cm and average size is bimodal (fine sand and 5 to 6 cm); weakly cemented, hard dry strength, slightly plastic; occasional carbonate stringers on clast and in matrix with e to e- HCl reaction; occasional disseminated charcoal; lower contact is smooth and wavy, distinct to gradual, upper portion includes thin A horizon that extends upslope on Units 3b through 3e, but is stripped west of st. 205.5 m; this deposit is truncated to the east by FZ1 and truncated to the west by FZ2.1.

Units FC2Wa and FC2Wb – Yellowish brown to brown to dark brown (dry: 10YR 4/3 to 5/4; wet: 10YR 3/3 to 4/3) fault-scarp colluvium associated with Event W_{FZ2}, the oldest event exposed on FZ2; silt sandy gravel with cobbles (Unit FC2Wb) to cobbley sandy gravel (FC2Wa (10 to 15 % cobbles, 40 to 55% gravel, 15 to 25% sand, 10 to 20% silt, 0 to 5% clay); clasts are

primarily angular to subrounded tan quartzite with some limestone, maximum clast size is 25 cm and average size is medium gravel; Unit FC2Wb has a strong slope-parallel fabric that steepens toward FZ2; clast-supported; Unit FC2Wb is very poorly sorted and has more matrix, Unit FC2Wa is generally moderately sorted with lenses of well-sorted sands and open-work gravels, but is jumbled and loose; Unit FC2Wa appears similar to Unit FC1X but has fewer cobbles and more silt; lowermost contact is distinct and wavy, contact between Units FC2Wa and FC2Wb is gradual to distinct and smooth; Unit FC2Wb includes intraclasts, krotovina, roots, abundant organics, and a buried A horizon in the upper 4 to 8 cm; weakly to moderately cemented; ev reaction to HCl; deposits only present between FZ2 and FZ3 in the slot trench.

Unit FC1Y – Yellowish brown to dark yellowish brown to brown (dry: 10YR 5/4 to 4/4; wet: 10YR 4/4 to 4/3) heterogeneous fault-scarp colluvium associated with the penultimate surface-faulting event on FZ1; silty sandy gravel with cobbles (occasional boulders, 10% cobbles, 45 to 55% gravel, 20 to 25% sand, 15 to 20% silt, 0 to 5% clay); clast- to matrix-supported, poorly- to moderately sorted deposit only locally present between FZ1 and FZ2; clast are dominantly subangular to subrounded calcareous sandstone, quartzite, gray limestone and some small red sandstone; maximum clast size is 38 cm and average size is 2 to 3 cm (pea gravel); clasts show strong slope-parallel fabric that steepens toward FZ1; amount of fines generally increases upward except in more concentrated pockets of gravel; cobble stone line marks top and distinctive pea gravel marks base; numerous intraclasts within lower portion, disseminated organics (including charcoal), dark grayish brown charring on some clasts; lower contact is distinct to gradual, and wavy, upper portion includes A and Bw horizons; some carbonate filaments and e- HCl reaction; slightly plastic, hard dry strength, weakly cemented; deposit truncated to the east by FZ1 and to the west by FZ2.

Unit FC1X – Yellowish brown to dark yellowish brown (dry: 10YR 5/4 to 4/4; wet: 10YR 4/4 to 3/4) probable fault-scarp colluvium associated with the oldest faulting event on FZ1; sandy cobbley gravel (occasional boulders, 25-35% cobbles, 35 to 45% gravel, 15 to 25% sand, 5 to 15% silt); clast-supported, moderately-sorted, loose, jumbled deposit only locally present between FZ1 and FZ2, but does appear similar to FC2Wa; clasts are dominantly subangular to rounded calcareous sandstone, gray limestone, quartzite, and some small red sandstone and yellow sandstone; maximum clast size is 28 cm and average size is 5 to 6 cm (medium gravel); weak clast imbrication parallels upper contact; lower contact not exposed; nonplastic, e+ HCl reaction, some charcoal and dark grayish brown charred coating on some clasts; deposit is truncated to the east by FZ1 and to the west by FZ2.1.

Units 4b(?) and 4bb(?) – Highly mottled light and dark brown (dry: 10 YR 8/3-carbonate stringers, 10 YR 5/3 to 3/3-A horizon and charred coatings on clasts, 10 YR 5/3-average matrix; wet: 10 YR 4/3-average matrix) heterogeneous, debris flow or possible colluvial deposit; sandy silty gravel with cobbles to gravelly sandy silt (5 to 10% cobbles, 15 to 40% gravel; 20 to 25% sand 25 to 50% silt 0 to 5% clay); clasts dominantly angular to subrounded tan quartzite, sandstone and limestone; maximum clast size is 24 cm and average size is silt; clasts appear randomly oriented but some apparent weak stratification with coarser basal cobbley horizon (lower 20 cm); very poorly sorted, matrix- to clast-supported; lots of roots and burrows; includes 5- to 10-cm thick buried A horizon overlying Bk horizon with Stage I+ morphology and grade 2 sbk structure (base not exposed); well- cemented (dense and very hard); medium plasticity; carbonate mottling, e- to ev+ HCl reaction of matrix and carbonate coats on clasts; intraclasts, charcoal and organic-rich pods present throughout (similar to Units 3e and 3g but denser and

more clay); unit only mapped between FZ2 and FZ3 but may correlate (with underlying Unit 4a) to upper portion of Unit 3, or possibly is an older colluvial wedge reworked from Unit 3.

Units 4a(?) – Very pale brown cobbly silty gravels; debris flow or possibly colluvial deposit; clasts mostly subangular to subrounded quartzite with limestone; maximum clast size is 26 cm; dense and well-cemented; appears clast supported and poorly sorted, but exposure is limited; intraclasts, charcoal and organic-rich pods are present similar to overlying Unit 4b and Unit 3g; lower contact not exposed; only mapped between fault strands FZ2a and FZ2b, but may correlate to upper portion of Unit 3, on the upthrown side of FZ1.

Unit 3g – Mottled orange, brown and tan (dry: 10 YR 5/6 [matrix] to 10 YR 7/3 [clasts]; wet: 10 YR 3/4) bioturbated debris flow deposit or package; silt cobbley gravel (25% cobbles, 30% gravel, 10% sand, 25% silt, 10% clay); clasts mostly subangular to subrounded quartzite with limestone; maximum clast size is 25 cm and average size is gravel; poorly-sorted, matrix-supported, generally massive except 5 to 30-cm thick basal lag of pea gravel; plastic and weakly cemented; highly bioturbated with abundant dark brown organic-rich pods, especially in lower portion; weak to no HCl reaction; top includes buried weak Bw horizon that appears stripped to the west; unit only present east of st. 217 m, in the footwall of FZ1, apparently truncated in angular unconformity by paleoslope.

Unit 3f – Yellowish brown to dark yellowish brown (dry: 10 YR 5/6 [matrix] to 7/3 [clasts]; wet: 10 YR 4/4) debris flow; silty cobbley gravel (occasional boulders, 35% cobbles, 35% gravel, 10% sand, 20% silt); clasts mostly subrounded to subangular quartzite (abundant red), some limestone and micrite; maximum size is 30 cm and average size is ≈15 cm; poorly-sorted, matrix to clast-supported with some weak stratification; matrix and clasts are similar to overlying Unit 3g and this unit appears to be a coarse basal lag of the overlying debris flow; non-plastic and no cementation; vigorous HCl reaction and some minor carbonate coatings on clasts; unit only present east of st. 217 m, in the footwall of FZ1, apparently truncated in angular unconformity to the west by paleoslope.

Unit 3e – Brown to dark yellowish brown (dry: 7.5 YR 5/3 [matrix] to 10 YR 6/3 [clasts]; wet: 10 YR 4/6) debris flow/flood deposit; cobbley gravel with silt (4% boulders, 20% cobbles, 55% gravel, 6% sand, 10% silt, 5% clay); clast-supported, poorly- to moderately-sorted with some thin lenses of concentrated pea-gravel; clasts are mostly subangular to subrounded quartzite with limestone and some micrite; maximum clast size is 52 cm and average size is15 cm; slightly plastic, none to weak cementation; lower contact is fairly distinct; some carbonate filaments and coatings on clasts, matrix shows vigorous HCl reaction; unit only present east of st. 221 m, in the footwall of FZ1, truncated to the west in angular unconformity by paleoslope with associated A horizon.

Unit 3d – Yellowish brown to dark yellowish brown (dry: 10YR 5/6 [clasts] to 6/3 [matrix]; wet: 10YR 4/6) debris flow with organic-rich horizon; highly variable, moderately- to poorly-sorted, matrix-supported, sandy silty cobbley gravel (1% boulders, 20 to 25% cobbles, 25% gravel, 10 to 20% sand, 20 to 25% silt, 9% clay); clasts are primarily subangular to subrounded quartzite with some sandstone and dark limestone; maximum clast size is 53 cm, average size is 15 to 20 cm; some lenses and small channels of pea gravels; deposit includes a thin, distinctively dark, organic-rich horizon near the top that pinches out at st. 24 m; medium plasticity; weakly cemented; discontinuous carbonate filaments in matrix and ev reaction to HCl; lots vesicles;

lower contact smooth and distinct; deposits only present east of st. 26 m, in the footwall of FZ1, truncated to the west in angular unconformity by paleoslope with associated A horizon.

Unit 3c – Yellowish brown to dark yellowish brown (dry: 10YR 5/6 [clasts] to 6/3 [matrix]; wet: 10YR 4/6) open-work channel deposit; moderately-sorted, clast-supported, cobbley gravel with sand (45% cobbles, 45% gravel, 5% sand, 5% silt); clasts are primarily subangular to subrounded quartzite with some limestone and sandstone; maximum clast size is 30 cm, average size is ~10 cm; stratified with some well-sorted pockets; likely is a sieve deposit associated with underlying debris flow deposits (with most of fines winnowed away); lower contact I gradational (over a few cm); no plasticity; no to weak cementation in localized pods; unit only present east of st. 27 m, truncated in angular unconformity by paleoslope with associated A horizon.

Unit 3b – Brownish yellow to dark yellowish brown (dry: 10YR 6/6[matrix] to 6/3 [clasts]; wet: 10YR 6/4) debris flow; poorly-sorted, matrix-supported sandy silty gravel with cobbles (1% boulders, 14% cobbles, 40% gravel, 20% sand, 20% silt, 5% clay); clasts primarily subangular to subrounded quartzite with minor limestone, generally randomly oriented, maximum clast size is 40 cm, average clast size is ~7 cm; some thin laterally discontinuous lenses of sandy fine gravels, otherwise deposit is nonbedded; non- to slightly plastic; medium to no dry strength; weak to moderate cementation; lower contact is abrupt to gradational; fines westward overall; unit only present east of st. 29 m, truncated by FZ1 and paleoslope with associated A horizon.

Unit 3a – Yellowish brown (dry:10YR 5/6-matrix, 10YR 6/3-clasts; wet: 10YR 4/6 – matrix) cobbley channel alluvium; silty cobbley gravel with sand (2% boulders, 40% cobbles, 30% gravel, 10 % sand, 18% silt); primarily subangular to subrounded quartzite, some limestone and orthoquartzite, maximum clast size is 35 cm and average size is medium gravel to cobbles; clast-supported, moderately to poorly sorted, grossly stratified (cobbles versus gravel layers); non-plastic and no cementation (loose); some vesicles in matrix; some thin discontinuous carbonate coatings on bottom of clasts, matrix effervesces violenty (ev); deposit only present in the footwall of FZ1.

Appendix B

Paleo Research Institute Report by Kathy Puseman on "Examination of Bulk Soil for Radiocarbon Datable Material From the Mapleton Megatrench, Utah"

EXAMINATION OF BULK SOIL FOR RADIOCARBON DATABLE MATERIAL FROM THE MAPLETON MEGATRENCH, UTAH

By

Kathryn Puseman
Paleo Research Institute
Golden, Colorado

Paleo Research Institute Technical Report 05-25

Prepared For

URS Corporation
Oakland, California

April 2005

Appendix B
Paleo Research Institute Report by Kathy Puseman on "Examination of Bulk Soil for Radiocarbon Datable Material From the Mapleton Megatrench, Utah"

INTRODUCTION

A total of 10 bulk soil samples from the Mapleton megatrench site on the Provo segment of the Wasatch fault zone, Utah, were floated to recover organic fragments suitable for radiocarbon analysis. One sample was collected from the trench, while the remaining nine samples were recovered from Boreholes B1 and B2. Botanic components and detrital charcoal were identified, and potentially radiocarbon datable material was separated.

METHODS

The bulk samples were floated using a modification of the procedures outlined by Matthews (1979). Each sample was added to approximately 3 gallons of water. The sample was stirred until a strong vortex formed, which was allowed to slow before pouring the light fraction through a 150 micron mesh sieve. Additional water was added and the process repeated until all visible macrofloral material was removed from the sample (a minimum of five times). The material that remained in the bottom (heavy fraction) was poured through a 0.5-mm mesh screen. The floated portions were allowed to dry.

The light fractions were weighed, then passed through a series of graduated screens (US Standard Sieves with 4-mm, 2-mm, 1-mm, 0.5-mm and 0.25-mm openings to separate charcoal debris and to initially sort the remains. The contents of each screen were then examined. Charcoal pieces larger than 1-mm in diameter were broken to expose a fresh cross section and examined under a binocular microscope at a magnification of 70x. The remaining light fraction in the 4-mm, 2-mm, 1-mm, 0.5-mm, and 0.25-mm sieves was scanned under a binocular stereo microscope at a magnification of 10x, with some identifications requiring magnifications of up to 70x. The material that passed through the 0.25-mm screen was not examined. The coarse or heavy fractions also were screened and examined for the presence of botanic remains. Remains from both the light and heavy fractions were recorded as charred and/or uncharred, whole and/or fragments.

Macrofloral remains, including charcoal, were identified using manuals (Core, et al. 1976; Martin and Barkley 1961; Panshin and Zeeuw 1980; Petrides and Petrides 1992) and by comparison with modern and archaeological references. The term "seed" is used to represent seeds, achenes, caryopses, and other disseminules. Because charcoal and possibly other botanic remains were to be sent for radiocarbon dating, clean laboratory conditions were used during flotation and identification to avoid contamination. All instruments were washed between samples, and samples were protected from contact with modern charcoal.

DISCUSSION

The Mapleton megatrench site is situated just below the Lake Bonneville shoreline at an elevation of about 5,000 to 5,060 feet. In this location, a 19-meter scarp offsets post-lake Bonneville fan deposits that range from about 13,000 yr B.P. to the historic. The fan deposits are mostly debris flows from Big Slide Canyon. Woody vegetation in Big Slide Canyon includes maple (*Acer*), scrub oak (*Quercus*), mountain mahogany (*Cercocarpus*), sagebrush (*Artemisia*), and juniper (*Juniperus*). On-site vegetation is dominated by sagebrush, scrub oak, and a variety of flowers, grasses (Poaceae) and invasive weeds such as bunch grass, rabbitbrush (*Chrysothamnus*), prickly pear cactus (*Opuntia*), and thistle (*Urtica*).

Sample MM-RC25 was extracted from the trench (Table 1). This sample contained seven fragments of charcoal weighing 0.009 g from a conifer other than pine (Table 2, Table 3), as well as possible

Rosaceae charcoal weighing 0.010 g. Two fragments of hardwood charcoal weighing 0.007 g were vitrified, which precluded further identification. Vitrified material has a shiny, glassy appearance due to fusion by heat, and the presence of vitrified charcoal might reflect wood that was burned while it was green with a high sap content. All three charcoal types are present in sufficient quantities for AMS radiocarbon analysis. In addition, the sample contained a moderate amount of uncharred rootlets from modern plants and an abundance of rock/gravel.

The remaining nine samples were collected from Boreholes B1 and B2, with six samples from Boring B1 and three from Boring B2. Sample MM-RC49 represents bulk soil from a dark brown mottled debris flow at a depth of 48.5 feet (Boring B1-10). This sample yielded several small fragments of charcoal weighing 0.002 g that might be of a sufficient weight for AMS radiocarbon analysis. These charcoal fragments were too small for identification and likely represent a mix of both conifer and hardwood charcoal. A few uncharred rootlets from modern plants and a small amount of rock/gravel also were present.

Sample MM-RC50/51 was recovered from the dark brown mottled debris flow at a depth of 49 feet (Boring B1-10). A few pieces of charcoal too small for identification and weighing less than 0.001 g were present. These charcoal fragments are not of a sufficient weight for AMS radiocarbon analysis.

Sample MM-RC53 from a lower, thin, brown debris flow at a depth of 41.5 to 42 feet (Boring B1-9) consisted mainly of rock/gravel. Very little organic material, and no charcoal fragments, were present in this sample.

Sample MM-RC54 was taken from the upper mud flow at a depth of 38 feet (Boring B1-8). This sample contained several very small fragments of conifer charcoal weighing 0.001 g that might be sufficient for AMS radiocarbon analysis. A moderate amount of rock/gravel also was recovered.

Sample MM-RC55 represents the middle mudflow at a depth of 39 to 39.5 feet (Boring B1-8). Several fragments of charcoal were present in this sample; however, they were too small for identification and weigh less than 0.001 g.

Several fragments of conifer charcoal weighing less than 0.001 g were present in sample MM-RC56 from buried soil on the debris flow at a depth of 33 to 33.5 feet (Boring B1-7). These charcoal fragments are not of a sufficient weight for AMS radiocarbon analysis. A moderate amount of rock/gravel also was present.

Sample MC-RC57 was collected from a possible buried soil on a dark brown debris flow at a depth of 9.5 feet (Boring B2-2). This sample contained several fragments of charcoal too small for identification weighing less than 0.001 g. A few uncharred rootlets from modern plants and a small amount of rock/gravel also were present.

Sample MM-RC58/59 represents bulk soil and small charcoal from loess at a depth of 12 feet (Boring B2-3). Charcoal in this sample was too small for identification and weighs less than 0.001 g, which is not a sufficient amount for AMS radiocarbon analysis.

Sample MM-RC60 was recovered from a very dark brown debris flow at a depth of 39 to 39.75 feet (Boring B2-8). This is the oldest sample from Boring B2. Several small fragments of conifer charcoal were present, weighing 0.002 g. Fragments of charcoal too small for identification yielded a weight of 0.001 g, while three fragments of charcoal too vitrified for identification weighed 0.003 g. Individual charcoal types might be present in sufficient quantities for AMS radiocarbon analysis. The charcoal can be combined to yield a total weight of 0.006 g, which could then be submitted for AMS radiocarbon analysis. An uncharred *Euphorbia* seed, an uncharred Poaceae floret fragment, and a few uncharred rootlets represent modern plants and indicate the introduction of some modern material into this area.

SUMMARY AND CONCLUSIONS

Flotation of bulk samples from the Mapleton megatrench site, Utah, resulted in recovery of charcoal that can be sent for AMS radiocarbon analysis. Sample MM-RC25 from the trench yielded conifer and possible rose family charcoal, as well as hardwood charcoal too vitrified for further identification. All of these charcoal types were present in sufficient quantities for AMS radiocarbon analysis. Charcoal fragments in sample MM-RC49 yielded a total weight of 0.002 g, which might be enough for AMS radiocarbon analysis. These charcoal samples were too small for identification and likely represent a mixture of both conifer and hardwood charcoal. Conifer charcoal fragments weighing 0.001 g were present in sample MM-RC54. Sample MM-RC60 yielded conifer charcoal weighing 0.002 g, as well as charcoal too small for identification weighing 0.001 g and vitrified charcoal weighing 0.003 g. It might be possible to submit one of these charcoal types for AMS radiocarbon analysis, although combining the charcoal would yield an adequate amount of charcoal for dating. Only sample MM-RC53 did not yield any charcoal fragments. The remaining samples contained small fragments of charcoal weighing less than 0.001 g. Four of the samples from this project yielded identifiable conifer charcoal, reflecting the presence of conifers in Big Slide Canyon, such as juniper.

TABLE 1
PROVENIENCE DATA FOR SAMPLES FROM THE MAPLETON MEGATRENCH SITE, UTAH

Sample No.	Location	Depth	Description/Provenience	Analysis
MM-RC25	Bench 1-HW	~2 m	Bulk soil from buried A horizon in Unit 6t, below Unit $FCA5Y_g$	Float/Charcoal ID prior to C-14 analysis
MM-RC49	Boring B1-10	48.5'	Bulk soil from dark brown mottled debris flow (silty sandy with gravel and clay) - correlates to Unit 3g?; above red/ochre quartzite cobbles	Float/Charcoal ID prior to C-14 analysis
MM-RC50/51	Boring B1-10	49'	Bulk soil and small charcoal from dark brown mottled debris flow - correlates to Unit 3g?	Float/Charcoal ID prior to C-14 analysis
MM-RC53	Boring B1-9	41.5'-42'	Bulk soil from lower thin brown debris flow (sandy silty gravel with cobbles) - correlates to Unit 6b?	Float/Charcoal ID prior to C-14 analysis
MM-RC54	Boring B1-8	38'	Bulk soil from upper mudflow (silty sandy with gravel and clay) - correlates to Unit 6j?	Float/Charcoal ID prior to C-14 analysis
MM-RC55	Boring B1-8	39'-39.25'	Bulk soil from middle mudflow (silty sandy with gravel and clay) - correlates to Unit 6d?	Float/Charcoal ID prior to C-14 analysis
MM-RC56	Boring B1-7	33'-33.5'	Bulk soil from buried soil on debris flow (brown silty gravel with cobbles) - correlates to Unit 5g?	Float/Charcoal ID prior to C-14 analysis
MM-RC57	Boring B2-2	9.5'	Bulk soil from possible buried soil on dark brown debris flow (silty sand with gravels and clay)	Float/Charcoal ID prior to C-14 analysis
MM-RC58/59	Boring B2-3	12'	Bulk soil and small charcoal from loess (sandy silt); may correlate to loess in SP3	Float/Charcoal ID prior to C-14 analysis
MM-RC60	Boring B2-8	39'-39.75'	Bulk soil from very dark brown debris flow (gravelly sandy silt) - correlates to Unit 3e or 3d?; oldest sample from Boring B2	Float/Charcoal ID prior to C-14 analysis

TABLE 2
MACROFLORAL REMAINS FROM THE MAPLETON MEGATRENCH SITE, UTAH

Sample No.	Identification	Part	Charred		Uncharred		Weights/ Comments
			W	F	W	F	
MM-RC25	Liters Floated						1.40 L
Bench 1-HW	Light Fraction Weight						2.22 g
	FLORAL REMAINS:						
	Rootlets					X	Moderate
	CHARCOAL/WOOD:						
	Conifer (not pine)	Charcoal		7			0.009 g
	cf. Rosaceae	Charcoal		5			0.010 g
	Unidentified hardwood - vitrified	Charcoal		2			0.007 g
	NON-FLORAL REMAINS:						
	Rock/Gravel					X	Numerous
MM-RC49	Liters Floated						0.40 L
Boring B1-10	Light Fraction Weight						0.31 g
	FLORAL REMAINS:						
	Rootlets					X	Few
	CHARCOAL/WOOD:						
	Unidentified - small	Charcoal		43			0.002 g
	NON-FLORAL REMAINS:						
	Rock/Gravel					X	Few
MM-RC50/51	Liters Floated						0.60 L
	Light Fraction Weight						0.003 g
Boring B1-10	FLORAL REMAINS:						
	Rootlet					1	
	CHARCOAL/WOOD:						
	Unidentified - small	Charcoal					<0.001 g
	NON-FLORAL REMAINS:						
	Rock/Gravel					X	Moderate
MM-RC53	Liters Floated						0.40 L
Boring B1-9	Light Fraction Weight						<0.001 g
	FLORAL REMAINS:						
	Leaf					1	
	Rootlet					1	
	NON-FLORAL REMAINS:						
	Rock/Gravel					X	Moderate

TABLE 2. (continued)

Sample No.	Identification	Part	Charred		Uncharred		Weights/ Comments
			W	F	W	F	
MM-RC54	Liters Floated						0.50 L
Boring B1-8	Light Fraction Weight						0.04 g
	CHARCOAL/WOOD:						
	Conifer	Charcoal		17			0.001 g
	NON-FLORAL REMAINS:						
	Rock/Gravel					X	Moderate
MM-RC55	Liters Floated						0.35 L
Boring B1-8	Light Fraction Weight						0.05 g
	CHARCOAL/WOOD:						
	Unidentified - small	Charcoal		28			<0.001 g
	NON-FLORAL REMAINS:						
	Rock/Gravel					X	Few
MM-RC56	Liters Floated						0.50 L
Boring B1-7	Light Fraction Weight						0.20 g
	CHARCOAL/WOOD:						
	Conifer	Charcoal		24			<0.01 g
	NON-FLORAL REMAINS:						
	Rock/Gravel					X	Moderate
MM-RC57	Liters Floated						0.20 L
Boring B2-2	Light Fraction Weight						0.33 g
	FLORAL REMAINS:						
	Rootlets					X	Few
	CHARCOAL/WOOD:						
	Unidentified - small	Charcoal		35			Few
	NON-FLORAL REMAINS:						
	Rock/Gravel					X	Few
MM-RC58/59	Liters Floated						0.25 L
	Light Fraction Weight						0.03 g
Boring B2-3	CHARCOAL/WOOD:						
	Unidentified - small	Charcoal		11			<0.001 g
	NON-FLORAL REMAINS:						
	Rock/Gravel					X	Few

TABLE 2. (continued)

MM-RC60	Liters Floated						0.80 L
Boring B2-8	Light Fraction Weight						0.33 g
	FLORAL REMAINS:						
	Euphorbia	Seed			1		
	Poaceae	Floret				1	
	Rootlets					X	Few
	CHARCOAL/WOOD:						
	Conifer	Charcoal		35			0.002 g
	Unidentified - small	Charcoal		17			0.001 g
	Unidentifiable - vitrified	Charcoal		3			0.003 g
	NON-FLORAL REMAINS:						
	Rock/Gravel					X	Moderate

W = Whole
F = Fragment
X = Presence noted in sample
g = grams
L = Liters
* = Estimated frequency

TABLE 3
INDEX OF MACROFLORAL REMAINS RECOVERED FROM
THE MAPLETON MEGATRENCH SITE, UTAH

Scientific Name	Common Name
FLORAL REMAINS:	
Euphorbia	Spurge
Poaceae	Grass family
CHARCOAL/WOOD:	
Conifer	Cone-bearing, gymnospermous trees and shrubs, mostly evergreens, including the pine, spruce, fir, juniper, cedar, yew, and cypress
Rosaceae	Rose family

REFERENCES CITED

Core, H. A., W. A. Cote and A. C. Day
1976 *Wood Structure and Identification*. Syracuse University Press, Syracuse, New York.

Martin, Alexander C. and William D. Barkley
1961 *Seed Identification Manual*. University of California, Berkeley, California.

Matthews, Meredith H.
1979 Soil Sample Analysis of 5MT2148: Dominguez Ruin, Dolores, Colorado. Appendix B. In *The Dominguez Ruin: A McElmo Phase Pueblo in Southwestern Colorado*, edited by A. D. Reed. Bureau of Land Management Cultural Resource Series. vol. 7. Bureau of Land Management, Denver, Colorado.

Panshin, A. J. and Carl de Zeeuw
1980 *Textbook of Wood Technology*. McGraw-Hill Book, Co., New York, New York.

Petrides, George A. and Olivia Petrides
1992 *A Field Guide to Western Trees*. The Peterson Field Guide Series. Houghton Mifflin Co., Boston.

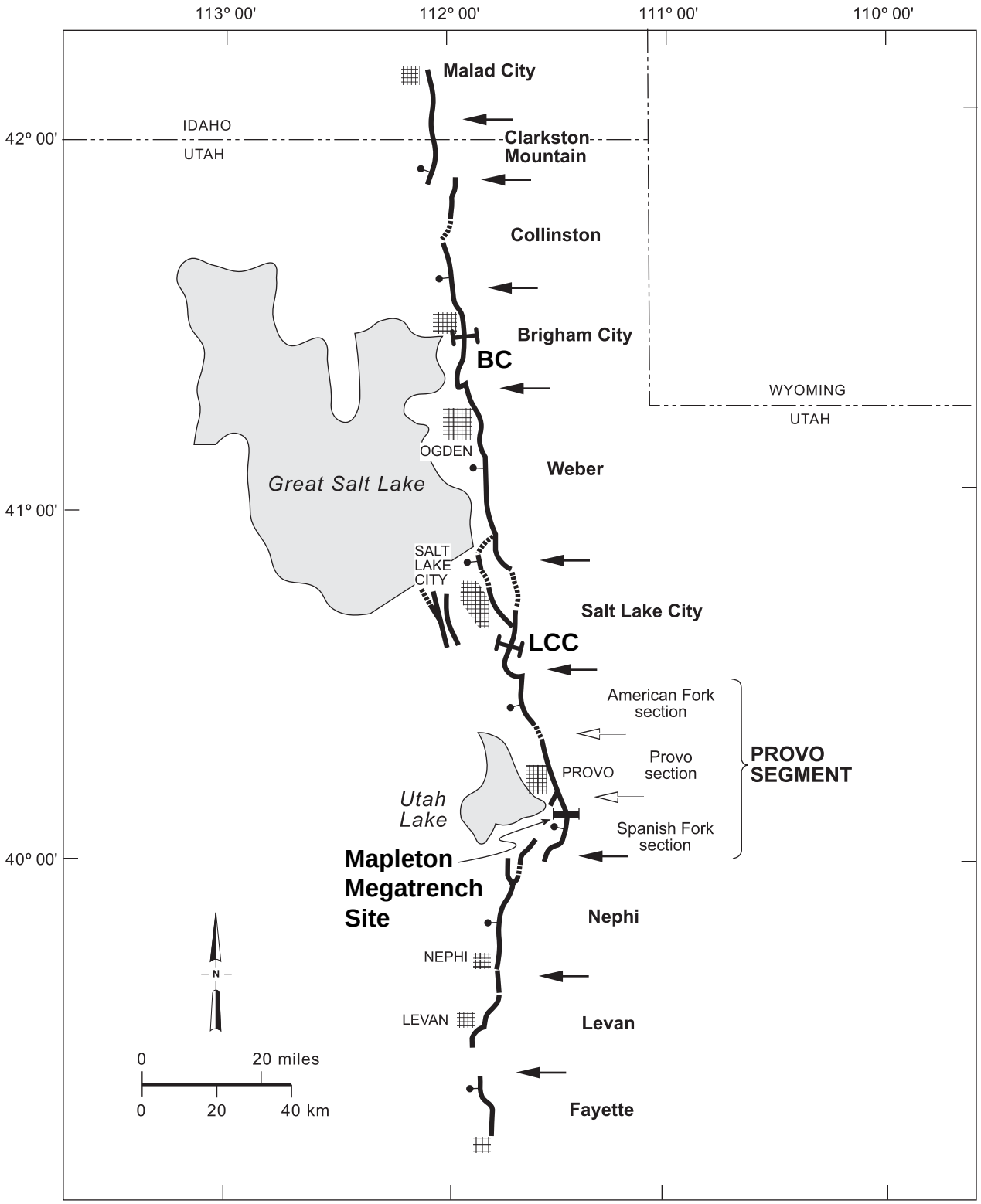

Figure 1. Map showing segments (in bold) of the Wasatch fault zone (after Machette et al., 1992), the location of this study, and the location of previous megatrench studies (BC – Brigham City site of McCalpin and Forman, 2002; LCC – Little Cottonwood Canyon site of McCalpin, 2002).

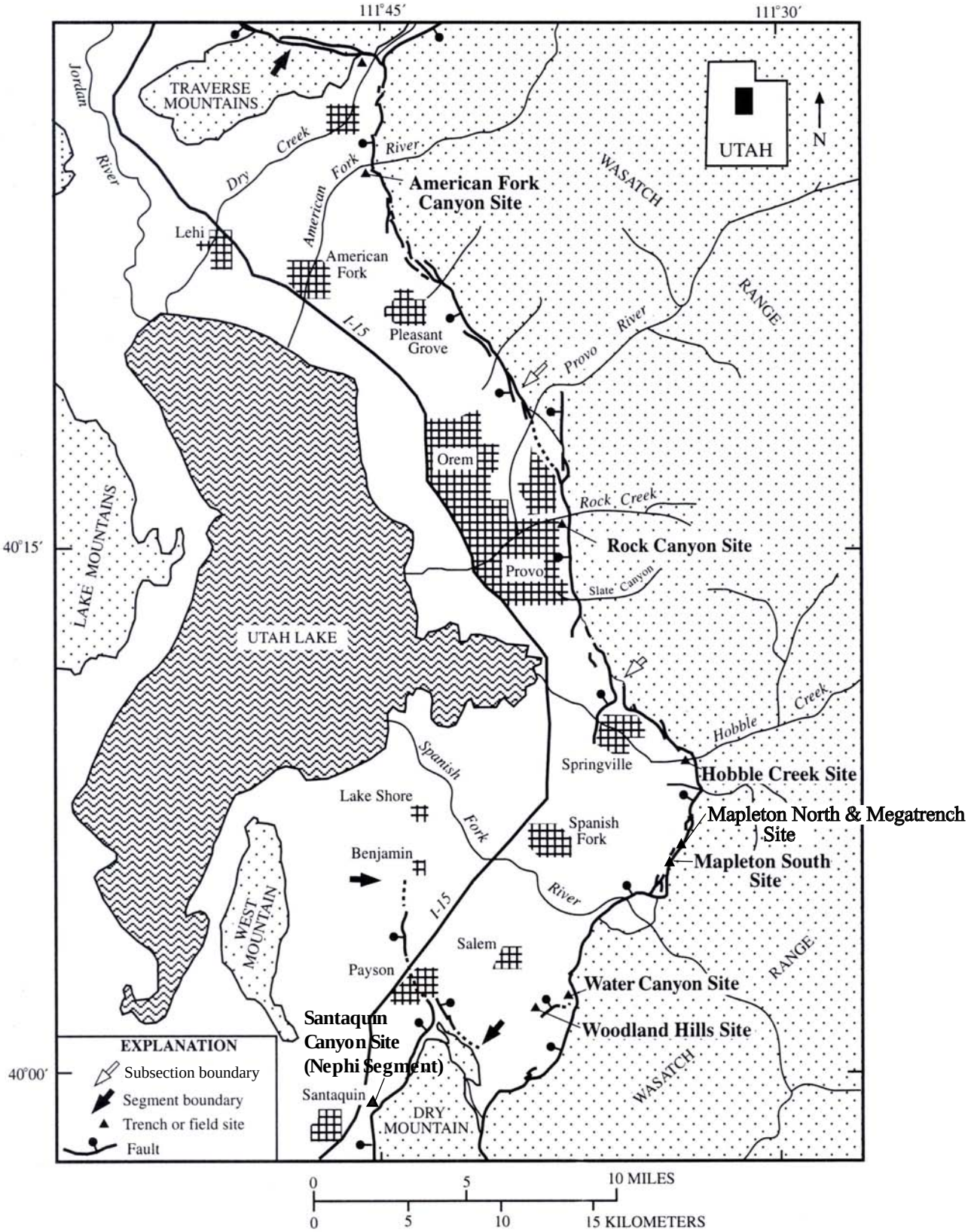

Figure 2. Location map of trench sites on the Provo and northern Nephi segments of the Wasatch fault zone (modified from Lund and Black, 1998).

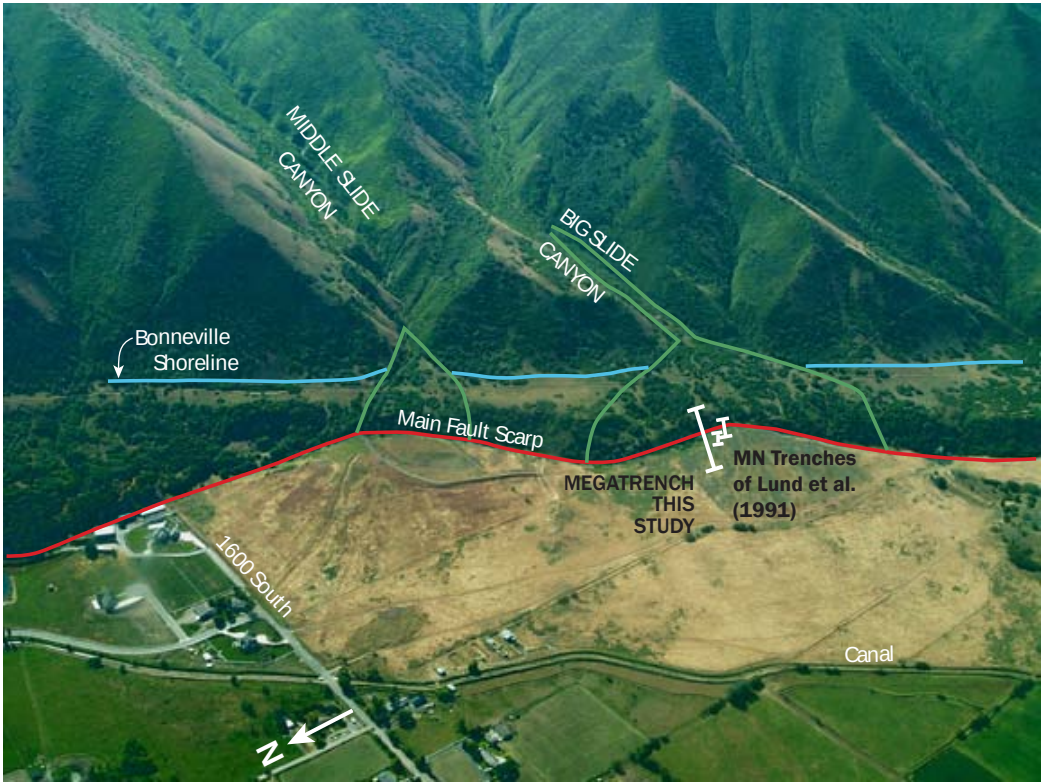

Figure 3. Aerial view looking east at the Mapleton megatrench site (photograph from R.L. Bruhn).

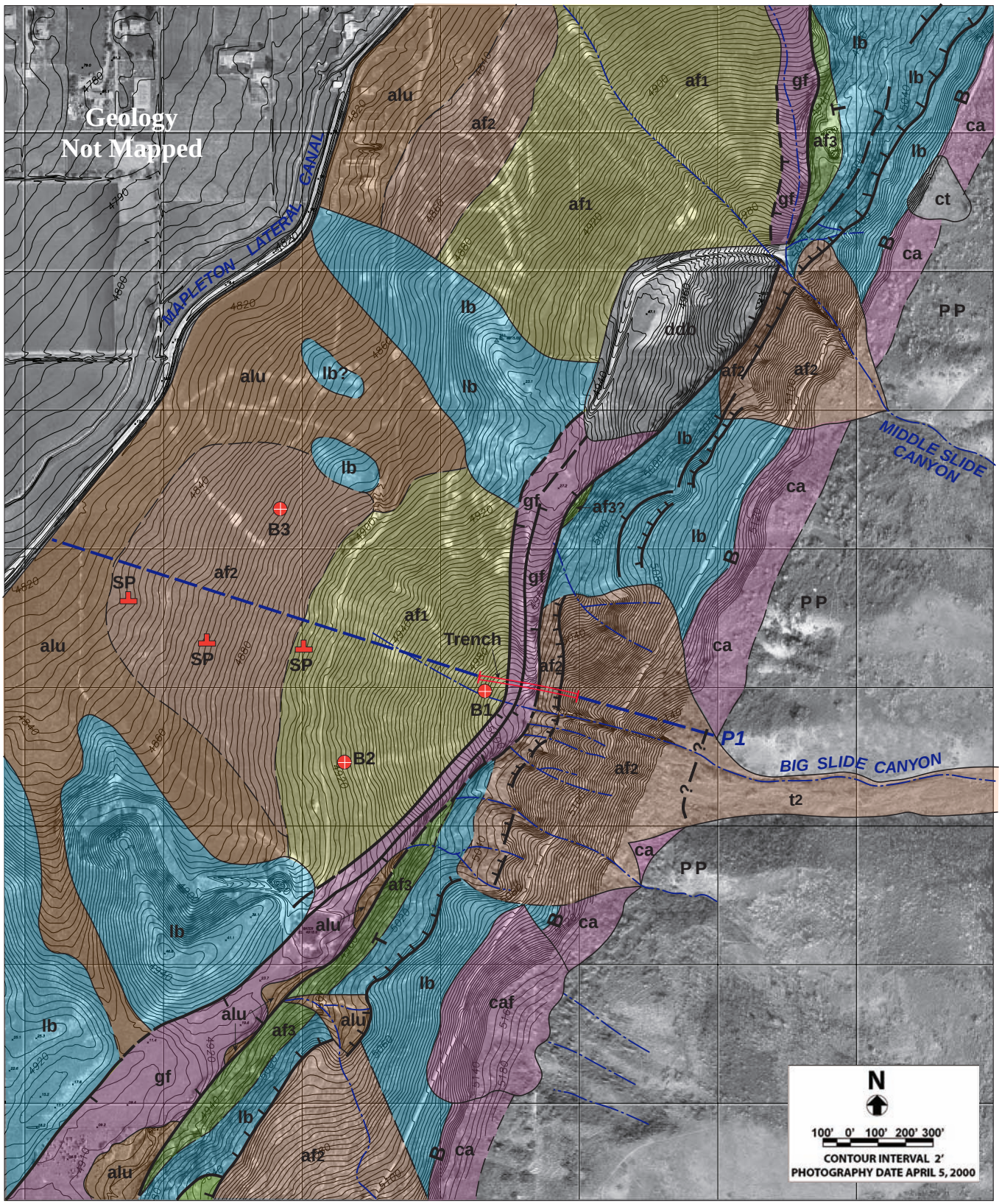

Figure 4. Surficial geology of the Mapleton Megatrench site.

EXPLANATION
Geologic Unit Descriptions

ddb Disturbed (Historic): Debris basin.

ct Colluvium (Holocene): Talus.

ca Colluvium and alluvium undivided (Holocene to upper Pleistocene): Includes talus, hillslope colluvium, and small alluvial-fan deposits that postdate the highest stand of Lake Bonneville (Bonneville shoreline).

caf Colluvium and alluvium undivided (Holocene to upper Pleistocene): Similar to "ca," but dominated by deposits of small, coalescing alluvial fans.

alu Alluvium undivided (Holocene to upper Pleistocene): Fine-to coarse-grained stream alluvium that postdates the high stand of Lake Bonneville and grades to the Provo shoreline; includes local areas of slope-wash colluvium.

gf Graben-fill alluvium and colluvium undivided (upper to middle Holocene): Fine- to coarse-grained alluvium deposited by debris flows or debris floods in graben which resulted from surface faulting along the Wasatch fault zone; includes scarp-derived colluvium adjacent to fault traces.

af_1 Fan alluvium (upper Holocene): Cobbley to locally bouldery gravel, matrix predominantly sand with silt and clay; frequently derived from the erosion of alluvial-fan deposits (af_2) on the upthrown side of the Wasatch fault zone.

af_2 Fan alluvium (middle Holocene to uppermost Pleistocene): Cobbley to locally bouldery gravel, matrix predominantly sand with silt and clay; deposited following regression of Lake Bonneville to the Provo shoreline; fan surfaces on the upthrown block of the Wasatch fault zone are moderately to deeply entrenched.

t_2 Terrace alluvium (middle Holocene to uppermost Pleistocene): Cobbley to locally bouldery gravel, matrix predominantly sand with silt and clay; terrace graded to af_2 fans.

af_3 Fan alluvium (upper Pleistocene): Cobbley to locally bouldery gravel, matrix predominantly sand with silt and clay deposited prior to and, at higher elevations, during the transgression of Lake Bonneville to the Bonneville shoreline; exposed in the main scarp of the Wasatch fault zone below the Lake Bonneville sediments.

lb Lacustrine deposits related to the Lake Bonneville highstand (upper Pleistocene): Bouldery sandy gravel at base ("T"), fining upward to interbedded silt and fine sand, with local coarse sand beds near top. Lower section deposited near shore as Lake Bonneville transgressed to the Bonneville shoreline. Upper section deposited in deep water as Lake Bonneville stood at the Bonneville shoreline. Uppermost section may include deposits related to the Keg Mountain oscillation.

PIPo Oquirrh Formation (Pennsylvanian and lower Permian): Gray to light-brown quartzitic limestone, brown quartzite, and gray to black limestone and cherty limestone.

Symbols

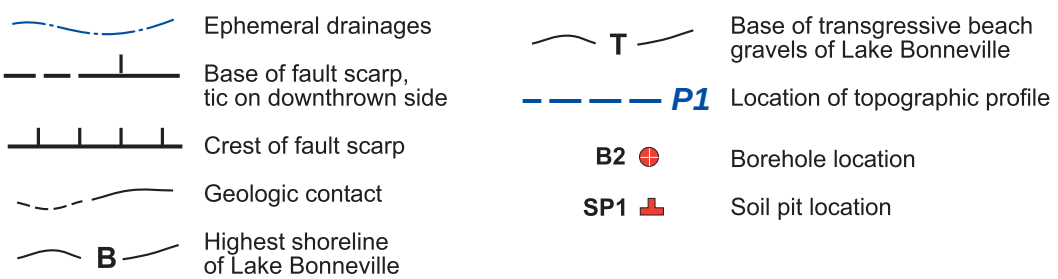

Figure 4. Continued

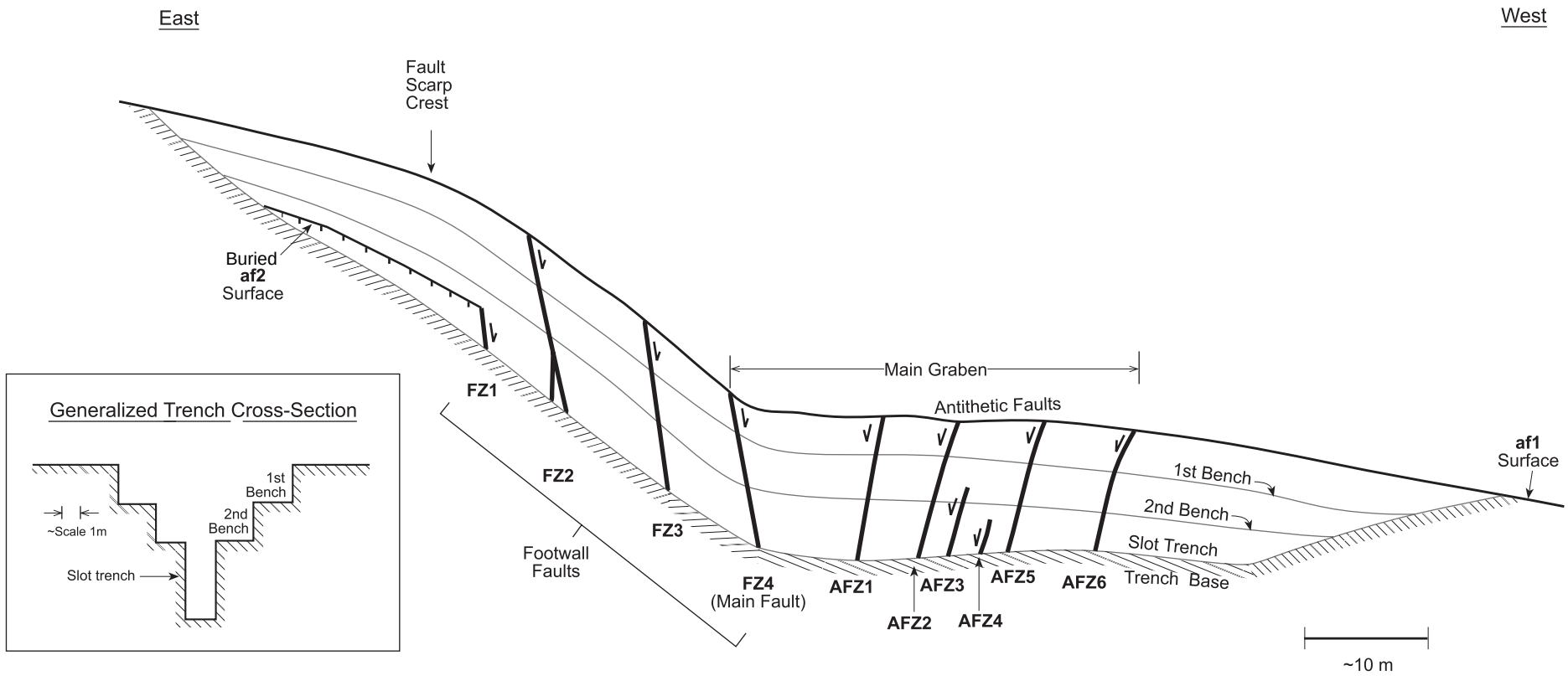

Figure 5. Schematic trench diagram showing general fault locations.

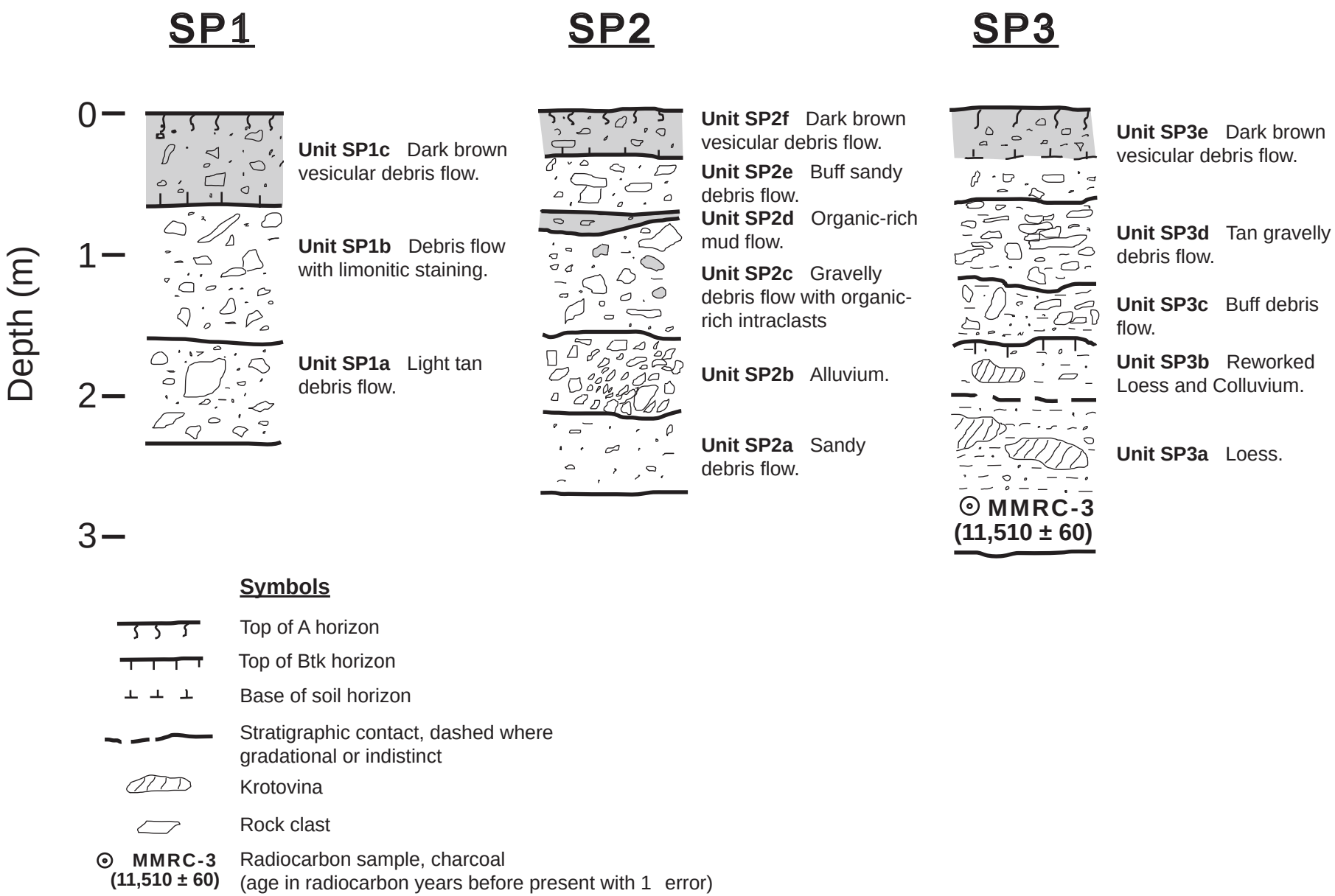

Figure 6. Logs of Soil Pits SP1 Through SP3.

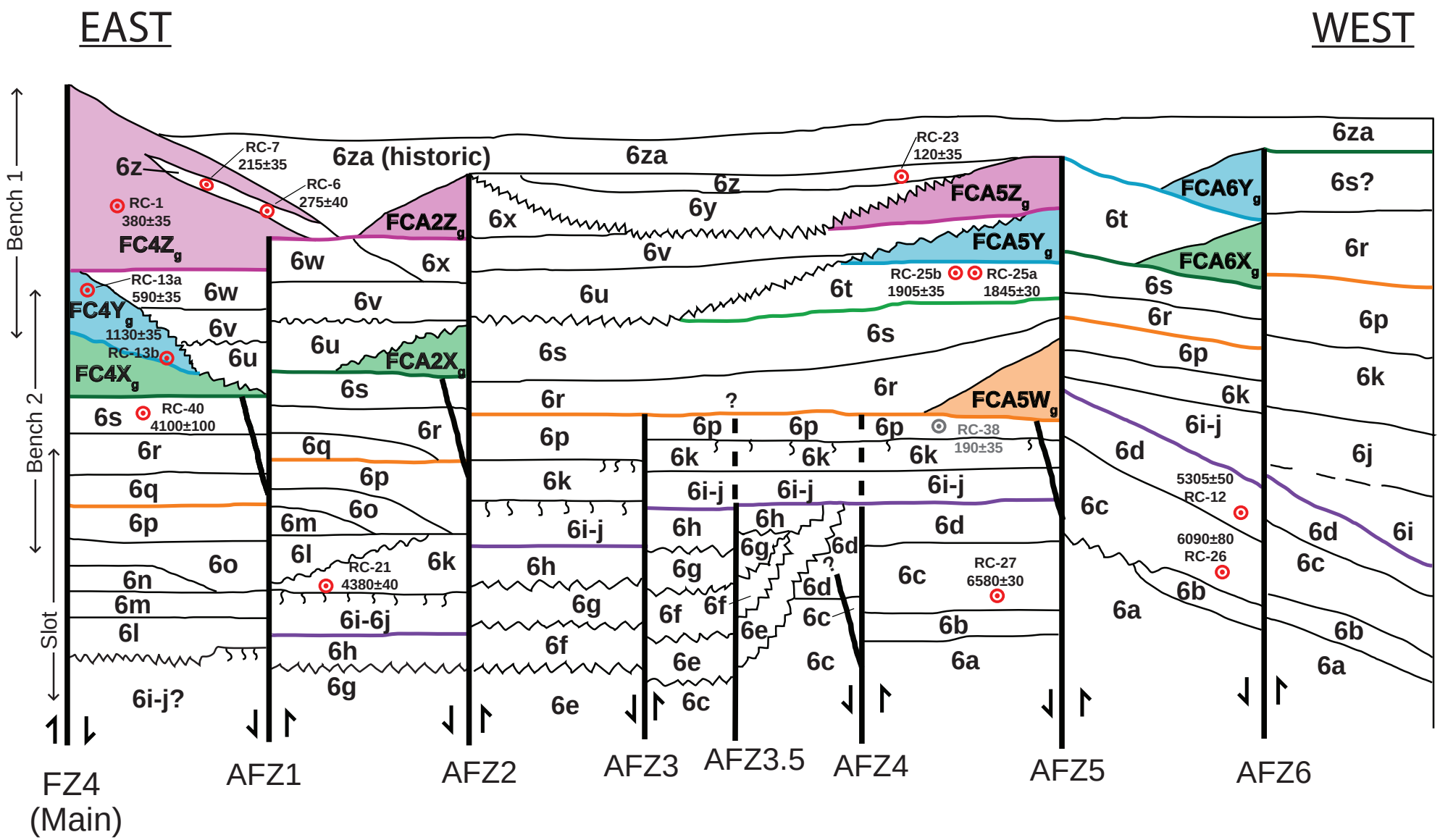

Figure 7. Schematic diagram of graben stratigraphy and surface-faulting event horizons (Event Zg – pink, Event Yg – blue, Event Xg – green, Event Wg – orange, and Event Vg(?) – purple). Red circles show radiocarbon samples and ages (with 1σ errors) used in the final analysis (see Figure 8). Gray circles show outlier samples not used in the analysis. Jagged lines indicate unconformities. Unit thicknesses and displacements are not to scale.

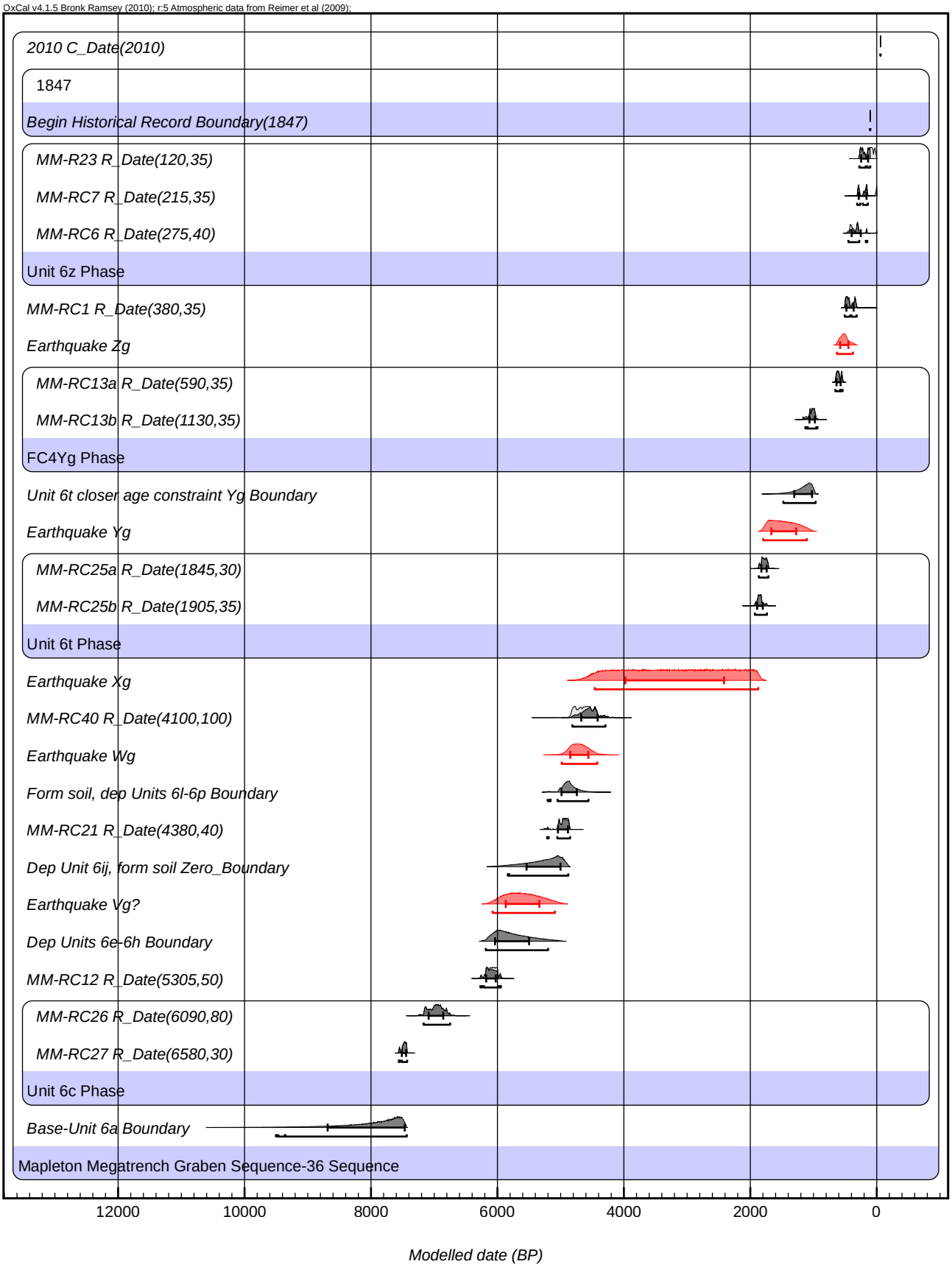

Figure 8. Age analysis of graben faulting events (shown in red). Ages (with 2 σ ranges) were calendar calibrated and modeled using OxCal v 4.1.5 (Bronk Ramsey, 2009) and the IntCal09 calibration curve (Reimeret al., 2009).

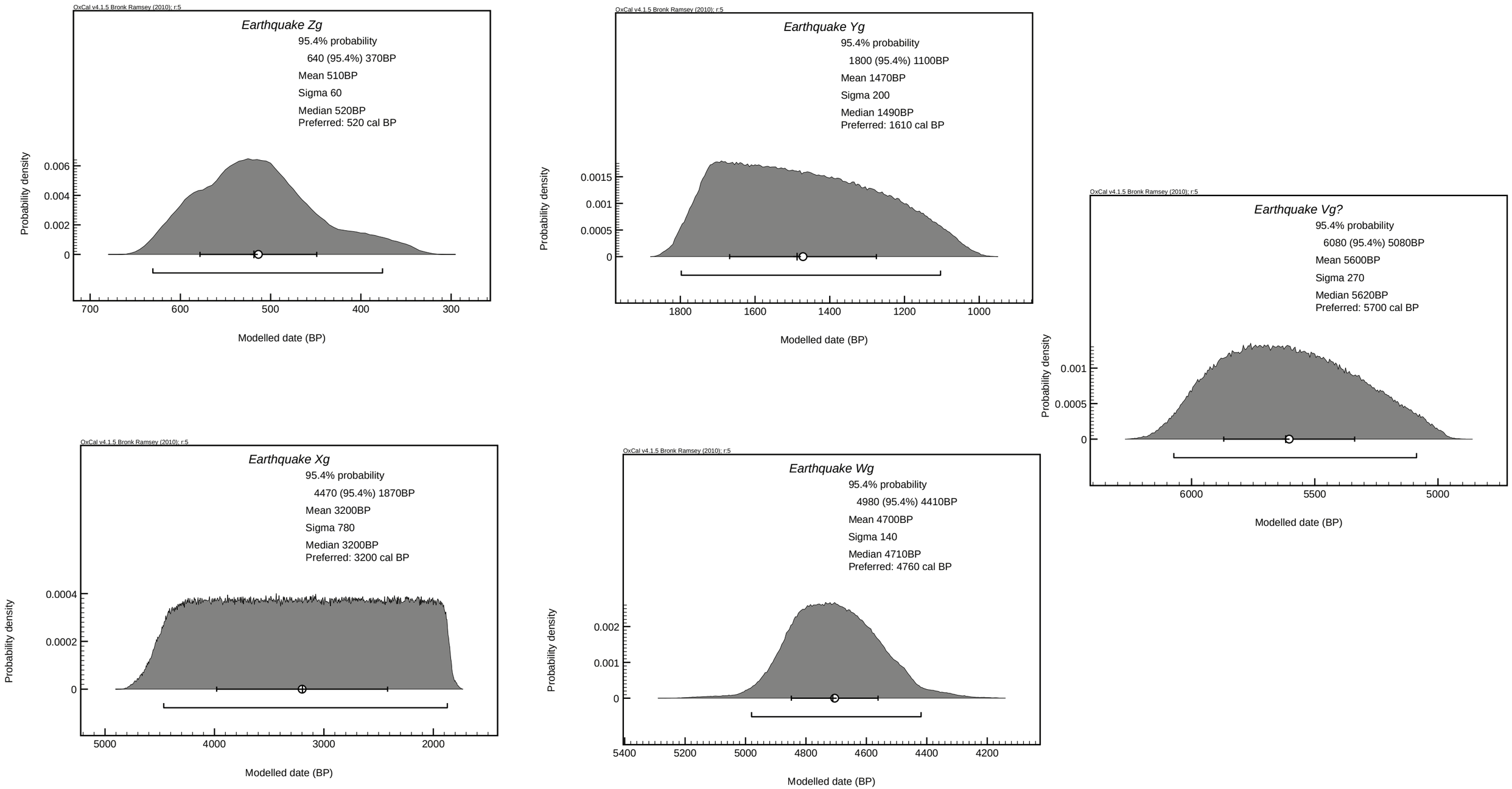

Figure 9. Modelled age distributions (in cal B.P.) of graben faulting events (from analysis showin in Figure 8). See Section 2.2.1 for discussion of selection of preferred ages.

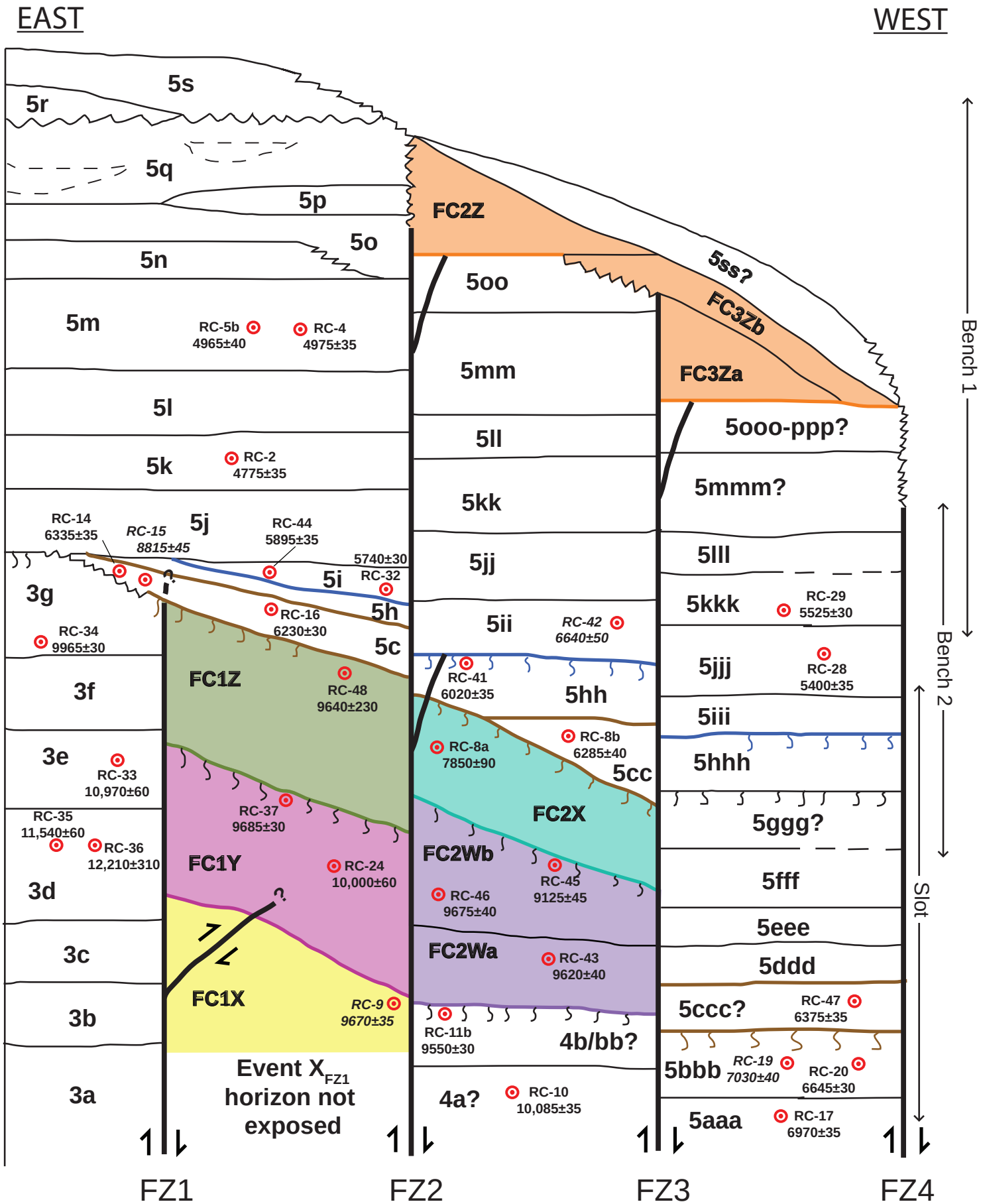

Figure 10. Preliminary schematic diagram of footwall stratigraphy and surface-faulting event horizons (Event ZFZ2&3 – orange, Events YFZ2 and YFZ3(?) – brown [uncertain if event pre- or post-dates deposition of Unit 5c/5cc/5ccc(?)], Event XFZ2 – teal, Event WFZ2 – lavender, Event ZFZ1 – green, Event YFZ1 – magenta). Dark blue indicates a non-tectonic slumping event horizon that included secondary faulting on FZ2. Jagged lines indicate unconformities. Red circles show radiocarbon samples and ages (with 1σ errors).

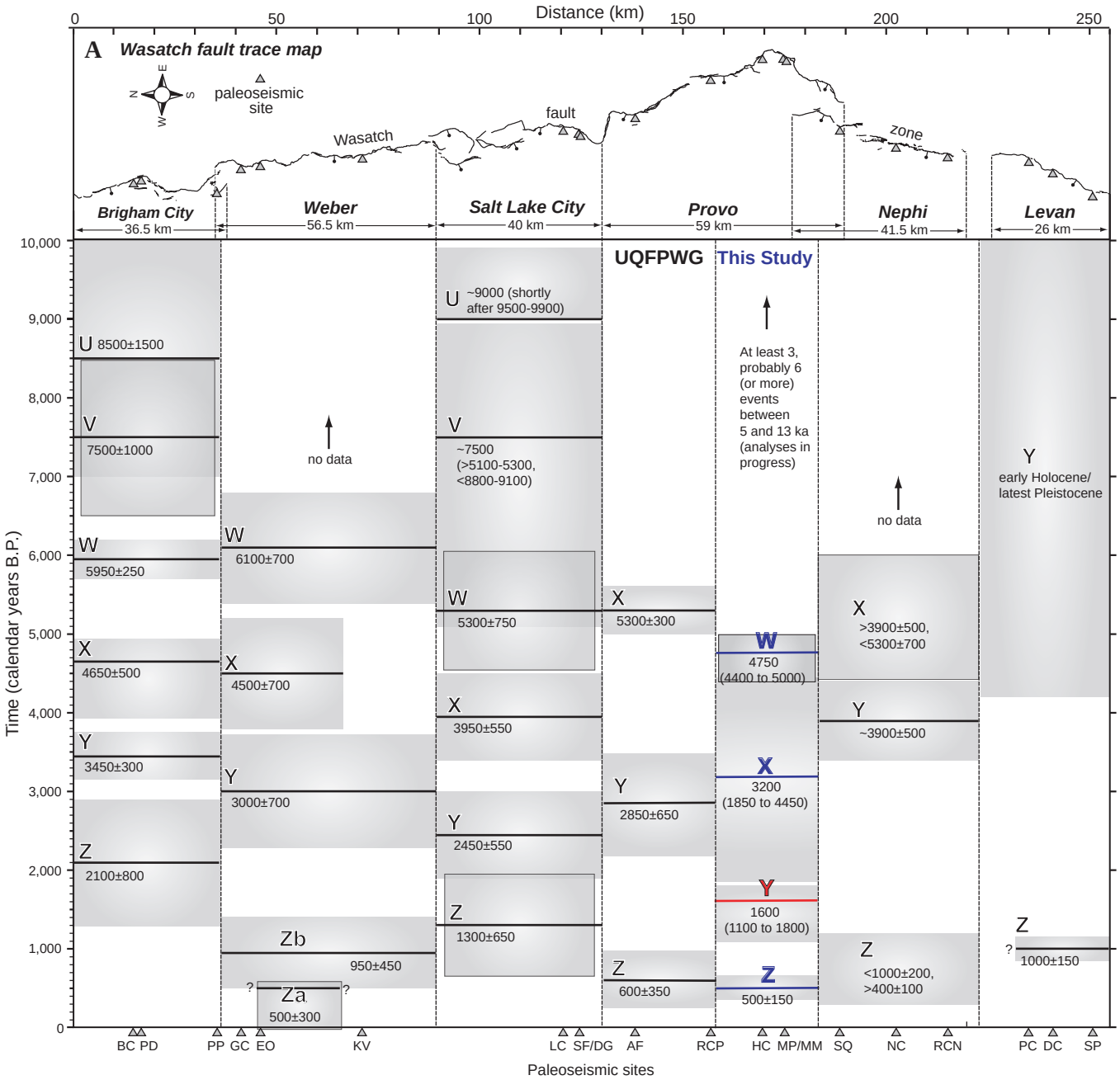

Figure 11. Paleoearthquake space-time diagram for central segments of the Wasatch fault zone comparing ages of the 4 youngest events in this study (shown in color) with consenus ages of the UQFPWG (Lund, 2005) determined from previous studies (modified from DuRoss, 2008). As discussed in the text, Event Y (in red) was previously unrecognized on the Provo segment.